2014

A study of effects of a new agricultural-based deicer on the properties of pavement concrete

Jianing Cao
Iowa State University

A study of effects of a new agricultural-based deicer on the properties of pavement concrete

by

Jianing Cao

A thesis submitted to the graduate faculty

in partial fulfillment of the requirement for the degree of

MASTER OF SCIENCE

Major: Civil Engineering (Civil Engineering Materials)

Program of Study Committee:

Kejin Wang, Co-Major Professor

Fatih Bektas, Co-Major Professor

Charles T. Jahren

Iowa State University

Ames, Iowa

2014

TABLE OF CONTENTS

Page

LIST OF FIGURES

Page

LIST OF TABLES

Page

ACKNOWLEDGEMENTS

First and foremost I would like to thank my major professor, Dr. Kejin Wang, and my co-major professor, Dr. Fatih Bektas for their guidance and support throughout this research and my M.S. study.

Dr. Wang's experiences and advices were instrumental in keeping me motivated to learn and improving my skills as a researcher. I'm grateful to Dr. Bektas for his support and guidance on my M.S. study at Iowa State University. I sincerely appreciate his patience with me and his contributions in this research work.

I'm truly grateful to Dr. Charles Jahren for his valuable time and efforts serving as a committee member.

In addition, I would also like to thank PCC research lab manager, Bob Steffes, for his help on my research work. I want to say thank you to all my friends, colleagues, the department faculty and staff for making my time at Iowa State University a wonderful experience.

Finally, thanks to my family for their encouragement and support during my study.

ABSTRACT

This study was aimed at evaluating effects of a new agricultural-based deicer named by the manufacturer as "Season I" on the properties of pavement concrete and its performance was compared with two traditional deicing salts: sodium chloride (NaCl) and calcium chloride ($CaCl_2$). The study can be divided into three parts and the first part evaluated physical frost damage including scaling and structural degradation of concrete/mortar. Strength loss, mass loss and scaling rating due to the damage were given. The second part inspected the effects of deicers on surface skid resistance and concrete permeability. The skid resistance indicator, BPN, and indirect concrete permeability indicators including electrical resistivity, air permeability index and water absorption rate were tested in this part. In the last part, the results of EDS point analyses were presented and discussed. The goal was to identify change/damage, if any, of micro-structures caused by the penetration of deicers.

The results of this study indicate NaCl and $CaCl_2$ solutions caused worse scaling and structural degradation comparing with Season I. Application of Season I greatly reduced the skid resistance comparing with NaCl and $CaCl_2$ solutions which had no apparent impacts. Season I reduced concrete permeability comparing with NaCl and $CaCl_2$ solutions based on electrical resistivity and water absorption rate. The EDS analyses found penetration depth of Season I was 13 mm and the penetration depth of NaCl was 19 mm. No salt precipitate or micro-structure change was found.

CHAPTER 1

INTRODUCTION

1.1 Organization of Thesis

This thesis is organized into five chapters:

- Introduction,
- Literature reviews,
- Experimental work,
- Results and discussion,
- Conclusions and recommendations.

Chapter 1 introduces the problems that currently exist about the durability of concrete pavement related to deicer application in winter environment. Efforts and funds spending on concrete pavement repairing and maintenance during the winter urge people to maximize the longevity of pavement by seeking for an effective and concrete-friendly deicer.

Chapter 2 covers literature review of past studies involving the physical frost-salt attack damages, the effects of salt application on concrete skid resistance and its permeability. Scaling and permeability change are addressed since the EDS point analysis was used to assess relationship between the penetration depth of deicers and scaling and explore the cause of concrete permeability change.

Chapter 3 includes the materials, specimen preparation and methodology adopted in experimental program of this study. The materials are discussed and the specimen preparation process is presented. Detailed information about each methodology employed can be found in last section.

Chapter 4 presents the test resulted and discusses the findings. The discussion is focused on:

- The difference in physical damage caused by different deicers,
- Skid resistance after deicer application,
- Difference in concrete permeability after deicer treatment,
- Findings of EDS analysis.

Chapter 5 gives final thoughts regarding the points achieved from this study. Recommendations for future work are provided to improve the quality of study on deicer performance and concrete durability problems.

1.2 Problem Statement

Transportation system plays a significant role in modern society. An efficient and reliable transportation system is considered as an engine to economic growth and the roadway system is particularly important since it has the largest number of users. However, based on Federal Highway Administration (FHWA), thousands of fatalities are reported

annually in winter weather related crashes and millions of dollars are spent on winter road maintenance in the snowy region of United States [1].

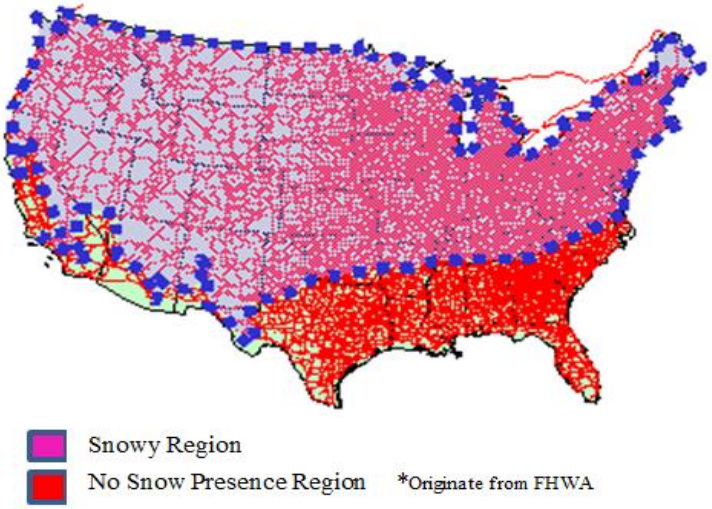

Figure 1. Snowy Region of United States [1]

A major contributor to unsafe road condition during the winter is the damages associated with application of deicing salts. Although many new deicing products are available on the commercial market in recent years, highway agencies are not satisfied with their performance.

1.3 Significance of This Study

It is well known that the most abundant and economical deicing material is rock salt which is primarily composed of sodium chloride. Other chloride salts like calcium chloride and magnesium chloride are also well adopted as deicing compounds. But, the aggressiveness of chloride-based deicers has been long proven [2-4]. Another common

type of deicing salts is acetates. Acetate-based deicers are most often used on airport pavement since they are considered non-corrosive to pavement reinforcement. However, the detrimental effects of calcium magnesium acetate (CMA) on Portland cement concrete (PCC) material was confirmed [5]. Previous studies have found drastic strength loss of concrete and signs of paste delamination. Agricultural-based (agro-based) deicer, which is made by adding agricultural additives to the liquid form of traditional chemical deicer, has been proven to be effective in recent decades. These agro-based additives are mainly agriculture by-products like complex sugars and proteins. The addition of these additives results in less physical and chemical damages on PCC materials [6].

Besides the differences of concrete mix and curing, the damage associated with deicers on PCC pavement is related to a variety of causes such as freezing and thawing environment, steel corrosion, physical distresses, leaching of cementitious material, chemical reactions between concrete constituents and the deicing chemicals, etc. These interrelated deleterious effects make the nature of this problem sophisticated and it is important to provide more information on this topic.

Thus, the intent of this is study is to evaluate the effects of a newly developed agro-based deicer on PCC in comparison with traditional deicing salts, namely sodium chloride and calcium chloride. The experimental work was designed to predict the concrete behavior with exposure to aforementioned deicers in winter environment as an indirect simulation of field conditions.

1.4 Scope of the Research

The assessment of the new agro-based deicer focused on following aspects:

- Frost damage to PCC materials
- Effects on skid resistance
- Effects on concrete permeability

The first part of the research work evaluated physical frost damage including structural degradation and scaling. Strength loss, mass loss and scaling rating were obtained. The second part inspected the effects of deicers on surface skid resistance and concrete permeability. Skid resistance and three indirect concrete permeability indicators including electrical resistivity, air permeability index and water absorption rate were tested in this part. SEM imagines and EDS point analyses were used to identify change/damage of micro-structures caused by the penetration of deicers.

CHAPTER 2

LITERATURE REVIEW

It is recognized that concrete is vulnerable to frost damage due to water inside concrete system. The presence of deicers accelerates the damage because deicing chemicals penetrate into concrete with water and deteriorate concrete materials in various ways. To better understand the role of deicer, it is necessary to review previous studies about frost damage on concrete. Scaling damage, which is one of the major frost damages, was discussed in details because of its importance in this study. Besides, the effects of deicer application on skid resistance and concrete permeability were reviewed to provide background knowledge for discussion in following chapters.

2.1 Frost Damage

The frost action or freezing and thawing cycling causes cracking and spalling of concrete by progressive expansion of the cement paste. The behavior of water in frost condition also contributes to internal pressures resulting cracking. The effects of frost action on two major components of concrete, cement paste and aggregate, can be different. But, both lead to frost damage [7].

Concrete's susceptibility to frost damage is explained by three major theories which are: the hydraulic pressure theory proposed by Powers in 1940s, the osmotic pressure theory and Litvan's theory proposed by G.G. Litvan in 1970s.

2.1.1 Hydraulic pressure theory

The first and the most well-known theory is the hydraulic theory proposed by Powers in 1949. The mechanism of this theory is relatively simple. When the temperature is below 0 ℃, water starts to freeze in capillary pores causing a volume increase. The theory assumes the paste material is fully saturated and this volume increase will force unfrozen water to move to spaces where it can freeze generating a hydraulic pressure. The distance and the amount of unfrozen water travels in a given time determine the magnitude of the pressure. If this pressure exceeds the strength of porous paste materials, mechanical damages will occur. The role of deicing salts in hydraulic pressure theory is limited. It is only considered as a depressant allowing the presence of liquid water in freezing temperature [8].

Since Powers considered only one single air bubble surrounded by paste, his theory is only valid for concrete having air voids of same size and equally spaced. Also, many experimental works later prove the unfrozen water in pores was actually moving towards capillary pores instead of being forced out. So, in the following years, Powers and Helmuth worked together and found the freezing water in capillary pores made the paste to dry and shrink. They explained their findings based on thermodynamic analysis and stated the growing ice crystals in capillary voids exerted a pressure on paste walls causing the system failure inside the concrete.

2.1.2 Osmotic pressure theory

Until 1970s, they realized that their assumptions in thermodynamic analysis which saying the water in pores and paste is pure water were not correct. They revised the theory and named it osmotic pressure theory because they realized the role of deicing chemicals. When ice started to form in capillary voids, thermodynamic equilibrium was broken between water in paste and pores in freezing temperature. Thus, the concentration of dissolved deicing chemicals in the unfrozen water increased. Then, due to the osmotic phenomenon, water in smaller pores or paste gels was attracted to larger pores in order to reach the equilibrium between different concentrations. As pore solution of low salinity moved into pores of high salinity, more water started to freeze because of declining salinity. The continuously built internal pressures led to mechanical damage on walls of capillary. The drawback of this theory was the protection of paste material by air voids cannot be explained clearly. Although the difference of specific volume between ice and water in hydraulic theory was still valid, it is hard to explain the results of unavoidable movement of water to pass through porous medium (paste material) to reach air voids for spaces. It was suspicious that pressure exerted on paste material would cause micro-cracking at rapid freezing rate.

2.1.3 Theory proposed by Litvan

Litvan also did tremendous amount of work to explain the effects of frost action on concrete damage. He claimed that, at a higher freezing rate, more water in pores tended to be unstable per unit time and higher risk of mechanical damage on paste materials. The mechanical damage occurred when the process of desorption can was not in an orderly

manner (ie. Fast moisture transfer caused quick drying of paste) [9]. His fundamental hypothesis was the water in capillary voids would not freeze in situ. This theory adequately explained the many fundamentals about mechanisms of frost damage proposed in Powers' hydraulic pressure theory. However, it did not establish a clear relationship between air void spacing and other factors like freezing rate.

The role of deicing salts was explained as the presence of salt in supercooled pore solutions will increase vapor pressure difference between unfrozen water and ice to amplify water movement. A study done by Cantor and Kneeter examined Litvan's hypothesis and they found the low salinity of pore solution exacerbated frost damage. [10-11].

2.1.4 Summary of frost damage

The theories of frost damage are interrelated because the pore solution movement, salinity and thermodynamic equilibrium are all affected by freezing temperature, moisture and the pore systems. It is essential to understand that three theories are all about internal pressures generated due to pore solution movement and cavity expansion. Besides, it has been found that chlorides cause leaching of calcium and decompose C-S-H gel (tobermorite) by chemical reactions [12-13]. In this study, chemical damages are not going to be addressed in details.

2.2 Salt Scaling

Scaling damage, as shown in Figure 2, is a superficial damage caused by freezing a saline solution and it is a progressive damage with esthetical hazard [14].

Figure 2. Typical Scaling Damage

It can be visually observed that thin pieces of surface cementitious materials are peeled off at random locations. The first theory of salt scaling mechanism was established in 1950s [15]. Being different from other frost damages, salt scaling does not harm the integrity of concrete body. However, scaling damage drastically increases the ingress of moisture offering a preferred environment for aforementioned chemical degradations including calcium leaching and C-S-H gel decomposition to occur. Moreover, the ingress of moisture due to scaling damage increases concrete's susceptibility to physical frost damage because of behavior of water with fluctuating temperature [16-17]. Another problem associated with the scaling damage is exposure of aggregates. Specific aggregates

with high porosity or reactive chemical constituents might propagate the damage on surface due to frost action and environmental chemical attacks [7].

In the following sections, previous studies were reviewed to summarize the characteristics and mechanisms of salt scaling to help understand scaling damage.

2.2.1 Characteristics of salt scaling

As mentioned in the beginning of section 2.2, scaling damage can be visually observed because of missing pieces of paste and the exposure of aggregates. It is unique because the presence of salts is a must for scaling to occur. Some reported scaling damages can be done without deicing salts [18-19]. Both studies have shown that the paste chips disintegrated were found when water was pooled in frost condition. However, none of these studies employed the standard test of salt scaling. Extreme long period of freezing and thawing cycling like 100 cycles used in these studies is twice that used in standard test. It is believed this extraordinary contributed to scaling damage although no salt solution was presented [14]. Another concern here is the poor quality of concrete mixes that has been used. High percentage fly ash substitution lowers the strength of surface materials.

The second significant characteristic of salt scaling is the most damage occurs at low concentration of salt solution pooled on concrete. One comprehensive study describes this phenomenon as “a moderate amount of salt solute will lead to the maximum scaling damage” and the concentration was called “pessimum concentration” [14-16, 20-22].

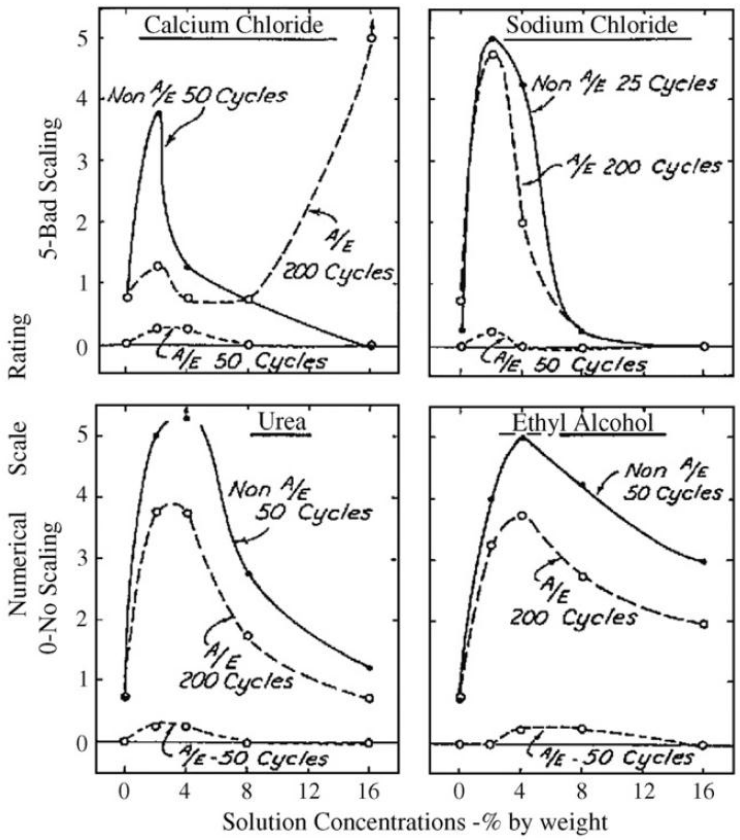

Figure 3. Scaling ratings at different solute concentrations of calcium chloride, sodium chloride, urea, and ethyl alcohol [15]

Figure 3 illustrates the existence of "pessimum concentration". Curves show that the most severe scaling damage was done when the concentration of the solution reached 3%. This is consistent with findings in review of frost damage. It indicates the mechanism of salt scaling might be related to proposed theories of frost damage. Also, research investigated the importance of deicing agent composition and found that the concentration is much more important than the composition of solute [23].

The point is the "pessimum concentration" is independent of solute type. But, this conclusion is questionable since it was based on test results of most chloride salts with

only a few others. Another interesting finding is that, as shown in Figure 3, air-entrained mixes have lower scaling rating with respect to non-air-entrained mixes. This is because air-entrainment is known to prevent damage from frost action and it has been concluded that an adequate air void system would improve the scaling resistance of concrete [24-28].

The last characteristic of salt scaling is the salt solution ponding. If the salt solution is not pooled on the concrete surface, no scaling damage will be done. Research finds no obvious scaling damage was occurring when the surface is flushed by concentrated NaCl solution in freezing and thawing conditions [15-16, 20].

2.2.2 Mechanisms of salt scaling

The review of frost damage and some characteristics of salt scaling have led to the suggestion that the mechanism of salt scaling is similar to the mechanisms of frost damage. However, if so, the most damage should be done with pure water pooled on concrete surface which is not true. Also, scaling damage is an esthetical damage. The strength loss of specimen in freezing and thawing resistance test was proven caused by frost action [29]. In spite of distinct nature of salt scaling and frost damage, it is necessary to discuss this topic for us to explain the mechanism of salt scaling. To evaluate the importance of hydraulic pressure and osmotic pressure as the cause of scaling, it is necessary to reconsider the role of salts. Recall that roles of deicing salts in hydraulic pressure theory and osmotic pressure theory. The pore salinity change due to ice formation results in a concentration gradient near concrete surface where scaling occurs. The salt concentration in brine adjacent to crystals is much higher comparing with the salt concentration of the

applied saline solution because the salt ions are not included in crystal layers when pore solution is frozen (Figure. 4) [30].

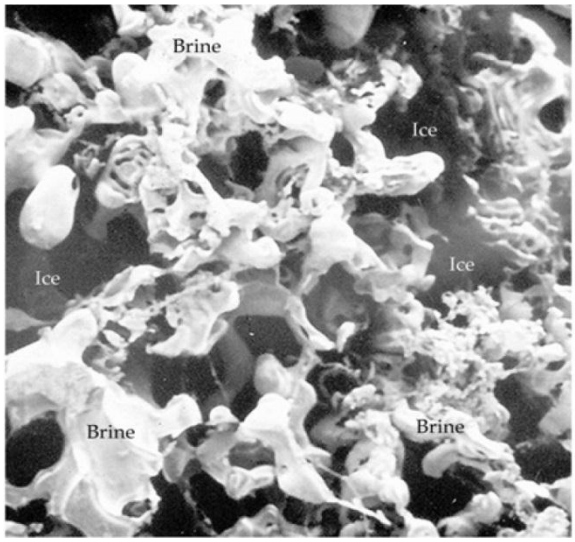

Figure 4. Brine ice with epoxy impregnated [30]

The osmotic pressure gradient near concrete surface drives the water to diffuse from low concentration to high concentration and surface paste material could be damaged in this process. However, several studies have reached a conclusion that such a magnitude of pressure is not destructive to surface paste material [31-32]. At the same time, salt might precipitate near the surface with temperature change. It is suspicious that, with increasing concentration of salt in pore solution, precipitation of salt will occur once the surface is dried. However, the precipitation of salt, for example NaCl, does not occur until the temperature drops to -21 ℃ [33]. This is much lower than lab freezing temperature of scaling test which explains salt precipitation is irrelevant to scaling damage. Table 1 summarizes some possible reasons of salt scaling that have been investigated in literature.

Table 1. Study of salt scaling mechanisms [34]

Proposed Reasons	Damaging Mechanisms	Reasons why not convincible
Hydraulic Pressure	Stress on paste material when pore solution is forced to move	Cannot account for characteristics of salt scaling like deicer ponding is required
Osmotic Pressure	Osmotic phenomenon caused by salinity difference	Limited by hydrodynamic relaxation
Vapor Pressure Difference	Vapor pressure difference between pore solutions drives mass transfer and change of state	Cannot account for characteristics of salt scaling like the existence of pessimum concentration
Salt Precipitation	Precipitation of salt crystals with temperature change	The temperature required to precipitate is too low to reach
Thermal Shock	Heat withdraw from concrete surface due to salts lowering melting point of ice	The magnitude of heat transfer is too small to cause scaling damage

There are other proposed reasons for salt scaling but none of these can adequately explain characteristics of salt scaling. The most recent proposed mechanism account for salt scaling is the glue spall mechanism which is originally a glass surface decoration technique (Figure. 5) [34-36].

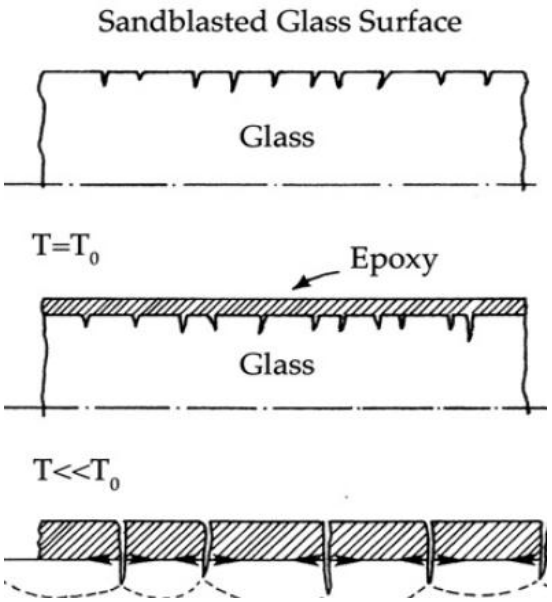

Figure 5. Glue spall technique [34]

For sand-blasted glass, a thin layer of epoxy can be spread over the surface of the glass at high temperature to make the surface smooth. And, when it cools down, the plasticized epoxy tends to solidify and contract more drastically comparing with the glass. Therefore, tensile stress will tear thin parts off from the brittle materials and propagate to flaws in an area. This phenomenon is very similar to salt scaling which is a progressive aggressive damage that starting with small thin piece of materials removed from the concrete surface. Some concluded that this mechanism adequately account for the salt

scaling because that, once the temperature is below the melting point of the saline solution, the ice formed on concrete surface contracts much faster than surface paste [37-38]. However, if it is the ice damaging the concrete surface with fracture caused by different contraction rate, pure water can at least do some damage since the ice contracts at different rate comparing with concrete which is contradicting with previous findings.

Even the mechanism of salt scaling damage has not thoroughly explained by scientists, factors affecting scaling damage were well studied. Water to cement ratio (designated as w/c), cement content, air-entrainment, freezing temperature, surface finishing treatment and the incorporation of supplementary cementitious materials (designated as SCMs) into ordinary Portland cement concrete were found having influences on the salt scaling resistance.

2.2.3 Factors affecting salt scaling

The w/c governs the properties of concrete mixture including strength and durability. As mentioned in the beginning of this chapter, moisture is the main reason for frost damage in concrete, so more water in pores makes the concrete vulnerable. It is important to control the w/c ratio to build a strong surface with fewer pores left by evaporated bleeding water to resist scaling damage.

Cement content is important for scaling resistance because, for a workable mixture, higher cement content means stronger concrete mixture and a strong surface absolutely reduces the scaling damage.

An adequate air system benefits the concrete durability including scaling resistance [24-28, 39]. Studies explain the possible two beneficial mechanisms: (1) AEA reduces bleeding which consequently lead to less segregation which makes the top surface stronger; (2) More voids below the surface will be provided so that the ice formed in these voids will damage surrounding aggregate and paste matrix below the surface.

Bleeding is important because it affects the w/c ratio, the most important factor of concrete design. The density variations from bleeding can be a reason that a weak surface presented during freezing and thawing environment. AEA reduces bleeding and, therefore, less segregation to minimize the effect of density variations. The stabilized air bubbles tend to adhere to paste materials and increase the average specific surface area. Deleterious effects of bleeding could also happen, if the concrete body dilates following nucleation of ice.

The next important factor is temperature. Several studies have investigated how the minimum temperature of in freezing cycle of scaling test can affect the amount of damage [17-18, 40]. A general conclusion has been reached that, if the minimum temperature in freezing cycle increases, the damage will be reduced in same condition. When the minimum temperature is hold above -10 ℃, there is no damage found. Moreover, it has been discovered that longer time at or below -10 ℃ causes more damage.

Surface treatment with specific chemical compounds will increase the strength of surface materials to improve scaling resistance. Figure 6 summarizes the effects of some of these factors on performance of concrete surface in standard test environment [41]. Air-

entrainment and a surface finishing treatment improve the scaling resistance as discussed earlier. The curing condition can be complicated and, in this study, air cured concrete is more vulnerable to scaling which makes sense because of poor cement hydration.

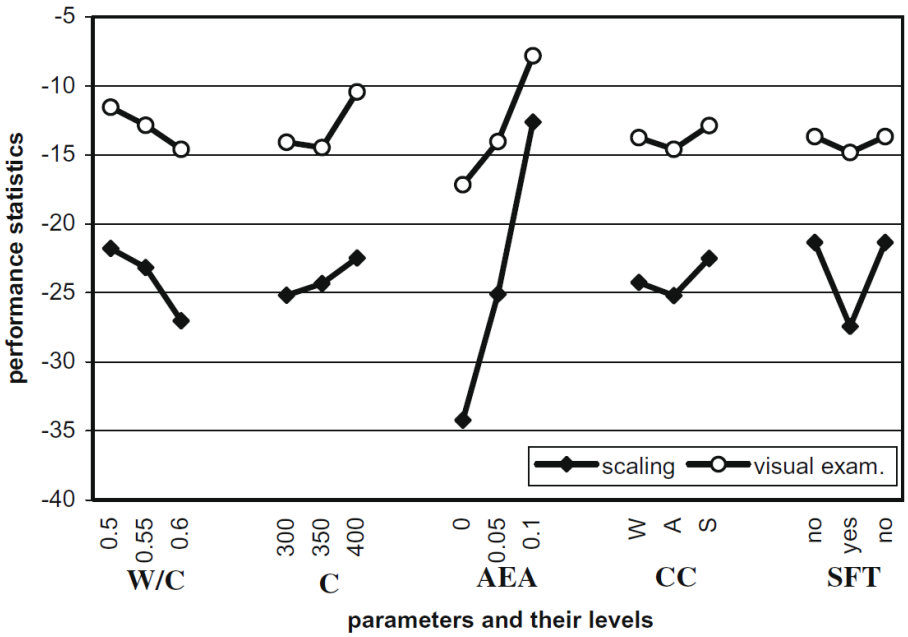

Figure 6. Effect of w/c, cement content (C), air-entrainment (AEA), curing conditions (CC) and surface finishing treatment (SFT) on scaling resistance [41]

Salt scaling resistance of concrete incorporating SCMs is a controversial topic. In Iowa, public agencies require at least 20% amount of SCM addition to concrete. Although SCMs incorporated concrete was not included in experimental work of this study, it is necessary to study this topic since Season I was designed for Iowa. Some claimed the mechanical properties and durability of SCMs incorporated concrete is generally better or at least comparable to ordinary Portland cement concrete (designated as OPC). But, studies

show that salt scaling resistance of concrete with fly ash or slag addition is poor [19, 42-43].

Table 2. Cumulative scaling residue and visual scaling rating of specimens exposed for 28 days (lab) and 180 days (natural exposure) [44]

	Cumulative scaling residue (kg/m^2)	
Mixtures	28 d	180 d
Control (V1)	2.60 (4)	0.29 (0)
35% FA (V2)	3.91 (5)	0.74 (3)
35% slag (V3)	1.25 (4)	0.25 (3)
25% FA (V4)	2.93 (4)	1.24 (3)
25% slag (V5)	0.75 (3)	0.26 (2)
TBC–FA (V6)	3.05 (5)	3.70 (5)
TBC–Sg (V7)	2.18 (5)	1.22 (3)

*Values in parentheses are the visual ratings.

Table 2 is a summary of a comprehensive study on salt scaling resistance of seven mixes (designated as V1 to V7) incorporated different percentage of fly ash (Class F), slag or ternary blends of fly ash and slag into the OPC [44]. The results show that, for lab testing environment, effects of SCMs addition did not drastically lower the salt scaling resistance of the slab specimens. Only three out of six mixes with high percentage SCMs replacement of cement exhibit more scaling damage. Salt scaling resistance of other three mixes with 35% of slag, 25% fly ash and 25% slag is actually superior or at least equivalent to control group which has no SCMs addition. However, in natural exposure to winter weather, the performance of SCMs incorporated concrete is much worse comparing with OPC. One explanation to this finding is that some found the standardized lab testing

environment is more severe than that occurring in the field [45-46]. Another research found that there was a thicker layer of porous top materials of concrete when SCMs were included [9].

Table 3. Effects of curing methods on scaling resistance with addition of high percentage of fly ash and slag [47]

Salt scaling resistance ranking of three different curing methods.

	25% fly ash	35% slag	Plain concrete
ASTM C 672	3	1	2
Presaturation 14-day curing	3	1	2
Presaturation curing compound	3	2	1
Presaturation 3-day curing	3	2	1

Note: 1 indicates the highest salt scaling resistance, 3 the lowest.

Table 3 summarizes another study which has found that the effects of different curing methods on salt scaling resistance with high percentage of fly ash and slag addition [47]. Presaturation in lime-water or with a curing compound was implemented for different periods of time to study the effects of curing. The conclusion has been made that, in same curing conditions, 25% fly ash addition always leads to most severe damage; the 35% slag addition shows less scaling damage when specimens were cured by following standard or presaturated for 14 days. However, presaturation in curing compound or a short presaturation in lime-water does not improve the scaling resistance of 35% slag incorporated concrete. It is interesting to find the opposite behavior of OPC (plain concrete in the Table) and slag included mixes. A problem associated with this study is that only

two slab specimen of each set were tested and the data is not consistent in terms of the mass loss per unit area.

Sometimes, the constituents of SCMs can determine the salt scaling resistance of concrete. One study used three types of fly ash with different siliceous contents (48, 50 and 53 weight percent) in different mixes and found the fly ash with higher siliceous content lowers the scaling resistance of concrete [48].

Silica fume is another common SCM used in concrete industry. Since it is an expensive material, studies on scaling resistance of silica fume incorporated concrete tend to focus on lower percentage of addition. Figure 7 shows the visual scaling ratings of specimen cured by different methods with addition of 5% and 10% silica fume [49]. It has been confirmed in this study that concrete containing less than 10% condensed silica fume still has a fair resistance to salt scaling. But, the most important factor that governing is the air void spacing factor. According to this study, the air void spacing factor must been at least 300 μm to satisfied the requirement of an adequate air system to guarantee a "reliable quality".

With the finding of these works, it can be figured out that the interrelationship between concrete workability that SCMs modified and air system of concrete actually determines the salt scaling resistance of SCMs incorporated concrete. It makes sense since the strength of surface material is affected by its porosity. Good workability of fresh concrete and well-distributed air system of hardened concrete is going to reduce the thickness of the porous layer aforementioned and increase the strength of surface material.

Phase composition observation of concrete surface by XRD technique in a study using slag rich cement concrete has verified that the air-entrainment improved resistance to deicer scaling [50]. The micro-fiber addition used in this work also benefited surface scaling resistance.

2.2.4 Summary of salt scaling

Salt scaling is a progressive superficial damage on concrete surface. Small pieces of paste materials are removed and some aggregates are exposed to environment. Salt scaling is resulted from deicing salt solution pooled on concrete surface in freezing and thawing conditions. Susceptibility to salt scaling is not related to theories of frost damage. Glue spall theory is sufficient to explain the mechanism and characteristics of salt scaling.

The factors affecting salt scaling include w/c, cement content, air-entrainment, minimum freezing temperature, surface finishing treatment, curing conditions and substitution of SCMs. Besides the influences on concrete performance of w/c, cement content and curing conditions, it should be noted that air entrainment improves the scaling resistance. No damage occurs when the minimum freezing temperature is above -10 ℃ and the most damage occurs when the concentration of salt solution is around 3%.

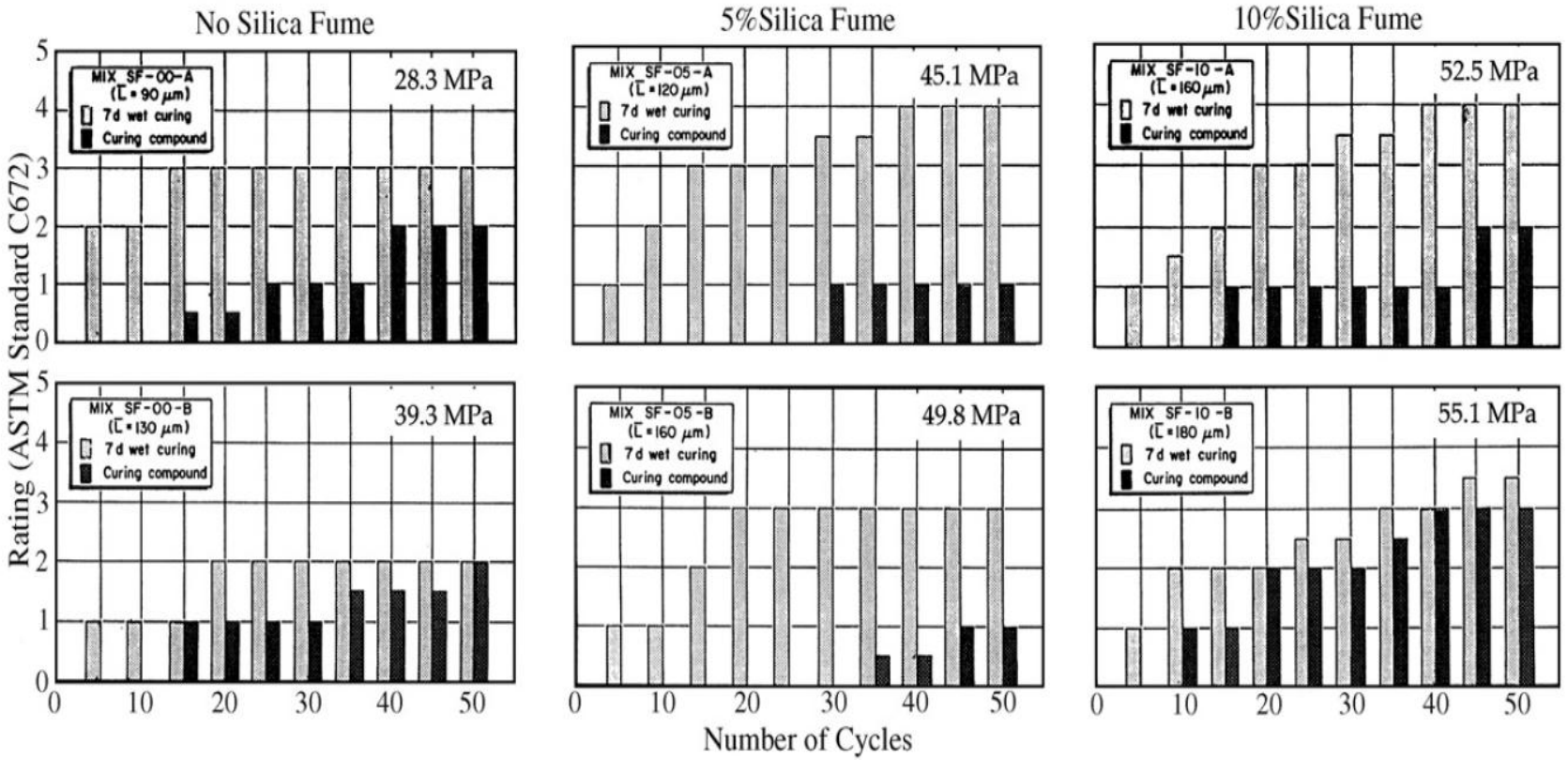

Figure 7. Scaling rates of silica fume addition concrete [49]

2.3 Effects of Salt Application on Skid Resistance

Skid resistance is a frictional property of test surface indicating the surface friction when abrasion occurs. Traditionally, the skid resistance is difficult to study in the past because of the equipment and weather [51-52]. After the development of portable skid resistance test which is called British Pendulum Tester, it is common for civil engineers to conduct test on wet roads to evaluate if the pavement is slippery. Although a lab test standard has been provided, it is still more common to see field tests to measure surface friction on locations where salt was presented.

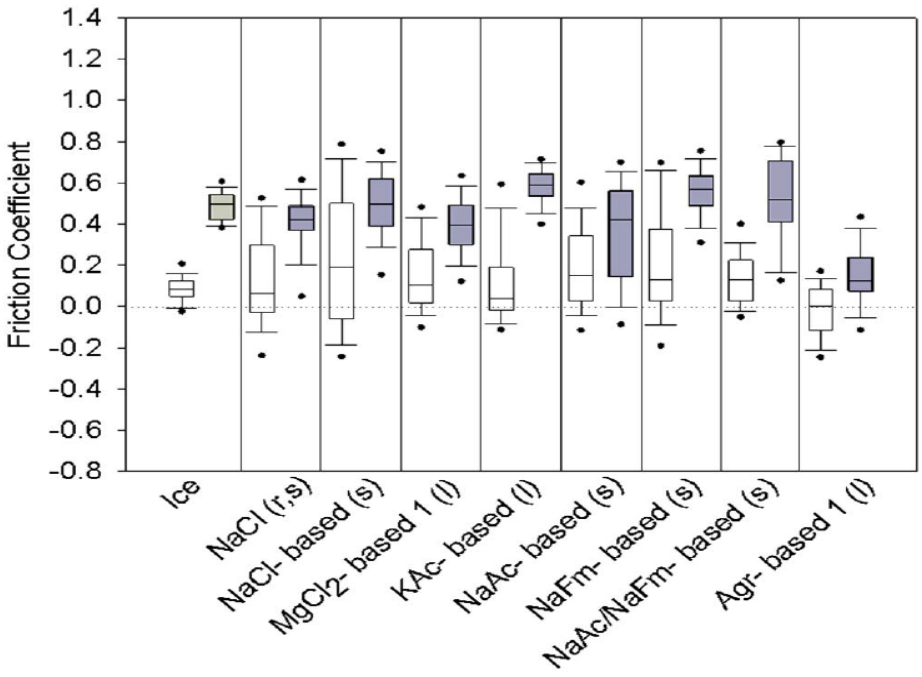

Figure 8. Tribometer data with friction coefficient of various deicers on ice and deiced surfaces [53]

The current practice of testing the impact of salt application on pavement surface is to measure the friction coefficient of deiced concrete surface by attaching a friction wheel to the back of a vehicle [53]. However, it is not applicable in the lab to analyze various effects of various deicers on surface friction. Therefore, they used a novel method to measure the friction of coefficients by using tribometer. Specific amount of water was allowed to freeze on the sample surface and deicers were applied to sit on the surface. Then, the friction coefficient was quantified by tribometer to indicate slippage of concrete surface.

In this particular study, three different types of agro-based deicers with high concentrations of either $MgCl_2$ or $CaCl_2$ were evaluated in terms of surface friction and these deicers led to the lowest friction on both the ice and deiced concrete surface as shown in Figure 8. Nonetheless, the viscosity of agro-based deicers was not described.

2.4 Effect of Deicers on Concrete Permeability

In concrete, the role of water in concrete can be complex. It is not only a required component for cement hydration but also an agent required to transport elements from place to place in concrete. As long as the water evaporates, the pores that were saturated are left empty and it makes concrete which is a porous material vulnerable to deterioration. Among all the parameters, the permeability of hardened concrete is the most important because the migration, dilution and leaching of minerals with excess water form localized stresses, varying with depth. This type of stress causes failures in

weak region of the concrete. Thus, there will be a strength loss and degradation of concrete mechanical properties [7, 13].

Because of the complexity of pore structure of concrete, it is extremely difficult to directly correlate pore structure and its distribution with permeability. Some measure the amount of pressured water passing through concrete disk to in a given time to calculate the hydraulic conductivity as an indicator of concrete permeability. However, the value of this hydraulic conductivity varies along the depth of concrete because the random distribution of voids. It is hard to guarantee the pore system is homogeneously distributed especially in the field when large quantity of materials is used. Therefore, in order to have a good understanding of permeability to control the quality of concrete, many indirect permeability measurements are used. These measurements imply the permeability of concrete because extensive research work established the correlation between the test measurements and permeability of concrete by modeling. In lab tests, water absorption, air permeability and electric resistivity are normally measured as indirect permeability indicators. All these three methods were employed in this study and the mechanisms were discussed in test methods part.

The effect of deicing salts on concrete permeability is limited because that the concrete permeability is determined by its pore structure. The deicer penetrates into concrete at various depths and may react with cementitious materials to modify pore structure. Also, salt application definitely will increase the water ingress due to surface cracking and scaling damages. But, no research has discovered any influence of

agriculture-based deicers on concrete permeability. It has been proposed by the deicer developer of Season I that the solution containing organic compound could penetrate into the concrete and seal the pore system to reduce the permeability to avoid water-related degradation.

The fundamental pore structure change could be observed by electron microscope and it may reveal if Season I has the sealing effect.

2.5 Summary of Literature Review

Previous studies show the damaging effect of exposure to frost-salt conditions. The experimental work follows was designed to provide quantitative analysis on physical degradation including mass loss, strength loss and scaling due to frost-salt attack. Also, to further expand previous research, the skid resistance and permeability change after application of three deicers (NaCl, $CaCl_2$ and Season I) were examined. Lastly, the EDS analysis was conducted to study the relationship between deicer penetration depth and the micro-cracking.

CHAPTER 3

EXPERIMENTAL WORK

3.1 Scope

In this study, experimental work was designed to analyze:

- Frost damage of Season I to pavement concrete,
- Effects of Season I on surface skid resistance,
- Effect of Season I on concrete permeability.

Frost damage of Season I to new concrete was assessed on mortar cubes and concrete slabs in terms of weight loss, strength loss and scaling rating.

The impact of Season I on surface friction of concrete slab was analyzed by using British pendulum tester. Standard test was conducted on surface of sand-blasted glass and concrete slab surface.

The effect of Season I on permeability was evaluated by using three indirect permeability indicators - air permeability index, water absorption rate (both initial and secondary), and electric resistivity of concrete surface. The specimens were moist cured for 14 days then immersed in deicing solutions for another 14 days. The compressive strength of differently cured specimen was also tested.

Same evaluations regarding 3% NaCl and 4% $CaCl_2$ solutions were also conducted to compare with the results of Season I. EDS point analysis was used to measure the penetration depth of deicers.

3.2 Materials

3.2.1 Concrete materials

The cement used in all concrete mixtures in this study was Type I/II hydraulic cement from Ash Grove Company. The coarse aggregate used was 1-inch nominal maximum aggregate size (NMAS) limestone from a local quarry. The fine aggregate used was local siliceous river sand which had fineness modulus of 3.05. The AEA 92 air entraining agent produced by Euclid Chemical was used.

3.2.2 Deicers

All liquid deicers (Season I, 3% NaCl solution, and 4% $CaCl_2$ solution) were either obtained from the manufacturers or prepared by deionized water and deicing salts. Season I was still in development and not on the commercial market yet. It is a brownish viscous liquid containing complex sugars and acetates.

The detailed composition of Season I was not provided by deicer developer due to patent considerations. Deionized water was employed as the control group. In case of concentration of deicing chemical solutions varies due to crystallization of chemicals at

lower temperature in winter, all the solutions were well-stirred before application. Five gallons of each deicer were used for this study.

3.3 Specimen Preparation

Six types of specimen were prepared for experiments:

1) 2-in^3 mortar cubes,

2) 4-in by 8-in concrete cylinders,

3) 4-in by 1-in concrete disks,

4) 4-in by 2-in concrete disks,

5) 10-in by 10-in by 5-in concrete slabs

6) 2-in by 1.5-in cylindrical half

The mortar cubes and the concrete slabs were used to assess the physical damages (cubes for mass loss and strength loss, slabs for surface scaling) caused by deicers to new concrete in freezing/thawing conditions. The cylinders and disks were used to study effect of deicers on concrete permeability and strength. The cylindrical halves were used in EDS analysis.

3.3.1 Mortar cubes and concrete slabs

In this research work, Twenty-four 2-in^3 mortar cubes (cube hereafter) were prepared in accordance with ASTM C109, "Standard Test Method for Compressive Strength of Hydraulic Cement Mortars". The cement to sand ratio is 1 to 2.75 and the

w/c is 0.485 (See Appendix A for batch quantities). The cubes were demolded after 24 hours and moist cured for additional 13 days then placed in an environmental chamber where the relative humidity was 50% for another 14 days.

To evaluate the scaling defects on concrete surface, 10-in by 10-in by 5-in concrete slabs (slab hereafter) were prepared. These slabs are from two similar mixes with 0.45 w/c ratio and 3.0~3.5 inch slump. The air contents of the two mixes are 5.0% and 5.5%. The mix designs and fresh concrete properties can be found in Appendix A. The curing method of the slabs is exactly the same to the curing method of cubes.

3.3.2 Concrete cylinders and disks

Twenty-four 4-in (diameter) by 8-in (height) cylinders (cylinder hereafter) were cast and cured following ASTM C192, "Standard Practice for Making and Curing Concrete Test Specimens in the Laboratory". The w/c ratio of the concrete mixtures of cylinders was 0.45 and the slump measured was 1.5 inch. The mix design and fresh concrete properties can be found in Appendix A. All the cylinders were moist cured for 14 days, and then 6 cylinders were immersed in each of three deicers. The remaining 6 cylinders were cured in 100% moisture for 28 days. The cylinders were used in electrical resistivity test and compressive strength test.

Figure 9. 2-in circular disks for water absorption test

Concrete disks of 1-in height (1-in. disk hereafter) and 2-in height (2-in. disk hereafter) were cut from cylinders after curing process (Figure 9). Sixteen 1-in disks were preconditioned at 50 ℃ for 7 days and used in air permeability test. Eight 2-in disks were preconditioned at 50 ℃ and 80% relative humidity for 3 days. These disks were sealed and stored at room temperature for another 15 days before being used in water absorption test.

3.3.3 Specimen for EDS analysis

Two 2-in long with 1.5-in diameter cylinders were cored from slabs 20 days after completion of scaling test. Each of these cylinders was split into halves along the centerline and one of the halves was scanned by SEM. Figure 10 shows the cross section of the one specimen used in this study.

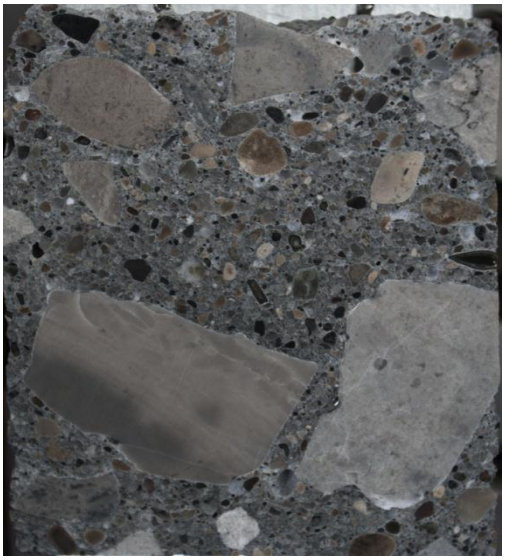

Figure 10. Specimen for EDS Analysis

3.4 Test Methods

As mentioned in the scope of experimental work, five most important tests and EDS analysis were performed. Table 4 summarizes the standards of test methods employed in this research and briefly explains the significance of each work. The compression tester used for compression test is shown in Figure 11 and the freezing chamber provided freezing and thawing condition is shown in Figure 12.

Table 4. Summary of Test Methods

Experiment	Standard	Significance/Measurement
Structural Degradation	SHRP H205.8 [54]	Mass loss and compressive strength after freezing/thawing cycles
Surface Scaling	ASTM C672/SHRP H205.9 [54-56]	Rate surface scaling level visually or by mass loss
Skid Resistance	ASTM E303/SHRP H205.10 [54, 57]	Surface friction
Electric Resistivity	FM-5-578 [58]	Electric resistivity of concrete surface
Water Absorption	ASTM C1585 [59]	The initial and secondary water absorption rate of concrete
Air/Gas Permeability	Durability Index Testing South African Method [60]	The air/gas permeability of concrete sample
EDS analysis on SEM	N/A	Examine penetration depth of deicer and assess micro-cracking

Figure 11. Compression tester

Figure 12. Freezing chamber

3.4.1 Structural degradation test

The structural degradation test was conducted following section H-205.8 in SHRP manual [54]. This test method evaluates the damage of deicers on the structural integrity of cubes under freezing/thawing condition. Before the freezing and thawing cycling, eight cubes were tested for compressive strengths for the purpose of evaluating strength loss.

Each specimen was labeled and the initial weight was measured to calculate density. Cubes must be presoaked in deionized water for at least 24 hours before being placed in test cell. Test cell used in this study were prepared with a container and sponges at the bottom as shown in Figure 13.

Figure 13. Structural degradation test cell

310 ml solution of deicer was poured into the test cell and the test cell was capped before being placed in freezer. It was important to make sure cubes in test cell were not in contact with each other and the walls of cell. Cubes must be touching with the sponge at the bottom to avoid the ponding of solution on cube surface. The cubes

freeze at 0 °±5 °F (17.8 °±2.3 °C) for 16 to 18 hours and thaw at room temperature 73 °±3 °F for 6 to 8 hours. The mass loss after 5 and 10 cycles were measured. Also, after 10 cycles, the largest intact part of each cube was dried and tested for compressive strength.

3.4.2 Salt scaling test

Salt scaling was examined in accordance with SHRP Manual and ASTM C672 [54-56]. Visual scaling rate and rating based on mass loss per unit surface area on horizontal concrete surfaces in freezing and thawing environment were given.

Slab with 9-in by 9-in ponding area was created by forming concrete dikes at the periphery as shown in Figure 14.

Figure 14. Concrete slab for salt scaling evaluation

The horizontal ponding area on the top of the slab was covered by 200 mL deicer. Each slab was covered with a secured polyethylene sheet to inhibit evaporation of water

and to prevent spilling before getting placed in freezing chamber. Scaling damage was evaluated at every 5 cycles in accordance with visual rating criteria and mass loss per unit area listed in Table 5. The polyethylene was removed and the deicer on the ponding area was carefully poured out. The loose materials were washed into the #200 sieve with a filter paper. Each filter paper was dried in the oven and the materials were weighed on a balance to nearest 0.1 gram. Photos to be used in visual examination of scaling surfaces were also taken after washing.

Table 5. Visual examination and unit mass loss evaluation criteria for scaling [55-56]

Rating	Surface Condition for Visual Examination	Equivalent Mass Loss in Unit Area, g/m^2
0	No scaling	0-50
1	Very slight scaling (1/8 in., 3.2 mm) depth, max., no coarse aggregate visible	51-210
2	Slight to moderate scaling	211-500
3	Moderate scaling (some coarse aggregate visible)	501-1300
4	Moderate to severe scaling	1301-2100
5	Severe Scaling (coarse aggregate visible over entire surface	>2100

3.4.2 Skid resistance test

The skid resistance test is included in section H-205.10 in SHRP Manual and ASTM E303, "Standard Test Method for Measuring Surface Frictional Properties Using the British Pendulum Tester", is the ASTM version of the test method [54, 57]. The British Pendulum Tester is a dynamic pendulum "impact-type" tester used to measure the energy loss when the rubber slider edge is propelled over the test surface. It can be used in field or laboratory to measure the frictional characteristics of pavement surface. This tester was originally developed in England back in 50s. Figure 15 shows the standard British pendulum tester.

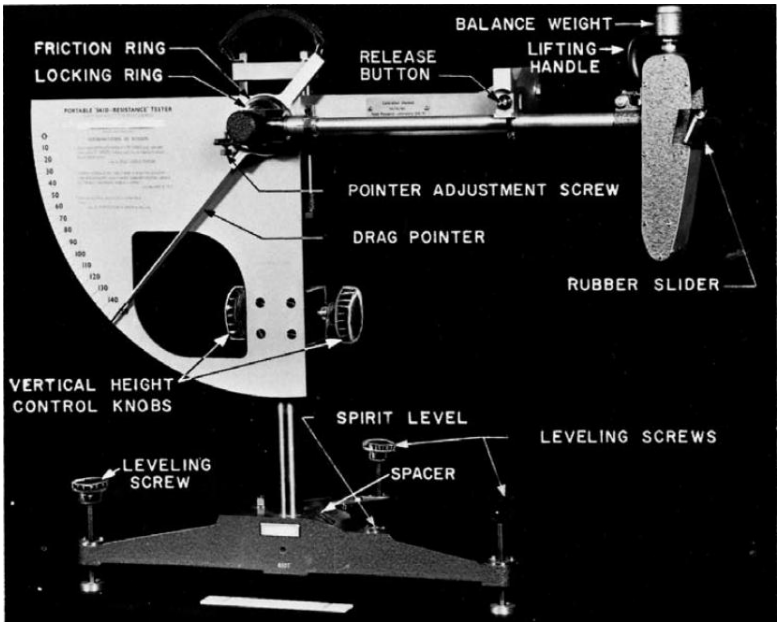

Figure 15. British Pendulum Tester [57]

The pendulum tester must be calibrated before each test because the starting point which represents the zero energy loss guarantees the quality of test results. Another

important adjustment is the slide length. Since the rubber slide is going to propel over the rough surface to reach its final position, the contacting length or area between the slider and the surface is critical. It is required to have a length of contact path between 4-7/8 and 5-inch (124 and 127 mm).

(a) Concrete slab

(b) Sand-blasted glass

Figure 16. Concrete slab and sand-blasted glass

The surface frictional properties of two different testing surfaces including concrete pavement and sand-blasted glass were measured after the application of deicers as shown in Figure 16. Once the pendulum tester had been set, deicer was applied to cover the test surface. The top layer of the test area was saturated by pre-wash. Tests were conducted on sand-blasted glass and concrete slab. The sand-blasted glass was used because that glass textures gave consistent results when different types of deicers were applied.

To obtain reliable indication of the surface friction, more than five swings were needed and each swing gave a reading. The reading was named BPN which was for British Pendulum Number. Higher BPN value accounted for rougher surface. The variations between readings could not be more than 1 as shown in Figure 17; otherwise, the results are not acceptable.

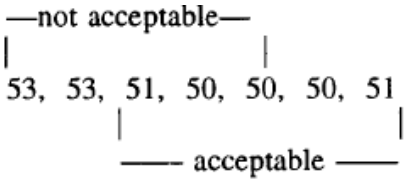

Figure 17. Acceptance level of test results [57]

Individual BPN value and temperature of the test surface was also reported with type, age, texture and location of test surface. An average value of five readings was used as the final result.

3.4.4 Electrical resistivity

The electrical resistivity test is a non-destructive test method measuring the electrical resistivity of saturated concrete. The electrical resistivity of water –saturated concrete is being increasingly used to indirectly evaluate concrete characteristics such as chloride ion diffusivity, permeability and properties of the pore water solution. By measuring the potential drop between the electrodes when a current is circulated, the electrical resistivity implies the distribution of pores since the resistivity of paste and saturated pores are different. With more saturated pores in give distance, it is more likely to have chemicals dissolved in the pore solution which could cause deterioration.

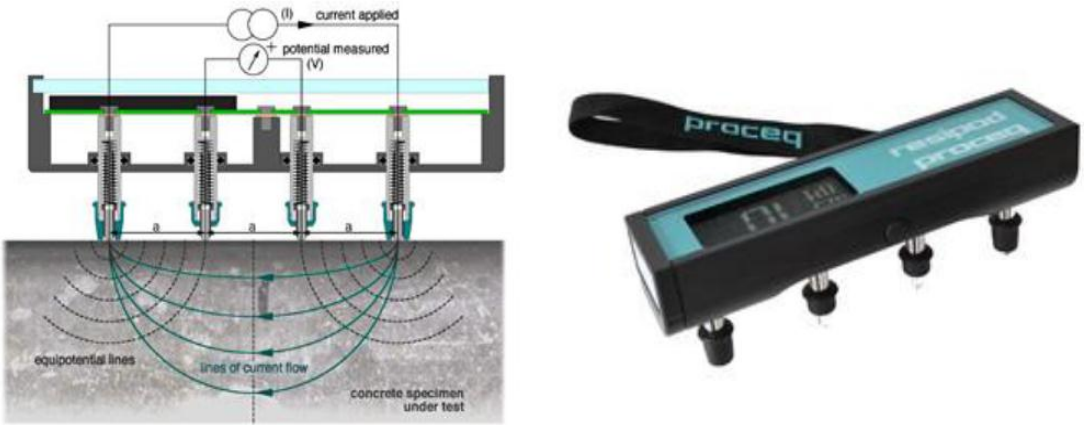

Figure 18. Wenner four-probe array [58]

The equipment used in this test is called Wenner linear four-probe array shown in Figure 18. This meter used a probe with four terminals set up in a linear array with a distance between points of array. The two outer points are the current insertion and removal points, whereas the two middle points are the measurement points of potential drop. Wenner array probe was placed along the longitudinal directions of cylinder and 8

readings were recorded in directions of 90 ° next to each other. Table 6 explains the correlation between surface electrical resistivity and chloride ion permeability. A low surface electrical resistivity indicates the specimen is the permeability of concrete is high.

Table 6. Surface Electrical Resistivity versus Chloride Ion Permeability [58]

Chloride Ion Permeability	RCP Test Charged Passed (coulombs)	Surface Resistivity Test 28 day test kΩ–cm
High	> 4,000	< 12
Moderate	2,000-4,000	12 - 21
Low	1,000-2,000	21 - 37
Very Low	100-1,000	37 - 254
Negligible	< 100	> 254

3.4.5 Water absorption rate

The water absorption rate was in accordance with ASTM C 1585, "Standard Test Method for Measurement of Rate of Absorption of Water by Hydraulic-Cement Concretes" [59]. This method was used to determine the water absorption rate (sorptivity) of unsaturated concrete.

2-in disks cut from cylinders were cured and conditioned at 50 ℃ in the oven to eliminate the moisture content. A completely unsaturated pore system of concrete is the fundamental hypothesis of this test method. Initial mass of each disk was measured and the disks were sealed with only bottom surface exposed to water to protect moisture ingress from ambient conditions through sides. The specimen was then place in water and the specimen should be supported to avoid touching the bottom of test cell to allow sufficient contact area.

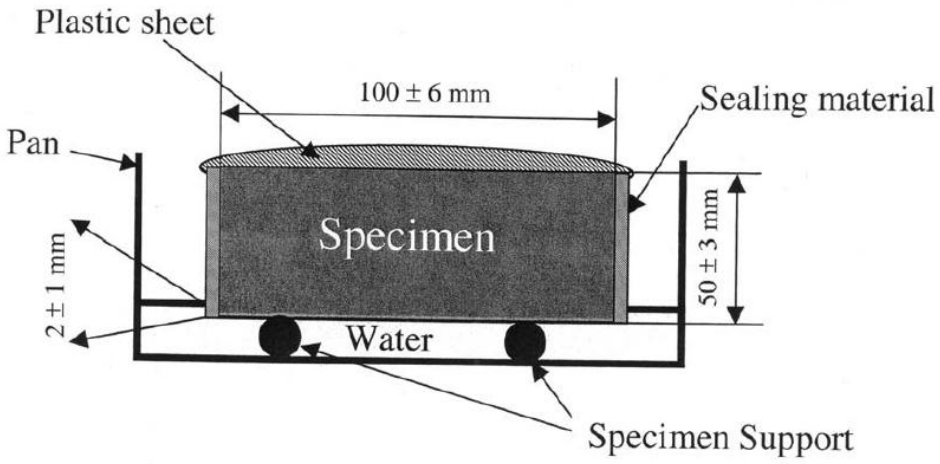

Figure 19. Water absorption test schematic [59]

Figure 19 shows the test set up described above. The water absorption rate was calculated by measuring mass change following equation below. Sample calculation is included in ASTM C1585. The linear regression analysis of the plot of I versus square root of time was used to obtain the slope of the best fitted line which is the value of water absorption rate of each specimen.

$$I = \frac{m_t}{a \times d}$$

Where:

I = absorption
m_t = change in specimen mass in grams, at the time t,
a = exposed area of specimen
d = density of the water

The assumption is the amount of water ingress is completely equal to the mass change of the specimen and the ingress depth is absorption. The water ingress of unsaturated concrete was dominated by capillary suction, so the water absorption rate

implies concrete permeability. It should be noted the mass measurement in given time can be unreliable due to short time period like 15 seconds. The removal of surface adherent water could also result in unreliable measurement.

3.4.6 Air permeability index

The air permeability index of each test specimen was calculated by using the coefficient of permeability, k. The coefficient of permeability was the slope of the simple linear regression model regarding the pressure change of an enclosed pressure chamber with one side covered by the 1-in concrete disk as shown in Figure 20 [60]. By recording pressure change in a given period of time, the rate of air passing through concrete was realized. Four specimens from same mixture were tested and each had an air permeability index value because of the differences of the diameter and thickness. The average value of four specimens represents the air permeability of a specific concrete.

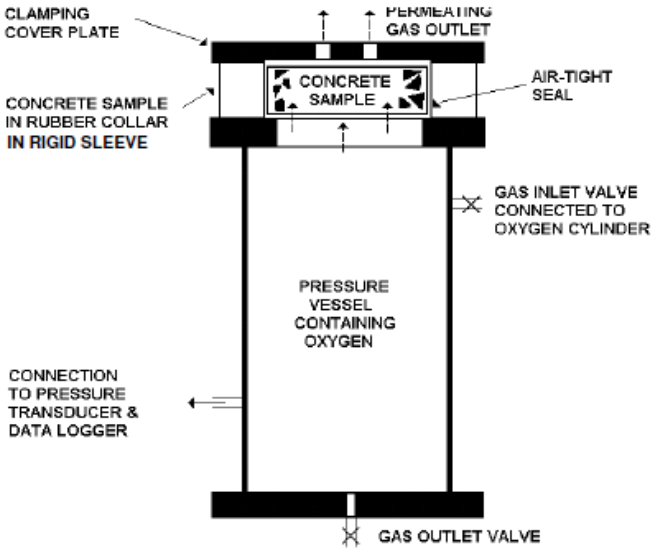

Figure 20. Air permeability test apparatus [60]

Before the test, the dimension of the concrete disk was measured and these disks were conditioned at 50 ℃ to eliminate the moisture content. High temperature conditioning must be avoided because the expansion of pores and other pore structure modification induced by drastic temperature change lead to unreliable results. Once cooled, 1-in disk was sealed in compressible collar within rigid sleeve before getting placed on top of the enclosed pressure chamber. An initial pressure was set at 15 MPa and the pressure changes were recorded by the sensors after the opening of valves.

The air permeability index was calculated by using linear regression model of pressure change against test time. The Darcy's coefficient of permeability equation had been used. It is important to know that, sometimes, the coefficient of correlation in linear regression model is less than 0.99 which is conflicting with the standard. It is acceptable since the meaning of this value has not been proved to be directly related to the quality of test results.

3.4.7 SEM imaging and EDS

A scanning electron microscope (SEM) is a type of electron microscope that generates images of scanned object with a beam of electrons. The signals produced by scattering electrons can be detected and the information about topography or composition of the scanned surface will be collected. SEM imaging is widely used in concrete material studies because it is a non-destructive technique providing views of the heterogeneous and complex microstructure of concrete. Many studies are focusing on quantify or locate micro-cracking of concrete by using SEM to observe the development of the mircostructure at various conditions like temperature or change the component of

concrete to find the influence [62-63]. In these studies, specimens taken from slabs in scaling test after 50 F/T cycles were used to perform in EDS analysis to determine the penetration depth of deicer. The schematic of a typical vacuum SEM is presented in Figure 21.

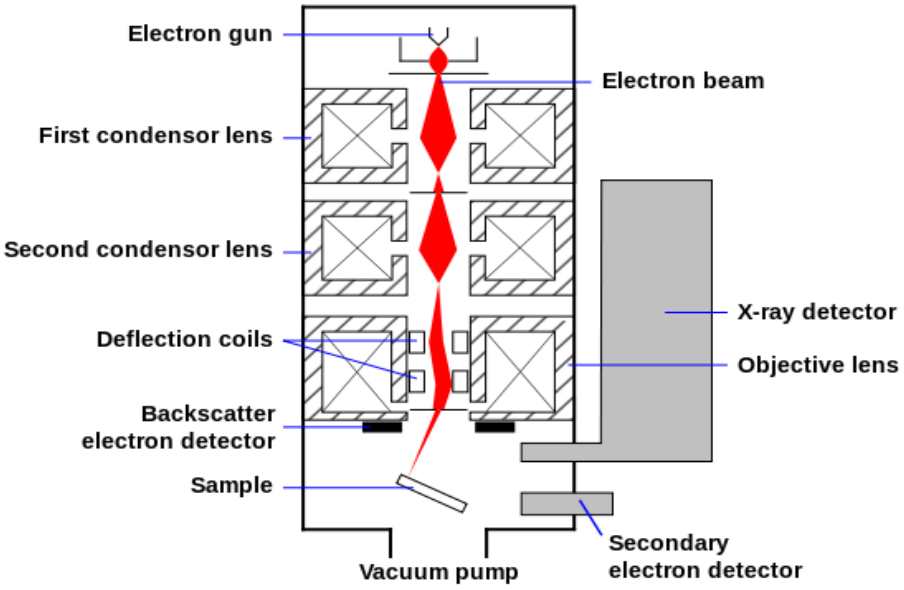

Figure 21. Schematic of SEM [61]

For this study, a Hitachi S 2460 reduced-vacuum scanning electron microscope with an accelerating voltage of 15 kV was used for imaging and EDS point analyses were obtained at 20 kV. Energy-dispersive X-ray spectroscopy (EDS or EDS) is an analytical technique used for the elemental analysis or chemical characterization of material. Each element with a unique atomic structure will reflect different peaks on EDS spectrum. As the energy of electrons of different energy is detected, EDS analysis allows the elemental composition of the specimen to be quantified. Elemental mapping was also employed to identify phase presented in the matrix.

CHAPTER 4

RESULTS, ANALYSIS, AND DISCUSSION

4.1. Physical Damage Caused by Frost-salt Attack

It is understood from literature that presence of deicers accelerates the damage by frost-salt attack because deicing chemicals penetrate into concrete with water and deteriorate concrete materials. In the following parts, physical damage due to frost-salt attack is presented in terms of mass loss, strength loss and scaling damage.

4.1.1 Structural degradation

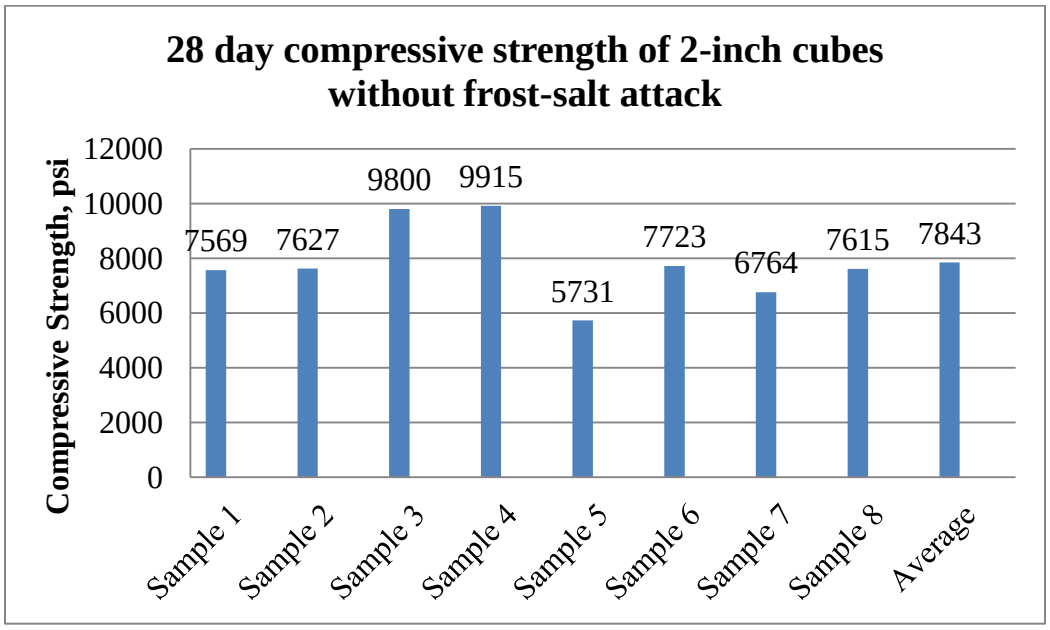

Figure 22. 28-day compressive strength of mortar cubes without frost-salt attack

Figure 22 shows the compressive strengths of eight 2-inch cubes which were tested at the age of 28-day without frost-salt attack. The average strength was 7843 psi with highest value of 9915 psi and the lowest of 5731 psi. The standard deviation of the data exceeded specified acceptable range because the highest/lowest value was 15% greater than the average strength. The reason why strength data of sample 3, 4 and 5 were questionable could be the dry curing of cubes in 50% relative humidity since it was known that dry curing hinders cement hydration.

Therefore, the value representing the average compressive strength of cubes before frost-salt exposure should be presented as 7460 $\pm$ 351 psi which accounts for the strength data of sample 1, 2, 6, 7 and 8. Strength results after 10 freezing and thawing cycles were summarized in Table 7 and presented in Figure 23. Being similar to strength data of cubes before frost-salt attack, strength data were corrected if the average value exceeded 15% more than the highest/lowest strength.

It could be seen from the summary that three groups of cubes having average compressive strength that was lower than the strength of cubes before frost-salt attack and one group of cubes was actually stronger than those without any damage. Remember all cubes from one mix which should have similar mechanical properties. This indicates Season I did not deteriorate mortar cubes in freezing and thawing cycles in comparison with other salts. The average strength of Season I group is actually a little bit higher than that of cubes without frost damage.

Table 7. Compressive strength of cubes after 10 cycles

Deicing Solution/Control	Compressive Strength, psi	Standard Deviation, psi	Average Strength, psi
Deionized Water	9253	2469	6,792 ± 2469
	7219		
	3364		
	7332		
3% NaCl solution	4028	550	3996 ± 550
	3942		
	4680		
	3335		
4% $CaCl_2$ solution	6495	1603	5275 ± 1603
	2917		
	5767		
	5921		
Season I	9537	1571	7973 ± 1571
	9077		
	6938		
	6341		

The largest strength difference occurred between cubes before and after frost-salt attack by 3% NaCl solution. The average strength of 3% NaCl group cubes was around half of average strength of cubes before frost-salt attack indicating that cubes in NaCl solution has a 50% strength reduction. The cubes of 4% $CaCl_2$ group also showed a relative large amount of damage. The average compressive strength was around 70% of average strength value of cubes before frost-salt attack meaning a 30% strength deduction. Deionized water also did damage cubes. The strength decline was roughly 10% comparing with the strength of those undamaged. The standard deviation of the strength results is large which might be caused by micro-cracking development after frost-salt attack. No microstructure observations have been made to verify this point.

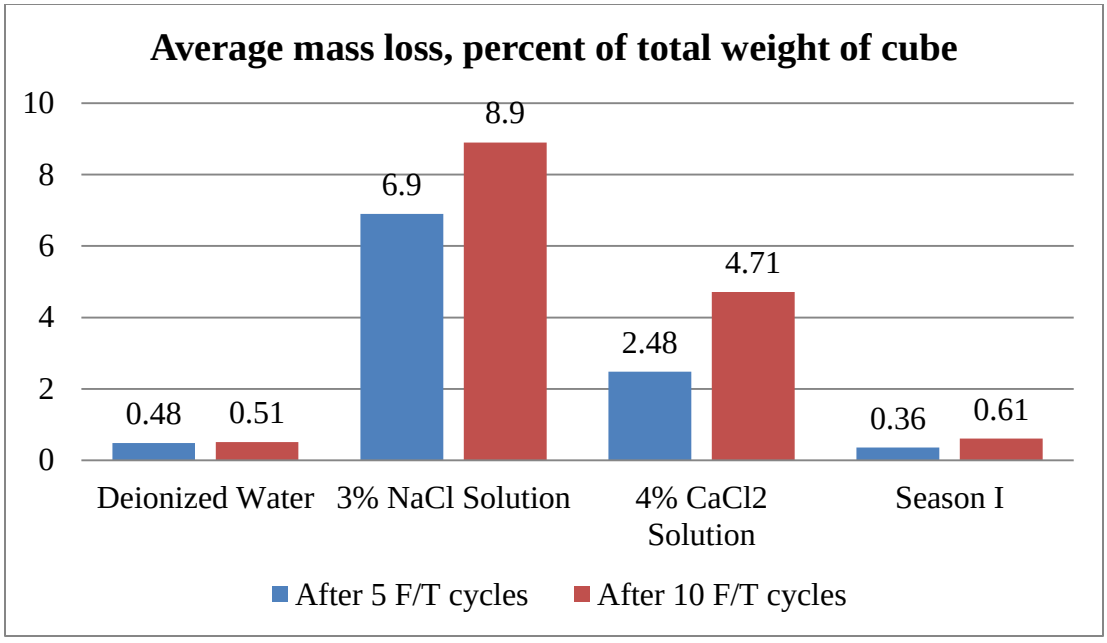

Figure 23. Average mass loss of damaged mortar cubes

Figure 24 demonstrated the average mass loss of damaged mortar cubes after 5 F/T cycles and 10 F/T cycles. According to this figure, cubes placed in the 3% NaCl solution had been damaged severely with 6.9% of weight loss after 5 cycles and 8.9% of weight loss after 10 cycles. 4% $CaCl_2$ solution also did a relatively high amount of damage on the specimen with 2.48% of weight loss after 5 cycles and 4.71% of weight loss after 10 cycles. Deionized water and the SI deicer had been done almost no damage after 10 cycles. It was important to notice the average mass loss also varies from sample to sample. Table 8 listed the deviation of mass loss data for each group after 5 and 10 cycles. It should be noticed that the mass loss of $CaCl_2$ group after 5 cycles was not very reliable since the deviation was over 50% of the average value.

Table 8. Deviation of mortar cube mass loss data

Deicing Solution/Control	Mass loss, %, percent of total weight of sample	
	After 5 Cycles	After 10 Cycles
Deionized Water	0.48 ±0.06	0.51 ±0.04
3% NaCl Solution	6.90 ±1.38	8.90 ±1.13
4% $CaCl_2$ Solution	2.48 ±1.37	4.71 ±2.07
Season I	0.36 ±0.11	0.61 ±0.14

A good correlation between the mass loss and the strength loss could be established. Table 9 shows the average mass loss versus average strength loss of each group. Besides the Season I group, a higher average mass loss indicated a higher average strength loss of cubes after frost-salt attack.

Table 9. Average mass loss versus average strength loss of deicers

Deicers/Control	Average Mass Loss, Percent of Cube Weight	Average Strength Loss, Percent of Undamaged Cubes
Deionized Water	0.51	9
4% $CaCl_2$ Solution	4.71	30
3% NaCl Solution	8.90	50
Season I	0.61	0

In spite of a direct relationship was established between average mass loss and average strength loss, there was an interesting finding that the structural integrity of cubes were harmed mainly due to the removal of surface paste materials instead of collapse of main concrete body as shown in Figure 25. No bulk piece of mortar was found loosen or disintegrated from of the most damaged cubes.

Figure 24. Cubes with surface materials removed after 10 cycles

Recall the characteristics of salt scaling in Chapter 2:

- Scaling is a progressive superficial damage without influence on concrete integrity
- Saline solution ponding is required during freezing and thawing cycles for scaling damage

It is suspicious that the structural degradation of mortar cubes was actually caused by same mechanism of scaling damage. However, scaling damage is only a problem for esthetics.

It should not influence mechanical properties (compressive strength) of concrete. A possible explanation to this is the most removed surface materials were at the corners of cubes and the cube in compression test was in relatively unstable geometrics as shown in Figure 26.

Figure 25. Unstable geometrics of damaged cube

When compression loads were applied on the cubes, such an unstable configuration of the specimen can be detrimental to strength results. Cubes with higher mass loss implying more materials removed at corners tend to break faster because of uneven loading conditions. Thus, the established correlation between the average mass loss and the average strength loss might be invalid.

4.1.2 Salt scaling

The scaling damage of 8 concrete slabs was assessed by visual examination and measuring mass loss per unit area in accordance with ASTM C672 and SHRP Manual [54-56]. Both visual rating and rating based on mass loss was given at every 5 freezing and thawing cycles until 50 cycles were completed.

Table 10. Scaling rating after 50 freezing and thawing cycles

Scaling rating after 50 freezing and thawing cycles		
Sample ID	Unit Area Mass Loss Rating	Visual Rating
Deionized water 1	0	1
Deionized water 2	0	1
3% NaCl 1	4	4
3% NaCl 2	4	4
4% $CaCl_2$ 1	3	3
4% $CaCl_2$ 2	3	4
Season I 1	0	1
Season I 2	0	1

The rating system was explained with “5” being the most severe scaling and “0” meaning no scaling. Figure 27 shows the visual difference from 0 to 5. From Table 10, it can be found that slabs in deionized water had almost no surface scaling. It is consistent with literature study that no scaling damage occurs without presence of deicing salts. The scaling damage of Season I was also negligible. Residues on surface were washed off from the slabs of Season I group and no scaling can be visually observed. It should be noted that, since the ponding area of slab surface is protected by molded concrete dikes around the periphery, loose materials from the frost damaged dikes can be washed into the sieve and measured as part of the mass loss.

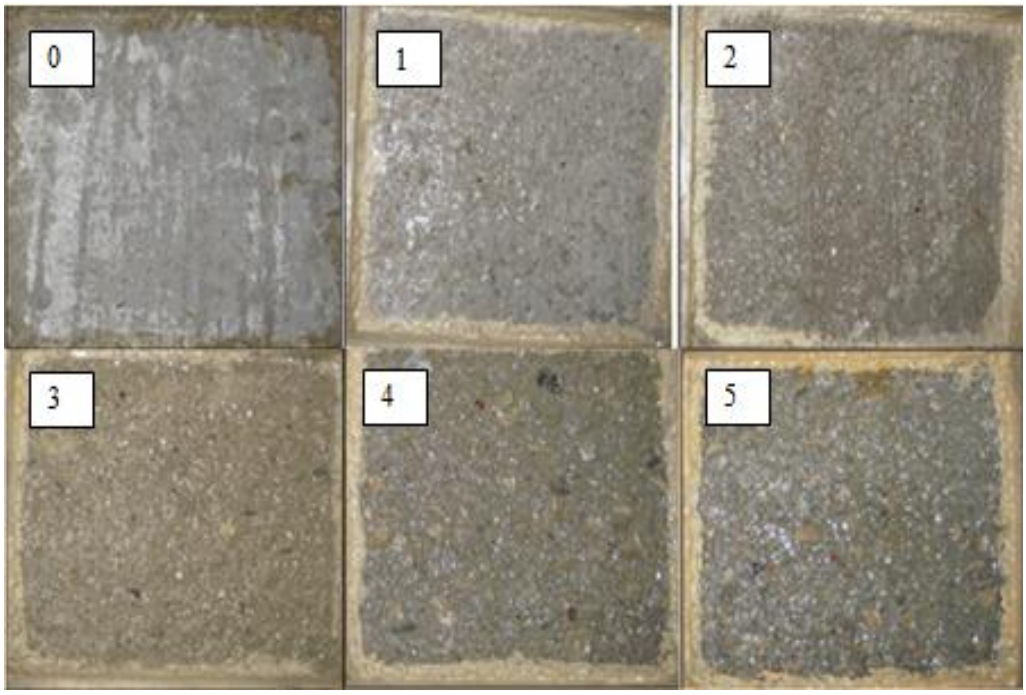

Figure 26. Scaling rating from 0 to 5

Although the amount of removed materials from the dikes is much smaller comparing with the removed superficial materials, it could contribute to an unreliable scaling rating. Remind of findings of the structural degradation test that cubes in 3% NaCl and 4% $CaCl_2$ solutions were damaged most severely. The scaling damage also followed this trend. Being slightly different from the degradation damage, scaling damage of the two groups (3% NaCl and 4% $CaCl_2$ solutions) was almost at the same level. Both 3% NaCl and 4% $CaCl_2$ solutions caused surface deterioration and the scaling rating after 50 freezing and thawing cycles was either 3 or 4 referring severe scaling. Figure 28 and Figure 29 summarized the visual rating and unit area mass loss rating, respectively, of the slabs at every 5 cycles until 50 cycles was reached.

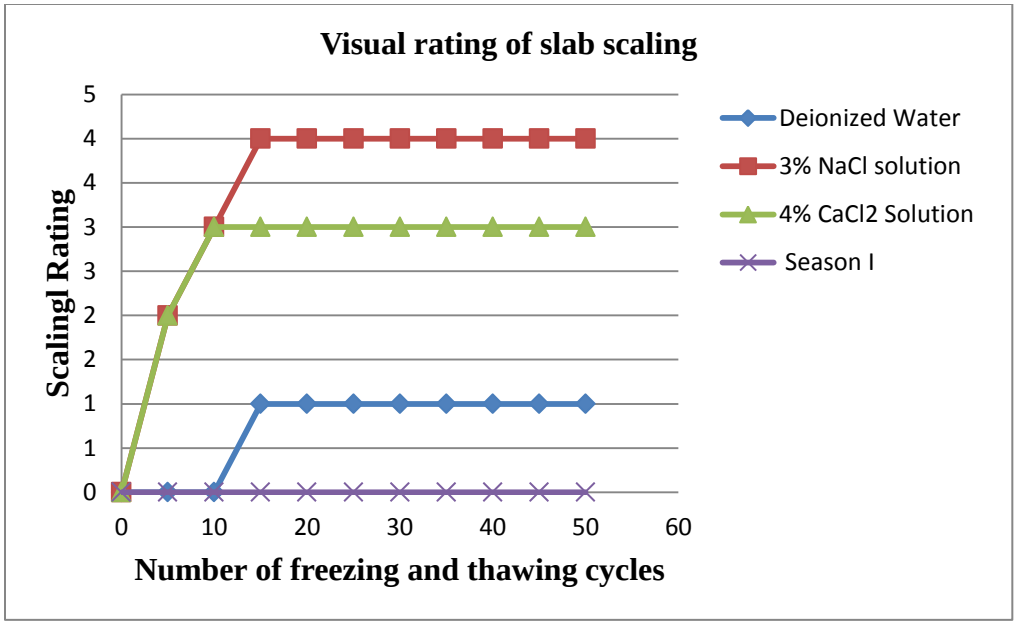

Figure 27. Visual rating of slab scaling

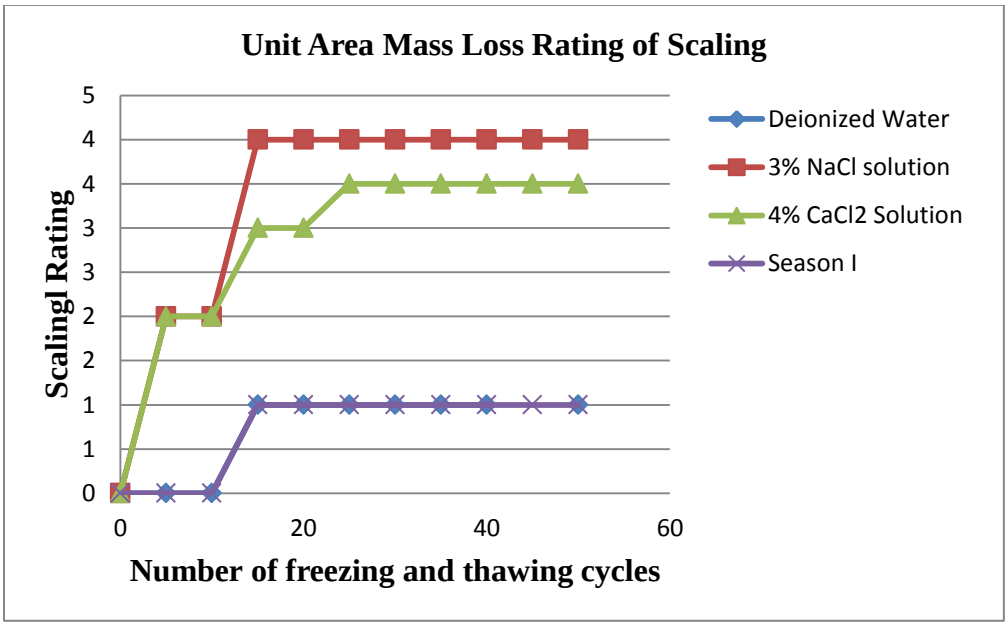

Figure 28. Unit area mass loss rating of scaling

The cumulative unit mass loss after each 5 cycles of each specimen is included in Appendix C. For both slabs and cubes in NaCl and $CaCl_2$ group, the mass loss is extremely high compared with specimen in Season I and deionized water. The same trend of mass loss in structural degradation test can be found in unit area mass loss on concrete surface in scaling test. This correlation of two sets of data is expected because the continuous exposure to deicers from the bottom surface of cubes in freezing and thawing condition is simply an "upside down version" of required deicer ponding in scaling test.

4.2. Effects on Surface Skid Resistance

Application of deicers after top snow has been removed on pavement can lead to slippery roads. The effect on pavement surface friction was studied and the summarized result of skid resistance was shown in Figure 30. All measurements can be found in Appendix C.

Recall that the higher BPN value indicating better skid resistance of tested surface. The surface after application of Season I had only 46.8 BPN on sand-blasted glass which was about 60% of the BPN of the other three. It was a great deduction on skid resistance which potentially increased the chances of having crashes in winter environment. As discussed in material section, Season I is a brownish viscous liquid which tends to lubricate rough surface like oil. The organic constituents including complex sugars might be the reason behind this lubrication.

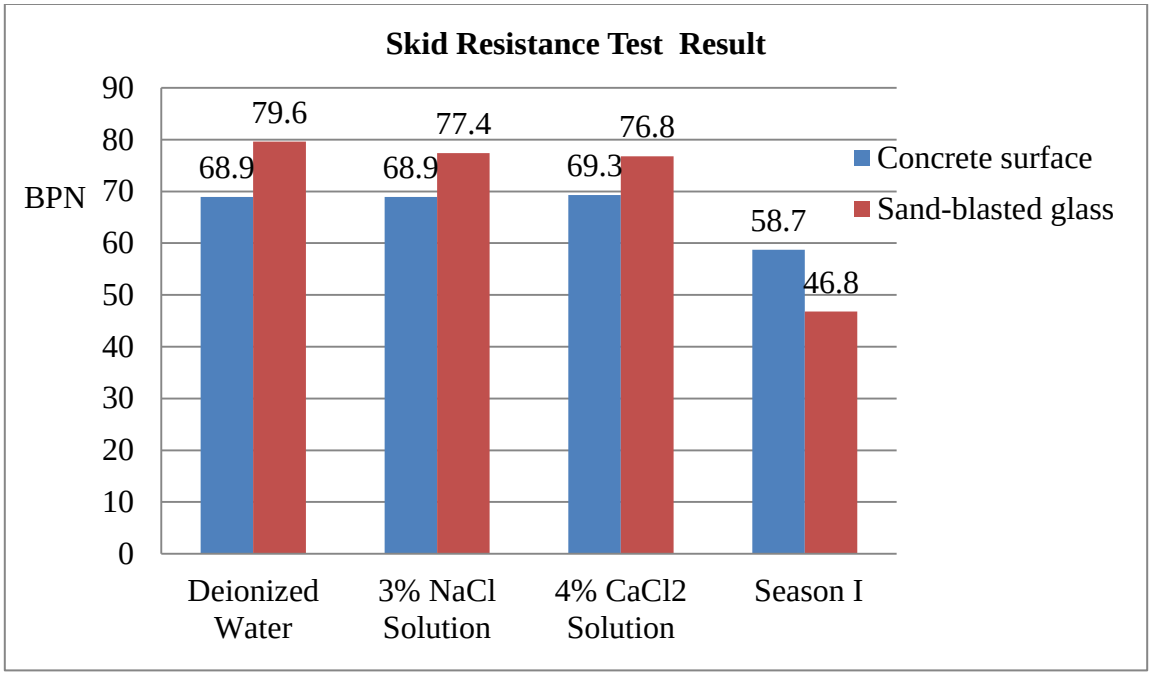

Figure 29. Skid resistance after application of deicers

Also, the BPN of concrete surface after application of Season I treated was higher than that on sand-blasted glass. This was because the texture difference between two tested surfaces. The concrete slab surface tested was apparently rougher than the sand-blasted glass. The sand-blasted glass was recommended to use because of the consistent results this texture providing. Moreover, the difference in BPN values on concrete surface between Season I and the other three solutions was 30% of the difference on sand-blasted glass. It means the skid resistance on concrete surface was not decreased too much after application of Season I. The difference in BPN values on different testing surfaces of each group was likely caused by the texture of tested surface and was not relevant to the applied deicers because same trend of increased BPN was

found after application of different deicers. FHWA suggested a minimum BPN of 65 representing acceptable skid resistance on pavement.

Second set of tests had also been carried out to evaluate the influence of other variables including testing surface temperature and drying time on skid resistance because the BPN measurements summarized in Table 11 is not sufficient to imply the influence of the temperature on surface friction measurement.

Table 12 shows the findings of the second set of tests. The BPNs at test site 1 and test site 2 which were both concrete surfaces were compared after application of Season I and 3% NaCl solution. The results did not explain the effect of temperature adequately. However, the results indicated the BPN was increased with longer drying time. It makes sense since, once the water of deicers was evaporated, the surface friction would increase because lack of lubrication on concrete surface.

Table 11. Skid resistance measurement

Deicer/Control	Test Surface	BPN	Temperature, ℉
Deionized Water	SG	79.6	65.3
	PCC	68.9	74.9
3 % NaCl Solution	SG	77.4	66.4
	PCC	68.9	74.8
4% $CaCl_2$ Solution	SG	76.8	66.2
	PCC	69.3	74.6
Season I	SG	46.8	67.5
	PCC	58.7	74.6

Table 12. Skid resistance at different surface temperatures and drying time

Deicer/Drying Time	Site 1		Site 2	
	BPN	Temperature, ℉	BPN	Temperature, ℉
Season I at 0 hr.	55-56	35.5-37.4	59-60	34.7-36.2
Season I at 2 hrs.	54-55	41.9-44.6	55-56	41.8-44.5
Season I at 4 hrs.	51-52	24.3-28.6	54-55	21.6-27.4
3% NaCl at 0 hr.	71-72	33.2-38.6	72-73	33.8-37.8
3% NaCl at 2 hrs.	72-73	42.9-45.3	72-73	41.9-43.8
3% NaCl at 4 hrs.	75-76	21.5-24.9	72-73	22.9-25.7

4.3. Effect on Concrete Permeability

Three different indirect permeability indicators including electrical resistivity, air permeability and water absorption rate were tested to evaluate the effect of different deicers on concrete permeability. Compressive strength of cylinders iterated in different deicers was also tested. Electrical resistivity, air permeability index and compressive strength results are summarized in Table 13. The compressive strength and the representative values of three indirect permeability indictors were presented in Figure 31 through Figure 34. Figures explaining calculation can be found in Appendix B.

Table 13. Electrical resistivity, air permeability and compressive strength of cylinders

	Electrical resistivity, kΩ-cm	Air Permeability Index	Compressive Strength, psi
Deionized Water	11.8 ±0.1	8.0 ±0.1	6407 ±242
3% NaCl Solution	11.4 ±0.1	8.1 ±0.2	6238 ±196
4% CaCl2 Solution	12.0 ±0.5	7.8 ±0.1	6422 ±95
Season I	16.9 ±1.9	7.9 ±0.1	6615 ±173

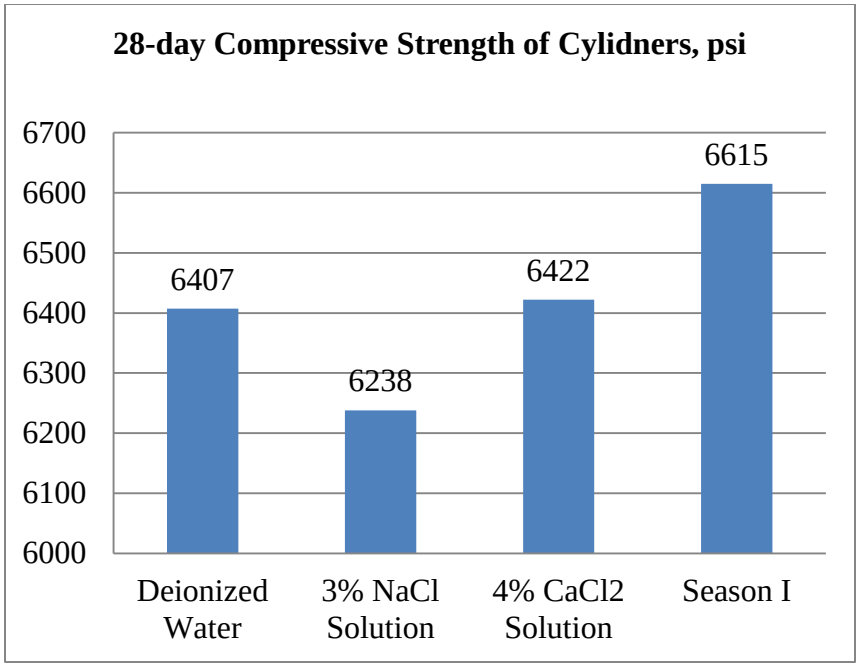

Figure 30. 28-day compressive strength of cylinders

For electrical resistivity readings, a higher value indicates lower permeability of chloride ions beneath the tested concrete surface [58]. A conclusion can be made that Season I greatly changed the surface electric resistivity of the concrete comparing with the other two deicers according to Figure 32. The average electrical resistivity is much higher than those of others implying the lowest permeability. This result matches with proposed sealing effect of Season I on concrete and it is suspicious that a specific constituent of Season I deicer clogged pores near the concrete surface when cylinders were immersed in Season I for 14 days. However, since the composition of Season I was not provided and no microscopic observation of micro-structure were conducted, it is difficult to reach a solid conclusion on this finding.

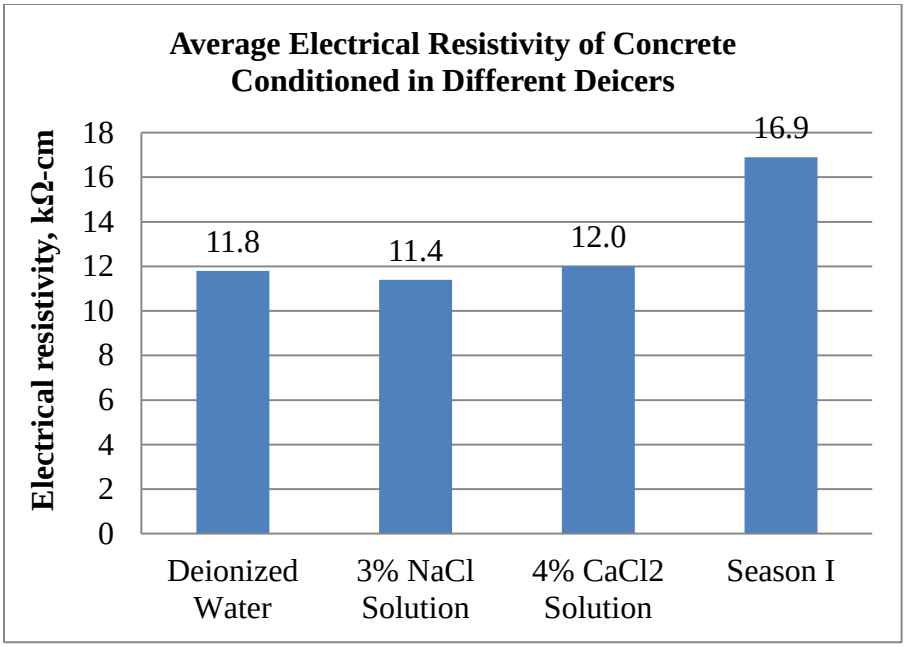

Figure 31. Average electrical resistivity of concrete conditioned in deicers

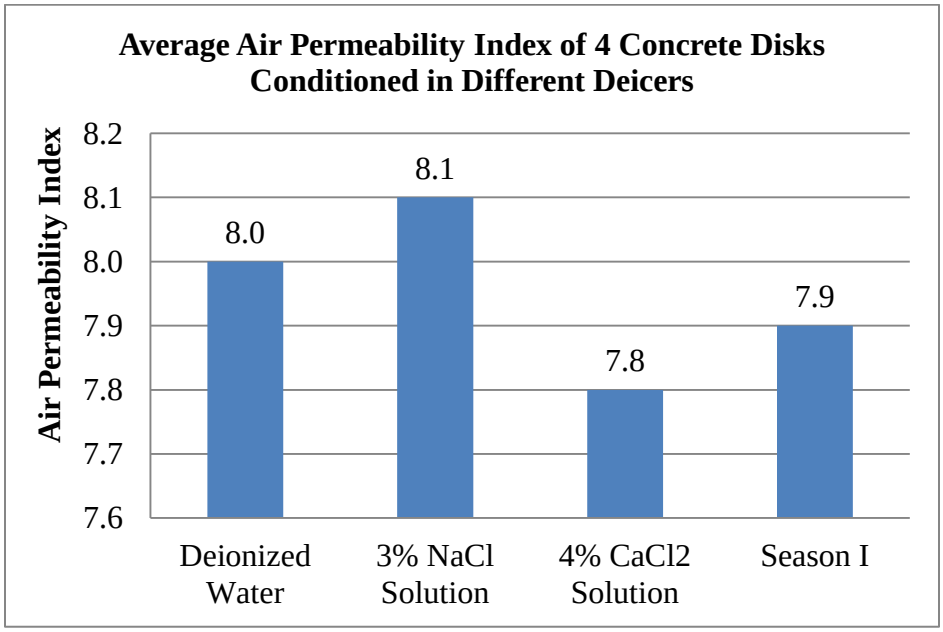

Figure 32. Average air permeability index of concrete conditioned in deicers

The second indirect indicator of permeability is air permeability index. As aforementioned, the coefficient of permeability, k, of each specimen was calculated based on pressure change over a given period of time. The plot of regression line and the slope value representing coefficient of air permeability can be found through Figure 43 to Figure 46 in Appendix B. The average air permeability index of specimens in each group is present in Figure 33 and, based on the chart, there is no obvious difference of air permeability index between disks cured by different deicers. It means that the air is able to penetrate through porous concrete disks at approximately same rate regardless of different deicer conditioning. It can be concluded that Season I and other deicers did not affect air permeability of concrete.

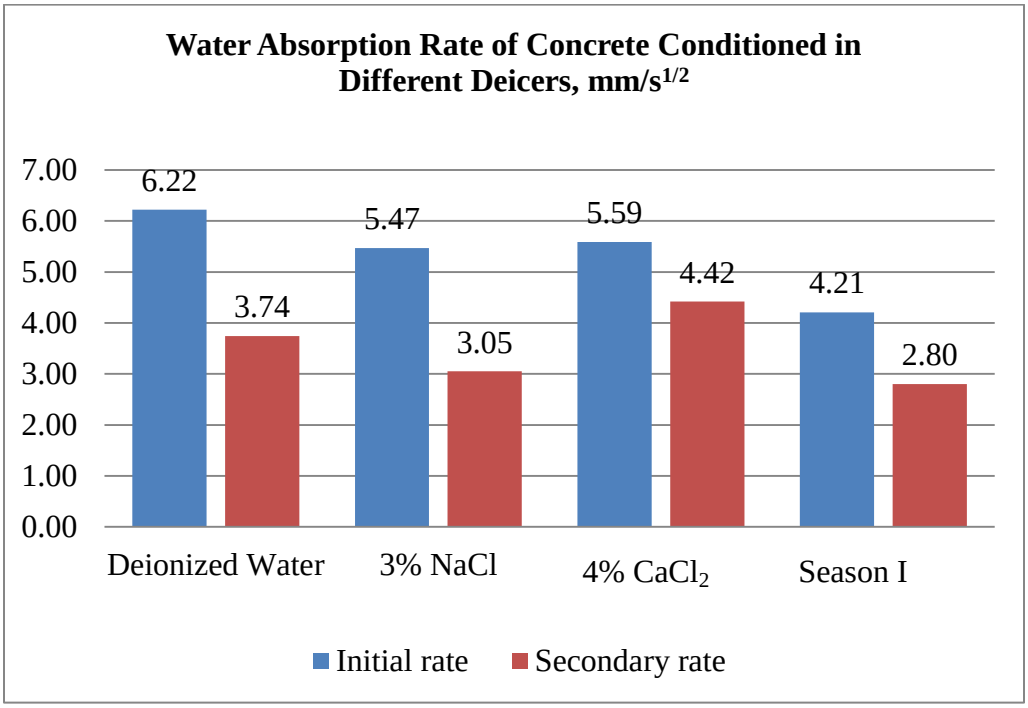

Figure 33. Water absorption rate of concrete

Water absorption rate of the 2-in disk was measured as the initial rate and the secondary rate. The absorption, I, of each specimen was calculated based on weight change of specimens in a given period of time following the equation in Chapter 3. The rate of absorption (both initial and secondary) is the slope of line that is the best fit to I plotted against square root of the time ($S^{1/2}$). Figure 47 through Figure 62 in Appendix B showed the regression line of each specimen. Since a higher water absorption rate meaning more water ingress in same test condition, specimens with higher water absorption rate are considered to be more porous. it can be concluded that specimens in Season I group had the lowest permeability because less water ingress were allowed by the porous concrete disks in same exposure conditions based on Figure 34.

In summary, two of three indirect permeability indicators, electrical resistivity and water absorption rate, supports the concept of sealing effect of Season I. However, air permeability index did not reflect any differences in the air permeability of concrete. It has been proven for long that higher permeability will result in a lower strength of concrete for the reason that high porosity results in lower density of concrete. Referring back to Figure 31, it can be found that this correlation is valid for Season I cured cylinders. Difference in compressive strengths between groups is not as drastic as the change of electric resistivity and water absorption rate. A possible explanation is that Season I had changed the surface permeability of concrete cylinders immersed in the solution but not able to penetrate deeper through the pore structure. It is very possible that the particle size of salt or other constituents contained within Season I is too large to penetrate through capillary pores.

The EDS analysis might resolve this uncertainty by examining the penetration depth of the Season I. Also, various factors including surface polishing and drying required by running EDS point analysis will alter the composition of substances left in pores.

4.4 Microscopic Analyses

Aforementioned physical damages and change of concrete permeability were caused by different effects of deicers on aggregates, paste and the pore structure of concrete. Each specific change of concrete properties studied so far could be amplified and observed at microscopic level. It is important to consider concrete as a two-phase material consisting of aggregate dispersed in a matrix of cement paste because the behavior of chemicals in deicer and the damage caused by frost action are different between regions. The chemical reaction in interfacial transition zone (designated as ITZ) was also a topic for people studying chemical deterioration of paste caused by deicer. The penetration depth of deicers is one of the key factors that can be related to deterioration rate and mechanism. Thus, by doing microscopic analysis, two questions should be addressed:

1. Is it possible to find a relationship between scaling damage and deicer penetration depth?
2. Is the surface permeability change of concrete actually resulted from the sealing effects of Season I?

4.4.1 Deicer penetration depth by EDS point analyses

The deicer penetration depth was evaluated by examining weight percent of different chemicals in two specimens taken from slabs in scaling test. One slab was pooled with 3% NaCl solution and another one was pooled with Season I during scaling. The tracked elements in EDS analysis for Season I sample is sodium, Na, and for 3% NaCl solution is chloride, Cl. Sodium was picked for Season I based on EDS analysis on a drop of the liquid. It was found the sodium content is extremely high comparing with other elements. Chloride was picked because the chloride penetration depth is normally used when NaCl solution was involved.

Results of the analysis are shown in Figure 35 and Figure 36 for NaCl solution penetrated sample and Season I penetrated sample. The NaCl solution penetrated about 19 mm where the weight percent of chloride drops drastically and Season I penetrated around 13 mm from the top surface of the cores. Table 14 and Table 15 are summarized results of chemical compositions versus the specimen depth. The exact relationship between scaling damage and deicer penetration depth is hard to interpret at this stage due to limited amount of samples in EDS analysis. However, the results suggest 3% NaCl solution penetrated 6 mm deeper than Season I deicer which might be resulted from more deicer ingress of slabs in scaling. Another contributing factor might be that, comparing with the NaCl solution, Season I is much more viscous due to the organic compounds it contained and it made Season I less flowable in pores. The particle size of these organic compounds might be too large to penetrate through capillary voids of concrete.

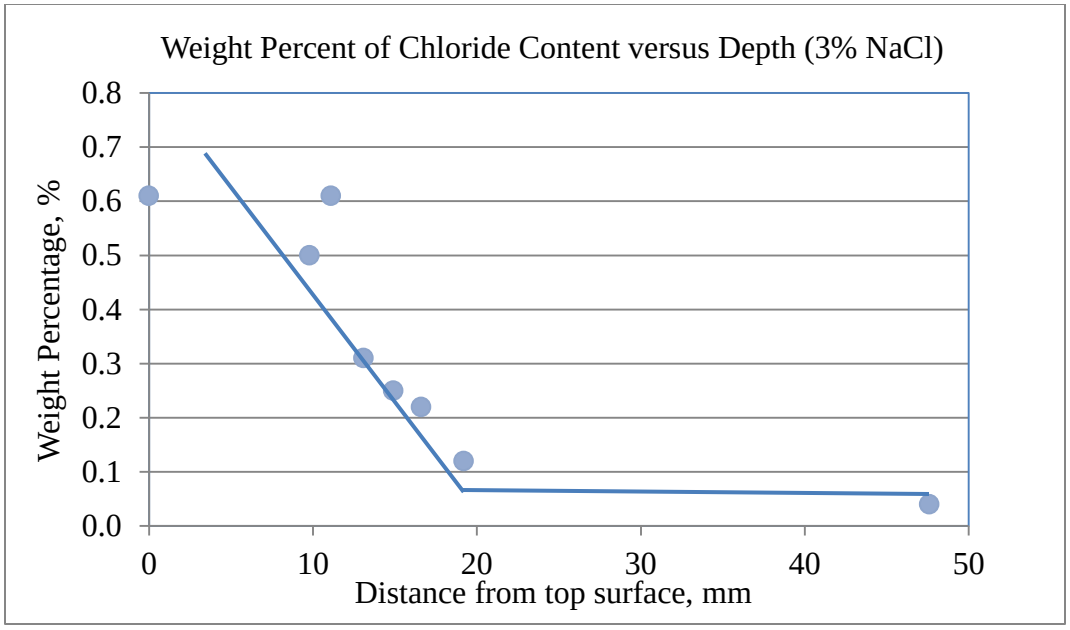

Figure 34. Chloride content versus depth for 3% NaCl specimen

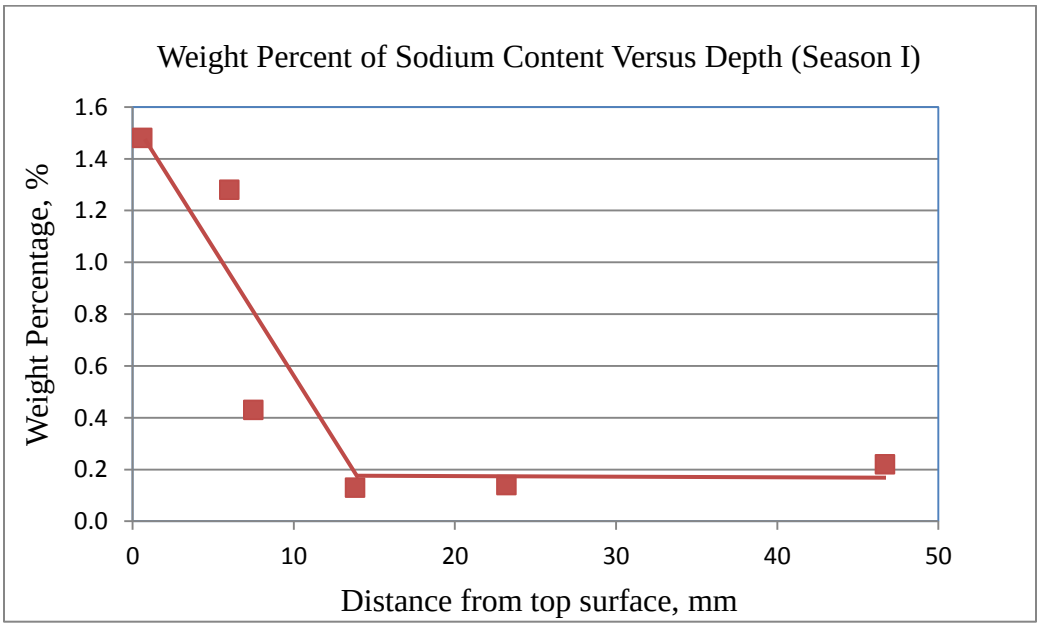

Figure 35. Sodium content versus depth for Season I specimen

Table 14. EDS analysis of chemical composition of NaCl sample

Spectrum Label	O	Na	Mg	Al	Si	S	**Cl**	K	Ca	Fe	Total
0.0 mm (Top) 500x	52.39	1.14	0.94	2.11	11.57	0.62	**0.61**	0.26	29.00	1.36	100.00
9.8 mm 800x	51.54	0.38	1.36	1.92	10.65	1.18	**0.50**	0.29	30.33	1.85	100.00
11.1 mm 800x	49.87	0.43	1.21	1.98	10.81	1.02	**0.61**	0.29	32.05	1.72	100.00
13.1 mm 800x	50.84	0.39	2.12	1.93	9.46	1.06	**0.31**	0.28	31.96	1.65	100.00
14.9 mm 800x	50.80	0.34	1.78	1.89	10.40	1.10	**0.25**	0.34	31.45	1.66	100.00
16.6 mm 800x	51.08	0.38	1.37	1.51	12.95	0.97	**0.22**	0.61	29.66	1.24	100.00
19.2 mm 800x	49.94	0.22	1.40	1.82	10.55	0.99	**0.12**	0.35	32.32	2.29	100.00
47.6 mm (btm) 800x	50.46	0.41	1.31	2.24	12.61	0.88	**0.04**	0.31	29.30	2.44	100.00

Table 15. EDS analysis of chemical composition of Season I sample

Spectrum Label	O	**Na**	Mg	Al	Si	S	Cl	K	Ca	Fe	Total
0.6 mm 800x	52.46	**1.48**	1.35	1.97	10.02	1.21	0.15	0.50	29.41	1.44	100.00
6.0 mm 800x	50.64	**1.28**	0.97	3.02	12.05	1.10	0.05	0.39	28.88	1.61	100.00
7.5 mm 800x	50.73	**0.43**	1.41	1.73	10.66	1.02	0.03	0.42	32.11	1.46	100.00
13.8 mm 800x	50.67	**0.13**	1.50	2.12	12.20	1.17	0.02	0.28	29.77	2.14	100.00
23.2 mm 800x	50.44	**0.14**	1.52	2.19	10.02	1.14	0.00	0.32	32.08	2.16	100.00
46.7 mm 800x	50.47	**0.22**	1.29	1.84	12.23	1.07	0.07	0.49	30.64	1.70	100.00

4.4.2 SEM photographic analysis

SEM images as Figure 37 through 40 show scanned cross sections at 500x and 800 x magnifications. All SEM images of the NaCl core and Season I core were analyzed by using EDS. Image of scanned surface was towards the top of the page and the points of where images were taken are shown in Figure 41 and 42.

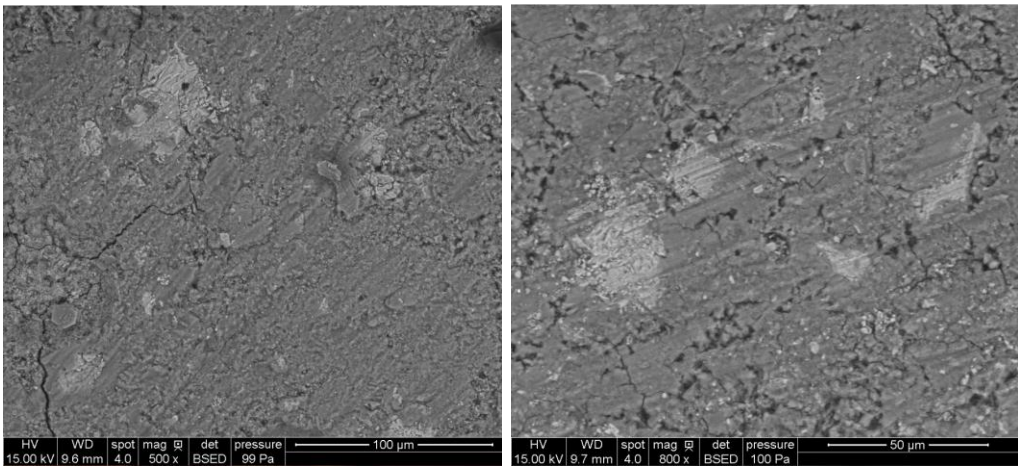

Figure 36. NaCl sample at 0 mm and Season I sample at 0.6 mm

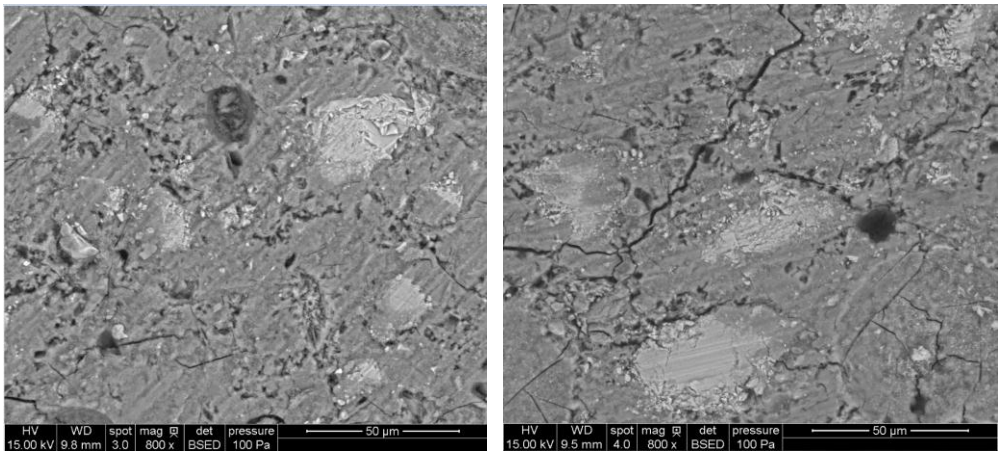

Figure 37. NaCl sample at 9.8 mm and Season I sample at 9.3 mm

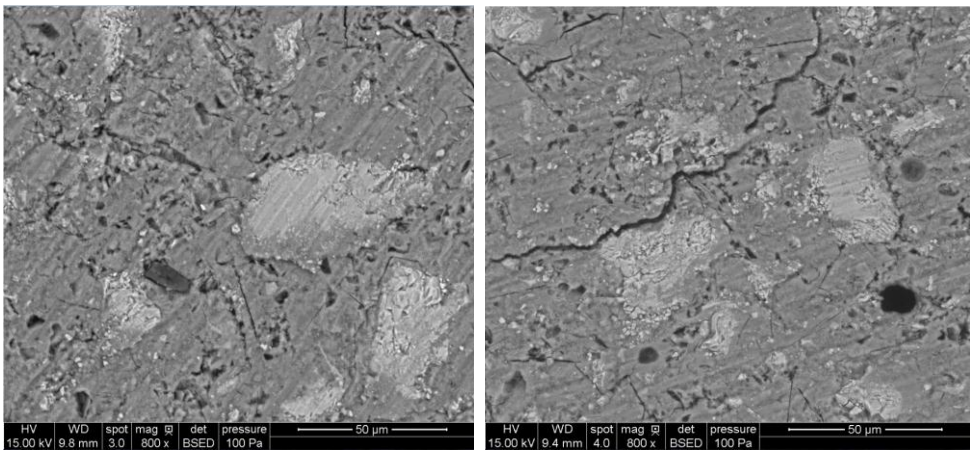

Figure 38. NaCl sample at 13.1 mm and Season I sample at 13.8 mm

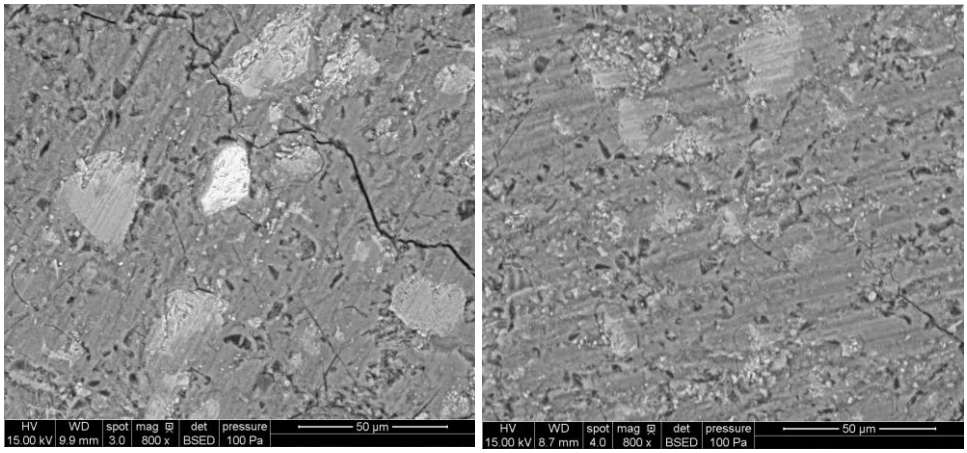

Figure 39. NaCl sample at 46.7 mm and Season I sample at 46.7 mm

The large white spots of Figure 37 through 40 are most likely unhydrated cement grains because the shape of these spots is irregular and the distribution is random. Although the surface of NaCl sample had more scaling damage, the image of Season I sample near the top surface in Figure 37 shows much more micro-cracking happened inside the concrete and some of the pores inside are connected by the cracking path. It is suspicious that these micro-cracking might be resulted from vacuum or polishing during sample preparation. Despite, these findings indicate the scaling is a superficial damage that has not much influence at micro-level. No clear salt precipitate is found near the top

surface of both samples. The high chloride content of NaCl sample surface is because the of the chloride treatment. Chloride concentration in this case might be due to formation of calcium chloride hydrate or to the adsorption of chloride by calcium silicate hydrate [64].

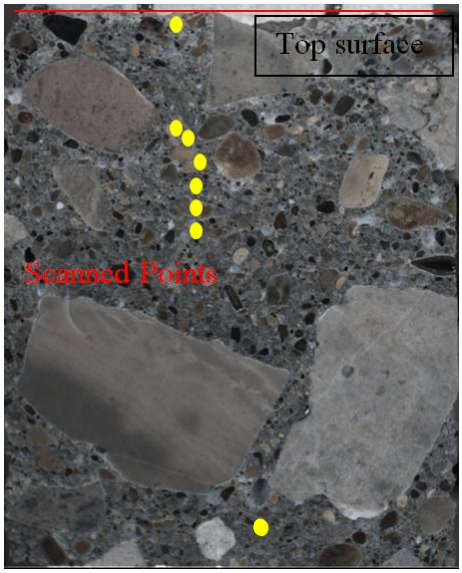

Figure 40. NaCl core cross section

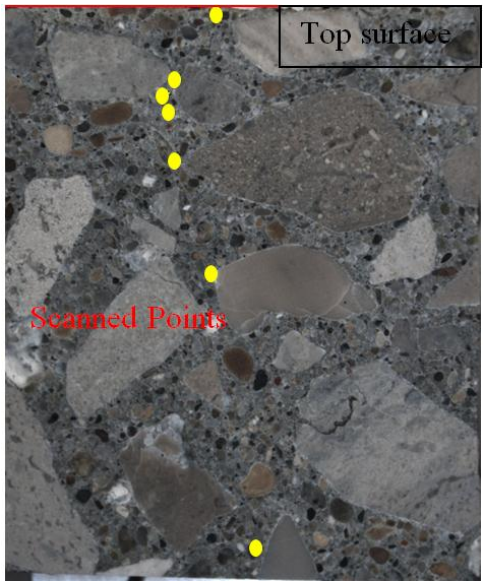

Figure 41. Season I core cross section

The image of NaCl core taken at 9.8 mm depth shows some crystaline structures with light color and only a few pores are clearly presented because some armophous phase filled the pores. These materials of crystaline structure might be salt precipatates instead of unhydrated cement grains because the difference in color. It is known chloride will promote the $Ca(OH)_2$ leaching and formation of porous C-S-H gel/phase which might be the reason why seeing pores are filled with armophous phaste. Nonetheless, no further evidence is obtained to verify this point. In the image of Season I sample, no obvious crystaline structure is presented. At approximately 13 mm, both samples show unhydrated cement grains, fine aggregate grains and pores as shown in Figure 39. Generally more micro-cracking can be seen in Season I sample which is consistent with findings in first two sets of images. Similar conclusions can be made from images of bottom parts of two cores in Figure 40.

CHAPTER 5

CONCLUSIONS AND RECOMMENDATIONS

5.1 Conclusions

The assessment of the new agro-based deicer, Season I, focuses on following aspects:

- Physical frost damage to pavement concrete
- Effects on skid resistance
- Effects on concrete permeability

The results indicate the effects of Season I deicer are acceptable, neutral or beneficial comparing with other chloride-based salt solutions which are traditionally used as deicers. The following conclusions can be made based on the findings:

1. No physical frost damage of mortar cubes is found in Season I solution. Mass loss of mortar cubes in Season I after freezing and thawing cycles is negligible comparing with mass loss of cubes in NaCl and $CaCl_2$ solutions.
2. Strength loss of mortar cubes in NaCl and $CaCl_2$ solutions after freezing and thawing cycles is due to instable geometrics caused by removal of surface materials around cube corners.

3. Scaling rating is given based on visual examination and mass loss per unit area. Results indicate slabs pooled Season I have no scaling damage and slabs pooled by 3% NaCl and 4% $CaCl_2$ solution have significant scaling damage.
4. Skid resistance results reveal the application of Season I deicer make concrete pavement surface more slippery than that of normal condition. The BPN value of Season I applied surface is lower than that of the surface treated by other two deicers.
5. The sealing effect of Season I deicer is reflected by higher electrical resistivity and higher water absorption rate comparing with specimens conditioned in water and other deicers. Air permeability index of all specimens is similar.

5.2 Recommendations for Future Study

The experimental work of this study has provided a comprehensive evaluation of a new agro-based deicer, Season I. To better understand the differences between this new product and traditional deicing salts, the followings are recommended:

1. To clearly explain the sealing effect of Season I, more EDS analyses and SEM images of different specimens tested in permeability evaluation are required for the study as to examine the micro-structure change.

2. The temperature of freezing and thawing cycles should be monitored and recorded to control the quality of frost damage results.

3. The frost resistance of concrete is determined mainly by its strength and air entrainment. If more mixtures containing SCMs or having different air content are provided, a more comprehensive understanding of effects of Season I on pavement concrete can be achieved.

REFERENCES

1. Federal Highway Administration, U.S. Department of Transportation, ROAD WEATHER MANAGEMENT PROGRAM, Weather Events, Snow and Ice., 2013.

2. Wang K., Nelsen D. E., Nixon W. A., Damaging effects of deicing chemicals on concrete materials, Cement and Concrete Composites, Vol 28, Issue 2, pp. 173-188, Feb 2006.

3. Nixon, W.A., Williams, A.D., 2001. A Guide for Selecting Anti-icing Chemicals. Ver. 1.0. IIHR Technical Report No. 420. The University of Iowa, Iowa City, IA, 21 pp.

4. Shi, X., Fay, L., Gallaway, C., Volkening, K., Peterson, M.M., Pan, T., Creighton, A., Lawlor, C., Mumma, S., Liu, Y., Nguyen, T.A., 2009b. Evaluation of alternate anti-icing and deicing compounds using sodium chloride and magnesium chloride as baseline deicers. Publication No. CDOT-2009-01 A Final Report Prepared for the Colorado Department of Transportation, Denver, CO

5. Fischel, M., 2001. Evaluation of selected deicers and based on a review of literature. Publication No. CDOT-DTD-R-2001-15. A Final Report Prepared for the Colorado Department of Transportation, Denver, CO.

6. Kahl, S., 2004. Agricultural by-products for anti-icing and de-icing use in Michigan. In:Trasportation Research Board (Ed.), Proc. 6th intl. Symposium on Snow Removal and Ice Control Technology: Transportation Research Circular E-C063: Snow and Ice Control Technology, pp. 552-555 (SNOW04-009).

7. Mehta, P.K., Concrete: Structure, Properties, and Methods. Emglewood Cliffs, NJ: Prentice Hall, pp. 125-128, 1993.

8. Power, T.C., The Physical Structure and Engineering Properties of Concrete, Bulletin 90, Portland Cement Association, Skokie, IL 1958.

9. Pigeon, M., Marchand, J., Pleau, R., 1996. Frost resistant concrete. Construction and Building Materials, Vol. 10, No. 5, pp. 339-348, 1996. Elsevier Science Ltd, Quebec, Canada.

10. Litvan, G.G., Frost Action in Cement in the Presence of De-Icers, Cem. Con. Res., Vol. 6, pp. 351-356, 1976.

11. Cantor, T.R. and Kneeter, C.P., Influence of Salt on the Freeze-Thaw Deterioration of Concrete, Material Performance, pp. 28-32, May 1997.

12. Hoffmann, Dirk W. Changes in Structure and Chemistry of cement Mortars Stressed by a Sodium Chloride Solution, Cem. Con. Res., Vol. 14, pp. 49-56, 1984.

13. Heukamp, F.H. et al. "Mechanical Properties of Calcium-Leached Cement Pastes Triaxial Stress States and the Influence of the Pore Pressures." Cem. Con. Res., vol 31, pp. 767-774, 2001.

14. Valenza, J.J., Scherer, G.W., A review of salt scaling: I . Phenomenology, Cem. Con. Res., Vol 37, pp. 1007-1021, 2007.

15. Verbeck, G.J., Kieger, P., Studies of "salt"scaling of concrete, Highw. Res. Board. Bull. Vol. 150, pp. 1-17, 1957.

16. Sellevold, E.J., Farstad, T., Frost/salt testing of concrete: effect of test parameters and concrete moisture history, Nord. Conce. Res., Vol 10, pp. 121-138., 1991.

17. Beckett, D., Influence of carbonation and chlorides chlorides on concrete durability, Conc., pp. 16-18., 1983.

18. Gunter, M., Bier, Th., Hilsdorf, H.,Effect of curing and type of cement on the resistance of concrete to freezing in deicing salt solutions, in: J. Scanlon (Ed.), ACI Special Publication SP-100, pp. 877-899., Amreican Concrete Institute, Detroit, 1987.

19. Gebler, S.H., and Klieger, P. Effect of fly ash on the durability of air-entrained concrete. ACI, Farmington Hills, Mich. pp. 483-519., 1986.

20. Studer, W., Internal comparative tests on frost-deicing salt resistance, International Workshop on the Resistance of Concrete to Scaling Due to Freezing in the Presence of Deicing Salts, pp. 175-187., Center de Recherche Interuniversitaire sur le Beton, University of Sherbrooke-University Laval, Quebec, August 1993.

21. Marchand, J., Pigeon, M., Bager, D., Talbot, C., influence of chloride solution concentration of salt scaling deterioration of concrete, ACI Mater. J., pp 429-435, Jul- Aug, 1999.

22. Lindmark, S. Mechanims of salt frost scaling of Portland cement-bound materials: studies and hypothesis, Ph.D. thesis, Lund Inst. Tech., Lund, Sweden, 1998.

23. Arnfelt H., Damage on Concrete Pavements by Wintertime Salt Treatment, Meddelande, vol. 66, Statens Vaginstitut, Stockholm, 1943.

24. Sommer, H., The precision of the microscopical determination of the air-void system in hardened concrete, Cem. Concr. Aggreg., Vol. 2, pp. 49-55., 1979.

25. Siebel, E., Air-void characteristics and freezing and thawing resistance of superplasticized air-entrained concrete with high workability, in: V.M. Malhotra (Ed.), ACI Special Publication SP-119, pp. 297-319 1989.

26. D.J. Corr, P.J. Monteiro, J. Bastacky, Mircroscopic characterization of ice morphology in entrained air voids, ACI Mater. J. 99-M18., pp. 190-195, 2002.

27. Powers, T.C., Helmuth, R.A. Theory of volume changes in hardened portland-cement paste during freezing, Proc. Highway Res. Board 32, 1953.

28. Jacobsen, S., Farstad, T., Gran, H.C., Sellevold, E.J., Frost salt scaling of no slump concrete: effect of strength, Nord. Concr. Res., Vol 11, pp. 57-71, 1991.

29. Powers, T.C. A working hypothesis for future studies for frost resistance of concrete, Journal of American Concrete Institution, Vol. 16, pp. 245-272, 1945.

30. Weissenberger, J. G Dieckmann, R. Gradinger, M. Spindler, Sea ice: a cast technique to examine and anlyze brine pockets and channel structure, Linmol. Oceanogr. Vol 37 (1), pp. 179-183, 1992.

31. Beddoe, R.E., Setzer, M.J., A low temperature DSC investigation of hardened cement paste subjected to chloride action, Cem. Concr. Res. vol 18., pp. 249-256, 1988.

32. Wall, F.T., Chemical Thermodynamics, Freeman, San Francisco, 1965.

33. Weast, R.C., Astle, M.J., CRC Handbook of Chemistry and Physics, 62nd ed., CRC Press, FL, 1981.

34. Valenza, J.J., Scherer, G.W., A review of salt scaling: II . Mechanisms, Cem .Con. Res., Vol 37, pp. 1022-1034, 2007.

35. Gulati, S.T., Hagy, H.E., Analysis and measurement of glue-spall stresses in glass-epoxy bonds, J. Am. Ceram. Soc. 65, pp. 1-5, 1982.

36. Gulati, S.T., Hagy, H.E., Theory of the narrow sandwich seal, J. Am. Ceram. Soc. 61, pp. 260-263, 1973.

37. Ciardullo, J.P., Sweeney, D.J., Scherer, G.W., Thermal expansion kinetics: method to measure the permeability of cementitious materials: IV. Effect of thermal gradients, J. Am. Ceram. Soc. 88, pp. 1213-1221, 2005.

38. Pounder, E.R., Physics of Ice, Pergamon Press, Oxford, 1965.

39. Van den Heede, P. Furniere, J. De Belie, N., Influence of air entraining agents on deicing salt scaling resistance and transport properties of high-volume fly ash concrete, Cem Con Com, Vol 37, pp. 293-303, 2013.

40. Hammer, T.A. Sellevold, E.J. Frost resistance of high-strength concrete, in. W.T. Hester (Ed.), ACI special Publication SP-121, Amreican Concrete Institute, Detroit, pp. 457-487, 1990.

41. R. Sahin, M. A. Tasdemir, R. Gul, C. Celik, Determination of the optimum conditions for de-icing salt scaling resistance of cocnrete by visual examination and surface scaling, Counstruction and Building Materials, Vol 24, pp. 353-360, 2010.

42. Johnston, C.D., Effects of microsilica and class C fly ash on resistance of concrete to rapid freezing and thawing and scaling in the presence of deicing agents. ACI, Farmington Hills, Mich. pp. 1183-1204., 1987.

43. Johnston, C.D., W/CM code requirements inappropriate for resistance to deicer salt scaling. ACI, Farmington Hills, Mich. pp. 85-105., 1994.

44. Bouzoubaa, N., et al. Deicing salt scaling resistance of concrete incorporating supplementary cementing materials: laboratory and field test data, Can. J. Civ. Eng. Vol. 35, NRC Research Press Web, November 2008.

45. Hooton, R.D., and Boyd, A. Effects of finishing and curing on deicer salt scaling reistance of concretes. In Proceedings of the International RiLEM workshop on Resistance of Concrete tot Freezing and Thawing With or Without De-cing Chemicals. University of Essen, germany, London, pp. 174-183., 1997.

46. Marchand, J., Jolin, M., and Machabee, Y. Deicer salt scaling resistance of supplementary cementing materials concrete: laboratory results against field performance. In Proceedings of the 6th International Congress Global Construction: Ultimate Concrete Opportunities, Dundee, UK. 5-7 July 2005.

47. Ahani, R.M., Nokken. M. R., Salt scaling resistance - The effect of curing and pre-saturation, Construction and Building Materials, Vol 26, pp. 558-564, 2012.

48. Nowak-Michta, A., Water-binder Ratio influence on De-icing Salt Scaling of Fly Ash Concretes, 11th International Conference on Modern Building Materials, Structures and Techniques, Procedia Engineering, Vol. 57, pp. 823-829., MBMST 2013.

49. Pigeon, M. Perraton, D. Pleau, R., Scaling Tests of Silica Fume Concrete and the Critical Spacing Factor Concept, ACI, pp. 1155-1182, 1958.

50. Deja, J. Freezing and de-icing salt resistance of blast furnace slag concretes, Cem. Con. Com., Vol 25, pp. 357-361, 2003.

51. Kummer, H. W., and Desmond F. Moore., Concept and use of the British portable skid resistance tester, No. 309, Pennsylvania State University, Dept. of Mechanical Engineering, 1963.

52. Giles, C.G., Sabey, E. Carden, W.W.F.. Development and Performance of Portable Skid-Resistance Tester, Road Research Technical Paper No. 66, Road Research Laboratory, Dept. of Scientific and Industial Resarch, England, 1964.

53. Fay, L. and Shi, X., Laboratory Investigation of Performance and Impacts of Snow and Ice Conctrol Chemicals for Winter Road Service, Journal of Cold Regions Engieering, Vol. 25, ASCE, 2011.

54. Chappelow, C.C., et al., Handbook of Test Methods for Evaluating Chemical Deicers, SHRP-H-332, Midwest Research Institute, Kansas City, MO, 1992.

55. Taylor, P., Hooton, R.D., Deicer Scaling Resistance of Concrete Pavements, Bridge Decks, and Other Structures Containing Slag Cement: Phase 2: Evaluation of Different Laoratory Scaling Test Methods, National Concrete Pavement Technology Center, Iowa State University, Ames, IA, July 2012.

56. ASTM C 672/C672M. 2003. Standard Test Method for Scaling Resistance of Concrete Surfaces Exposed to Deicing Chemicals, ASTM International, West Conshohocken, PA.

57. ASTM E 303. 2003. Standard Test Method for Measureing Surface Frictional Properties Using the British Pendulum Tester, ASTM International, West Conshohocken, PA.

58. FM 5-578. January 27, 2004. Florida Method of Test For Concrete Resistivity as an Electrical Indicator of its Permeability, State Matarials Office, FDOT, Florida.

59. ASTM C 1585. 2003. Standard Test Method for Measurement of Rate of Absorption of Water by Hydraulic-Cement Concretes, ASTM International, West Conshohocken, PA.

60. Durability Index Testing Procedural Manual. May, 2005. PART 2. STANDARD PROCEDURE FOR OXYGEN PERMEABILITY TEST, University of Cape Town and University of the Witwatersrand.

61. Wikipedia, http://en.wikipedia.org/wiki/File:Schema_MEB_(en).svg

62. Wang. X.S., Wu. B.S., and Wang. Q.Y., Online SEM invesitgation of microcrack characteristics of concretes at various temperature, Cement and Concrete Research, Vol 35, pp. 1385-1390, 2005.

63. Aggarwal. Y., Siddique. R., Mircostructure and properties of concrete using bottom ash and waste foundry sand as partial replacement of fine aggregates, Construction and Building Materials, Vol 54, pp. 210-223, 2014.

64. Lee, H. et al., Effects of Various Deicing Chemicals on Pavement Concrete Deterioration, Mid-Continent Transportation Symposium Proceedings, Iowa State University, Ames, Iowa.

APPENDIX A

SUPPLEMENTS TO MATERIALS AND METHODS

Mortar Mix Design

	Batch Quantities	Note	Number of Samples
2*2*2 in mortar cube	cement 1973 g	1 part cement 2.75 sand	24
	sand 5425.8 g	w/c = 0.485	
	water 956.91 g	C109	

Concrete Cylinder Mix Design

Coarse Aggregate (Dry):	115.1	lb
Fine Aggregrate (Dry):	83.2	lb
Cement:	36.6	lb
Waterproofer	-	lb
Pozzolan (2):	-	lb
Air Entrainer :	4.0	ml
Free Water	16.48	lb
Water adjustment	**1.59**	lb

Slump:	1.5	in
Concrete Temp:	70.2	˚F
(%) Air:	3.1	%

Concrete Slab Mix Design

Mix 1

Coarse Aggregate (Dry):	115.1	lb
Fine Aggregrate (Dry):	83.2	lb
Cement:	36.6	lb
Waterproofer	-	lb
Pozzolan (2):	-	lb
Air Entrainer :	9.5	ml
Free Water	16.48	lb
Water added	**1.5**	**lb**

Fresh properties of mix 1

Slump:	3.5	in
Concrete Temp:	69	˚F
(%) Air:	5.5	%

Mix 2

Coarse Aggregate (Dry):	115.1	lb
Fine Aggregrate (Dry):	83.2	lb
Cement:	36.6	lb
Waterproofer	-	lb
Pozzolan (2):	-	lb
Air Entrainer :	9.5	ml
Free Water	16.48	lb
Water added	**1.65**	lb

Fresh properties of mix 2

Slump:	3	in
Concrete Temp:	69	˚F
(%) Air:	5	%

APPENDIX B

SUPPLEMENTARY FIGURES

DI Water Group Air Permeability

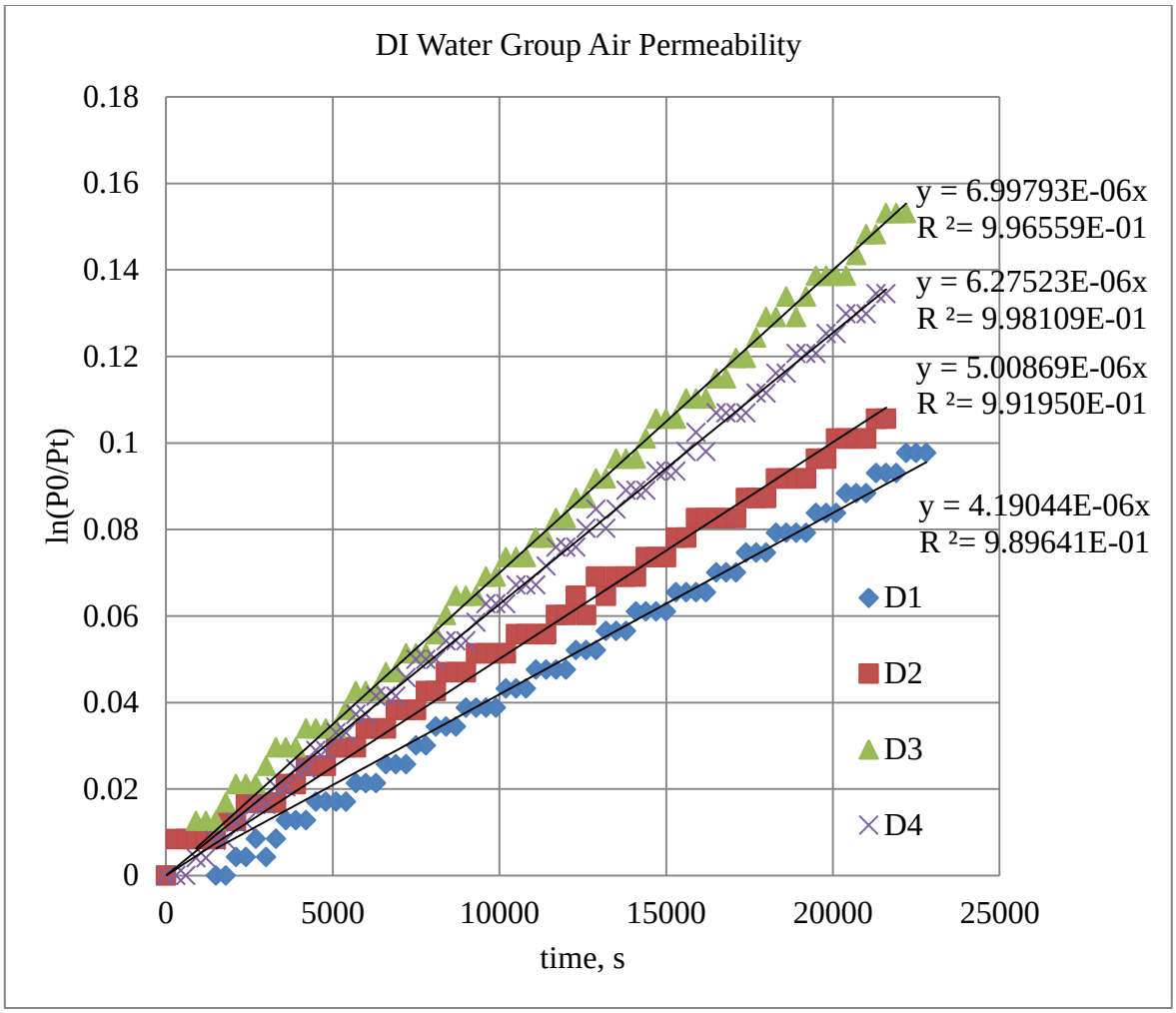

Figure 42. Permeability of concrete disk immersed in DI water

NaCl Group Air Permeability

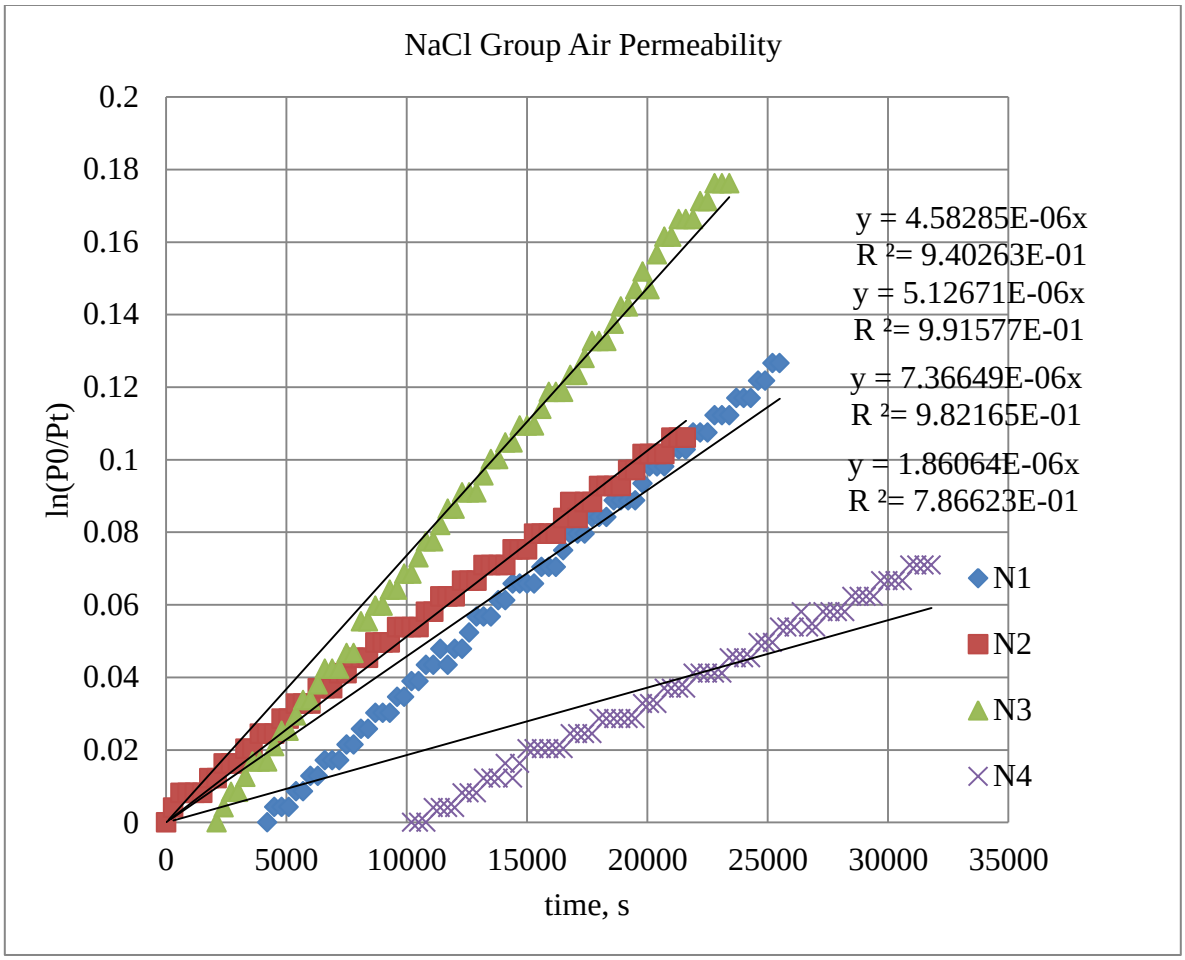

Figure 43. Permeability of concrete disk immersed in NaCl solution

$CaCl_2$ Group Air Permeability

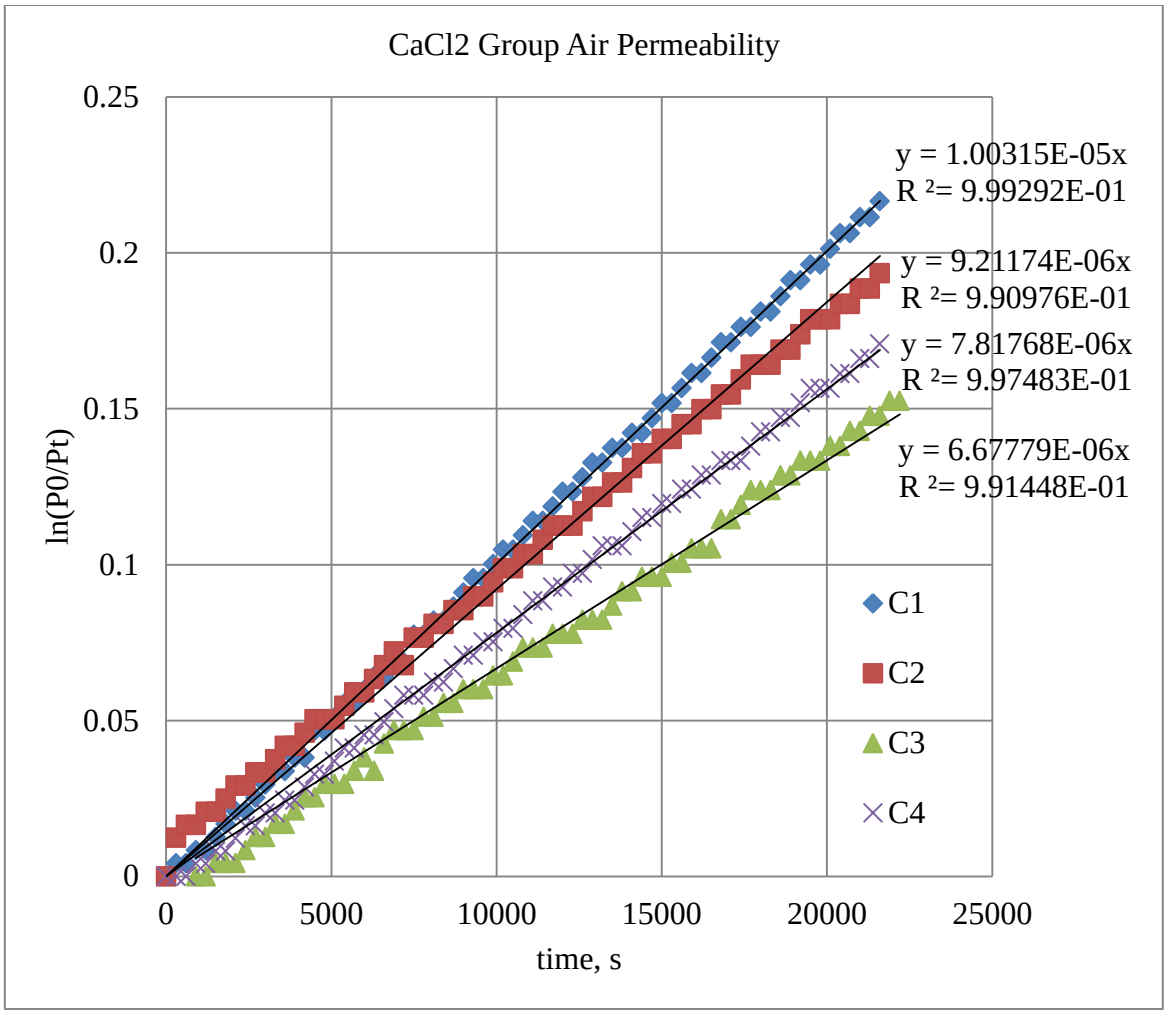

Figure 44. Permeability of concrete disk immersed in $CaCl_2$ solution

Season I Group Air Permeability

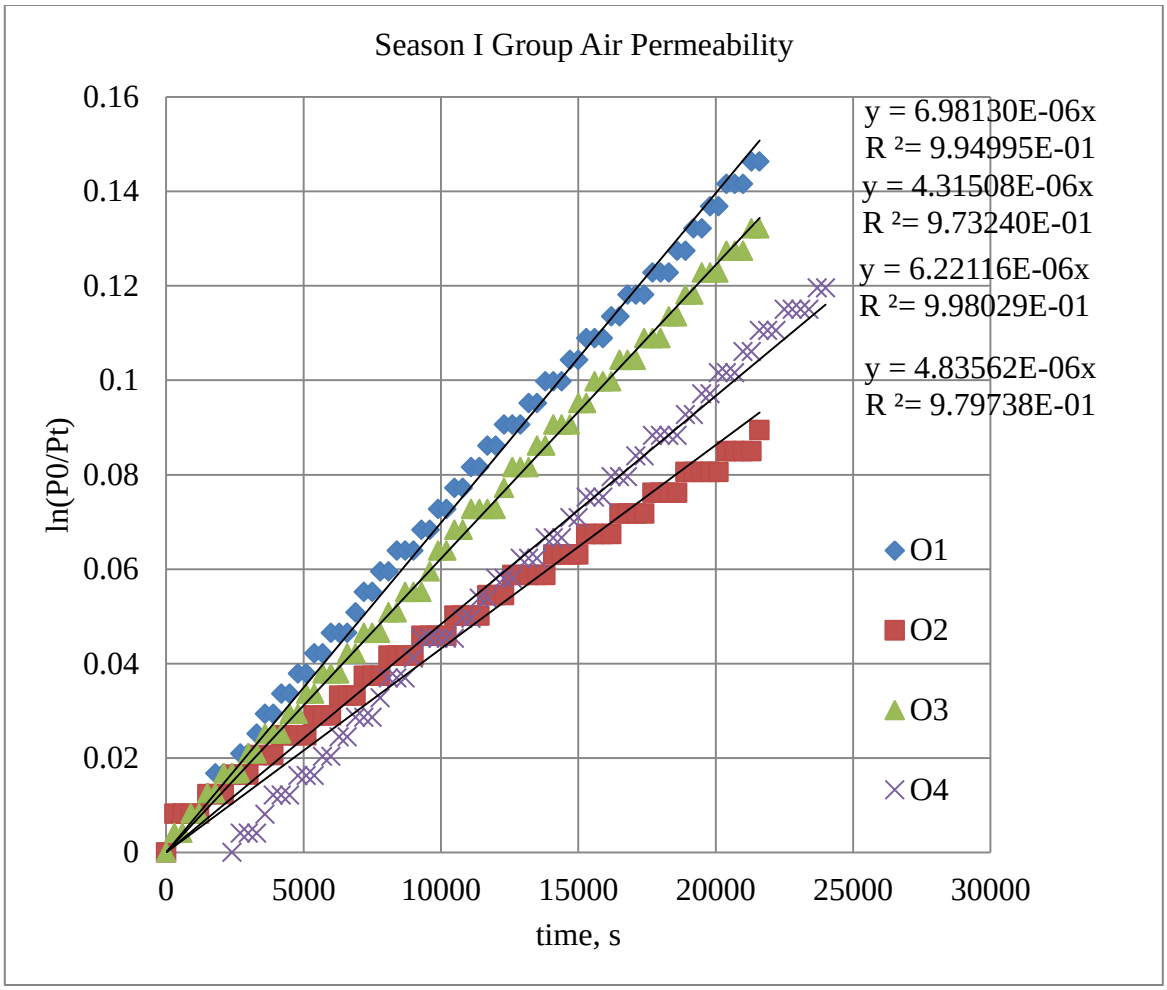

Figure 45. Permeability of concrete disk immersed in Season I

Water Absorption (DI Water Sample)

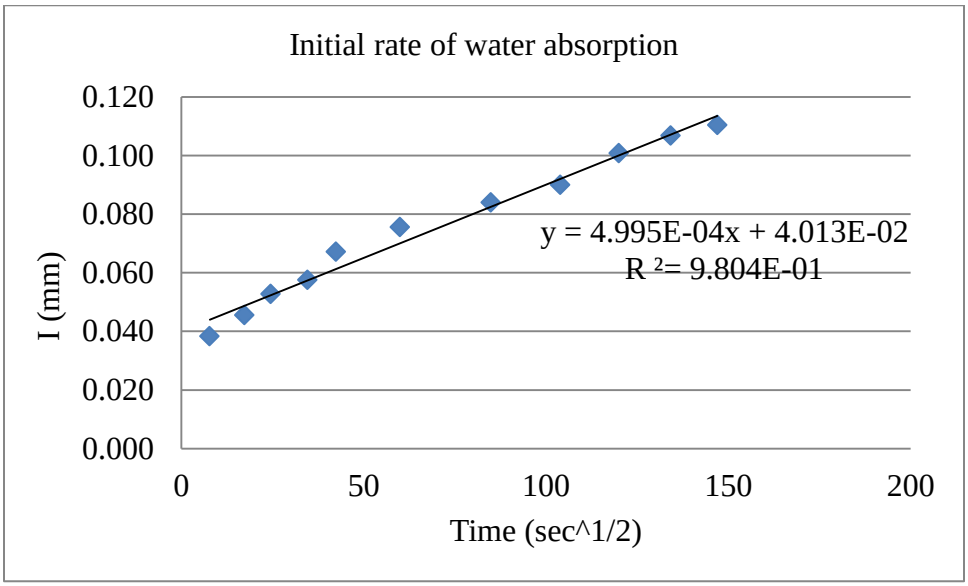

Figure 46. Initial rate of water absorption (DI Water Sample 1)

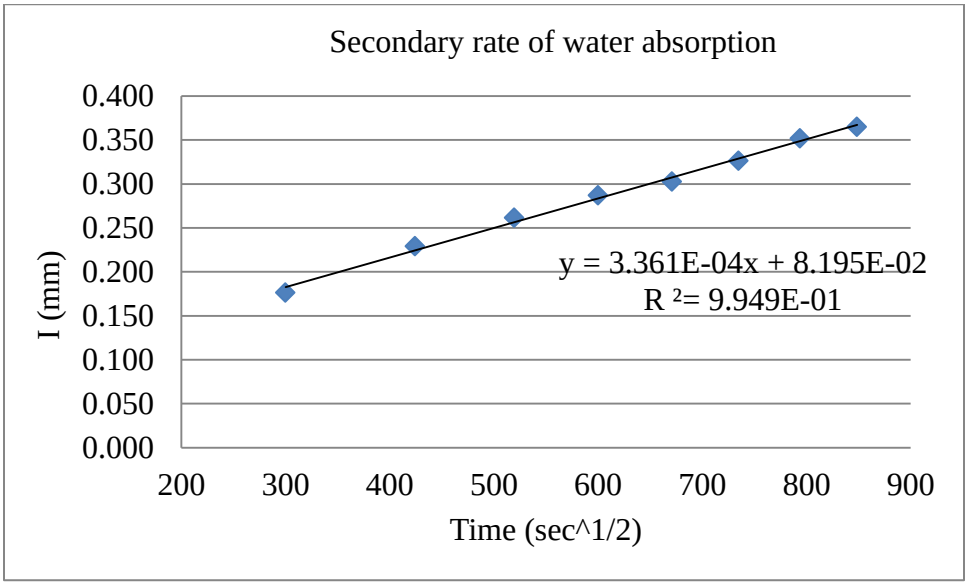

Figure 47. Secondary rate of water absorption (DI Water Sample 1)

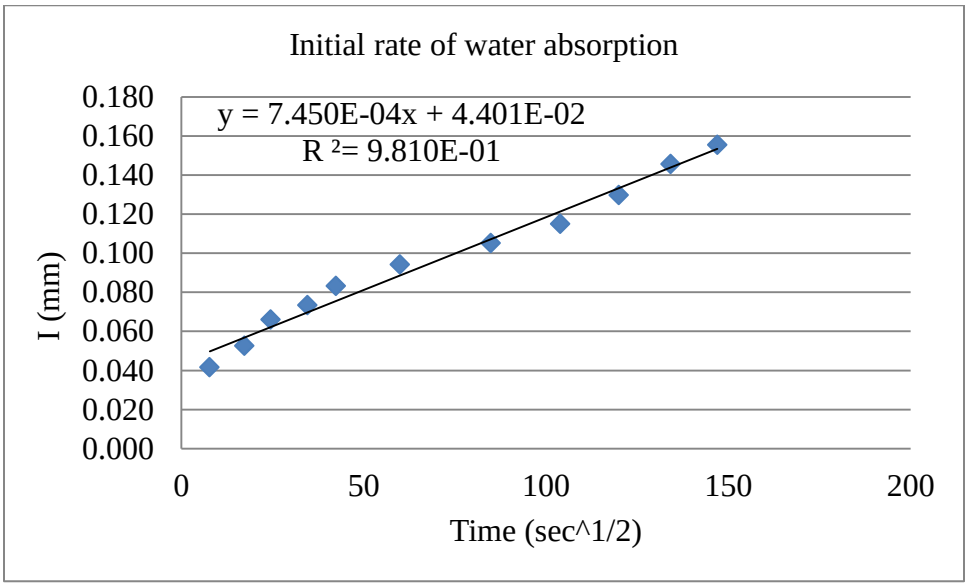

Figure 48. Initial rate of water absorption (DI Water Sample 2)

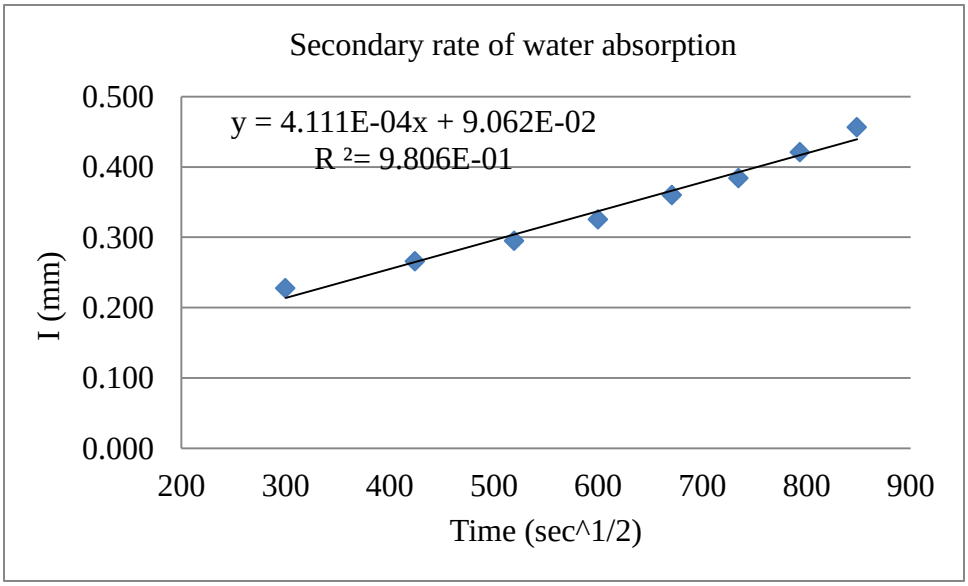

Figure 49. Secondary rate of water absorption (DI Water Sample 2)

Water absorption (NaCl Sample)

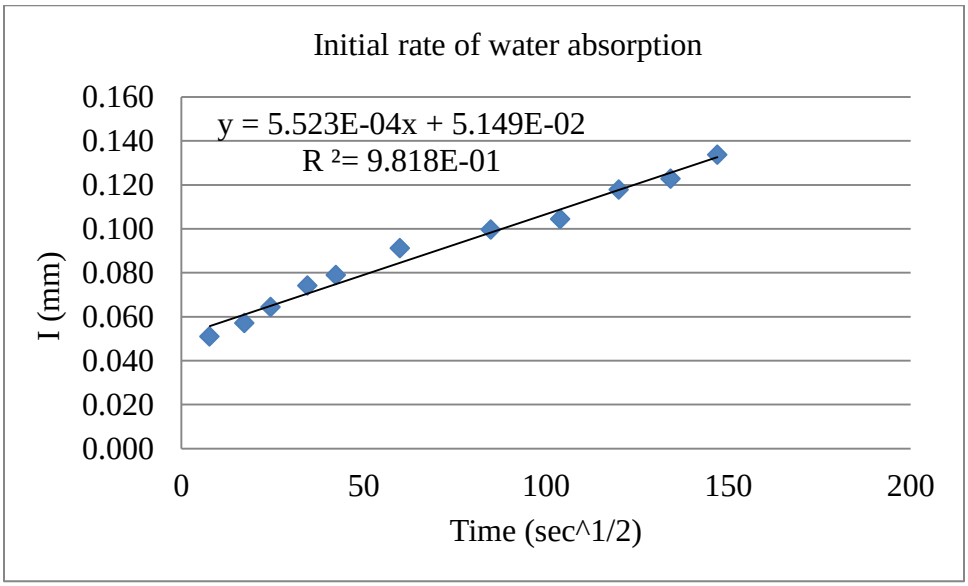

Figure 50. Initial rate of water absorption (NaCl Sample 1)

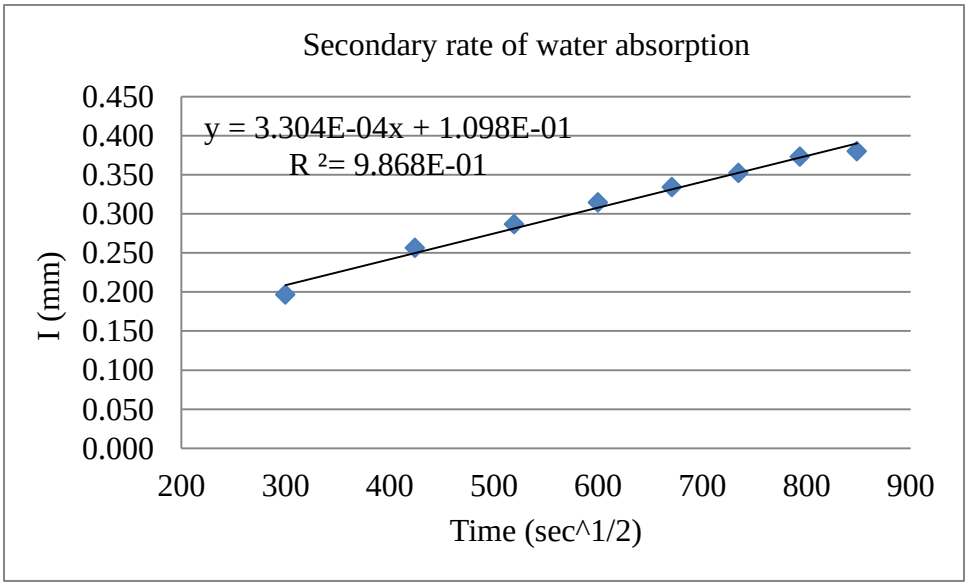

Figure 51. Secondary rate of water absorption (NaCl Sample 1)

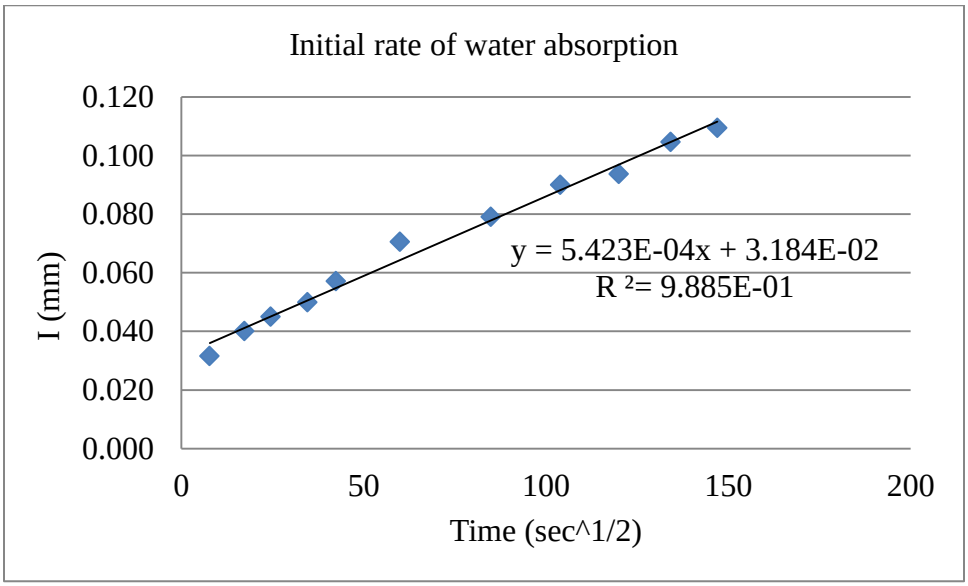

Figure 52. Initial rate of water absorption (NaCl Sample 2)

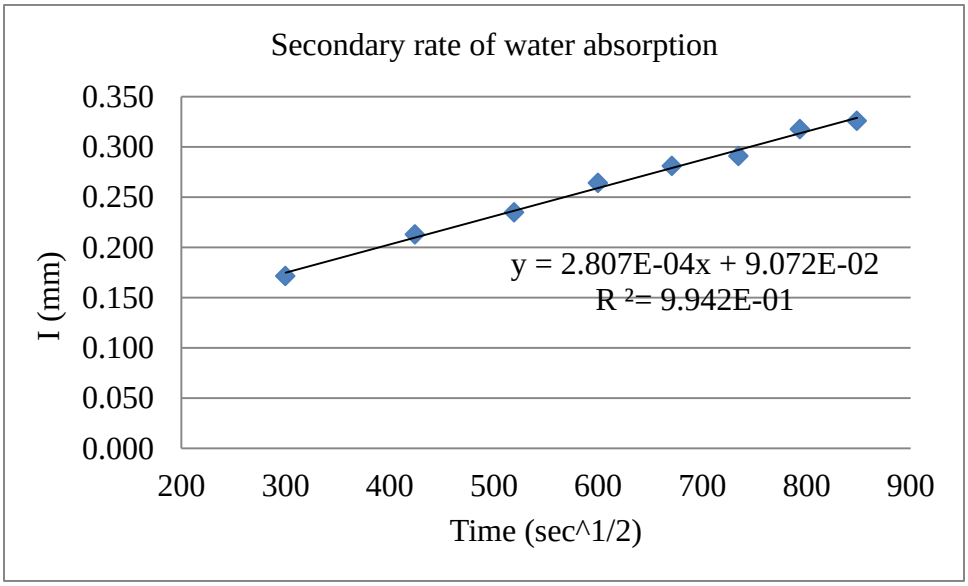

Figure 53. Secondary rate of water absorption (NaCl Sample 2)

Water absorption ($CaCl_2$ Sample)

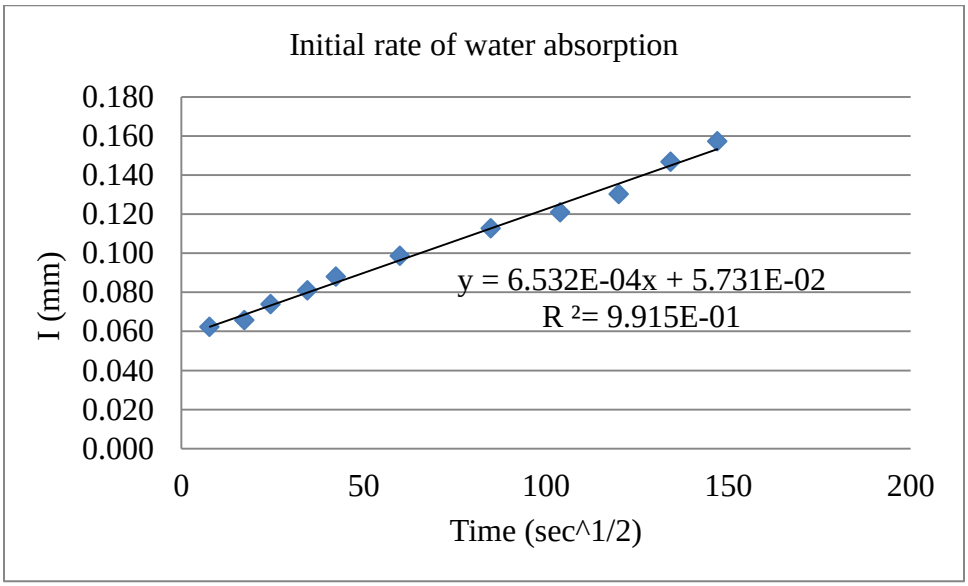

Figure 54. Initial rate of water absorption ($CaCl_2$ Sample 1)

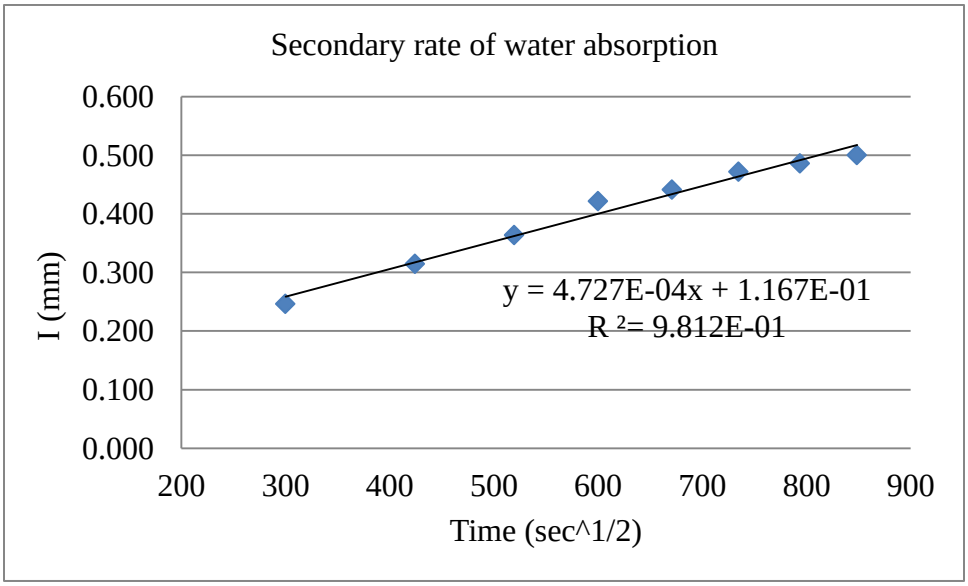

Figure 55. Secondary rate of water absorption ($CaCl_2$ Sample 1)

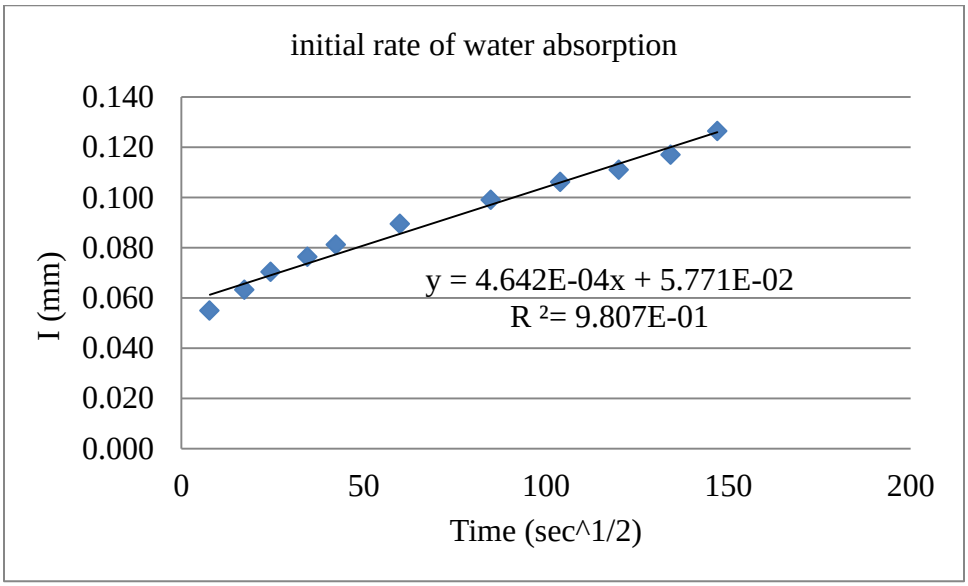

Figure 56. Initial rate of water absorption ($CaCl_2$ Sample 2)

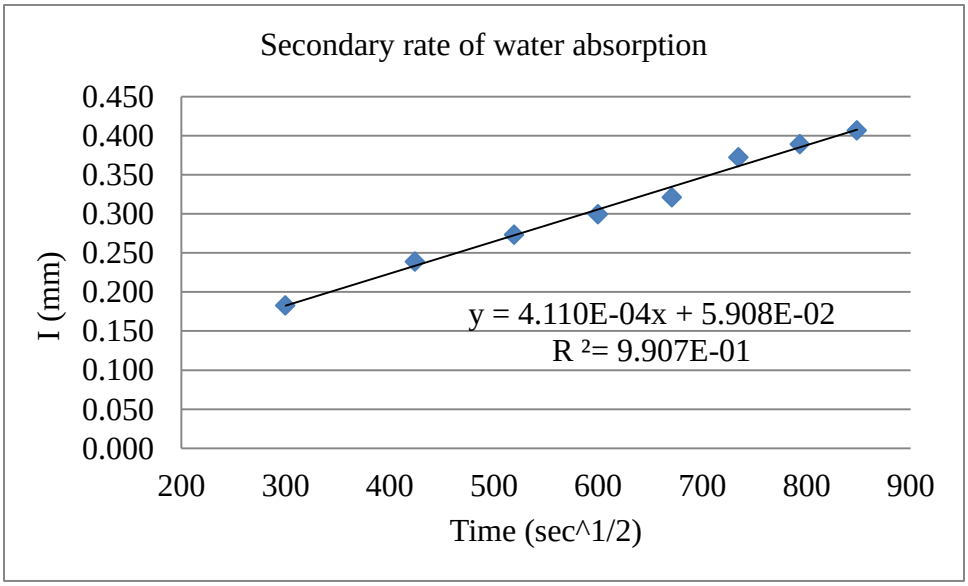

Figure 57. Secondary rate of water absorption ($CaCl_2$ Sample 2)

Water absorption (Season I Sample)

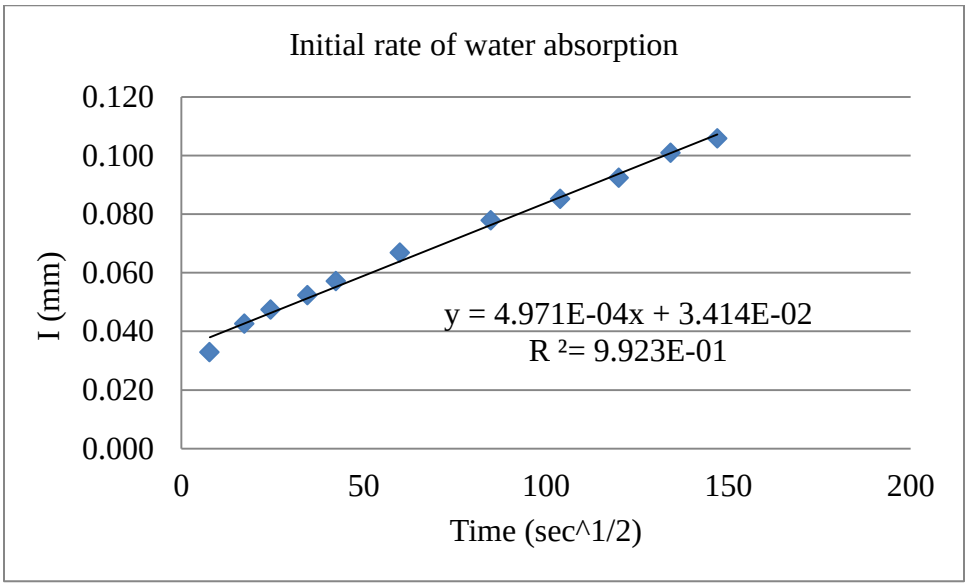

Figure 58. Initial rate of water absorption (Season I Sample 1)

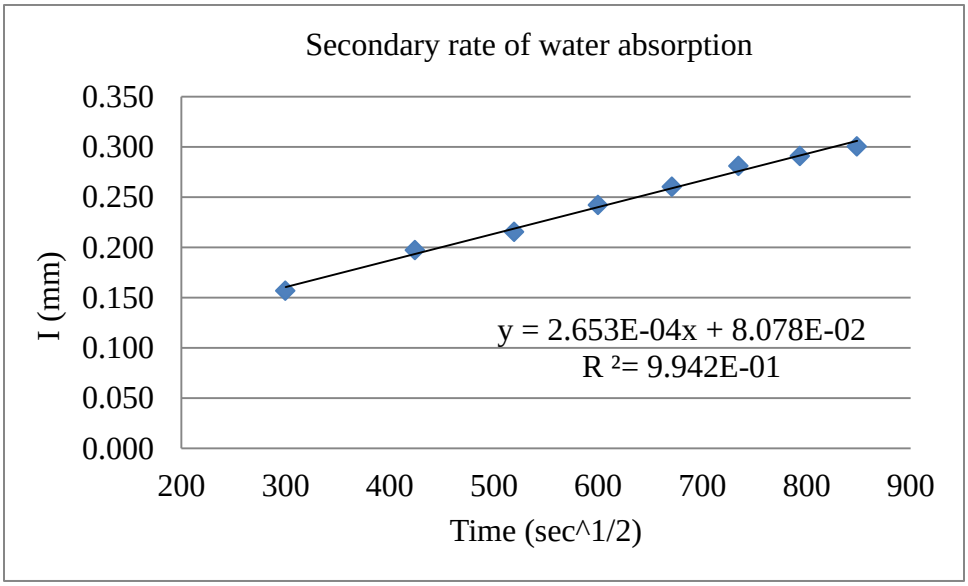

Figure 59. Secondary rate of water absorption (Season I Sample 1)

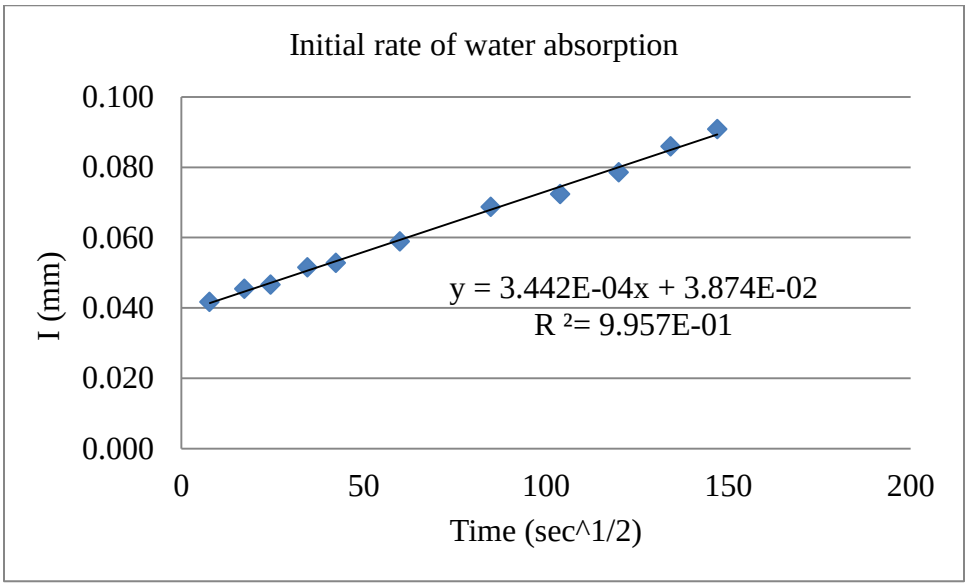

Figure 60. Initial rate of water absorption (Season I Sample 2)

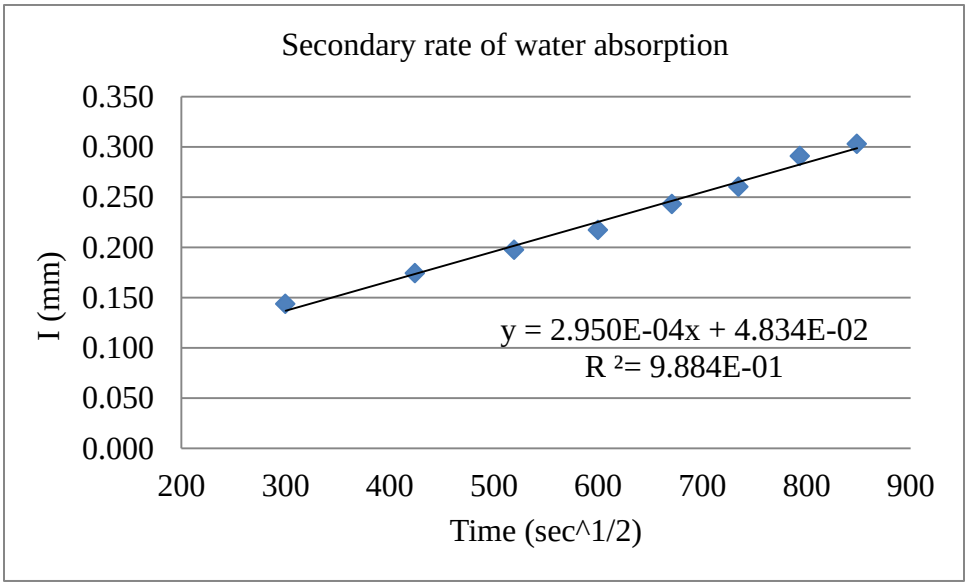

Figure 61. Secondary rate of water absorption (Season I Sample 2)

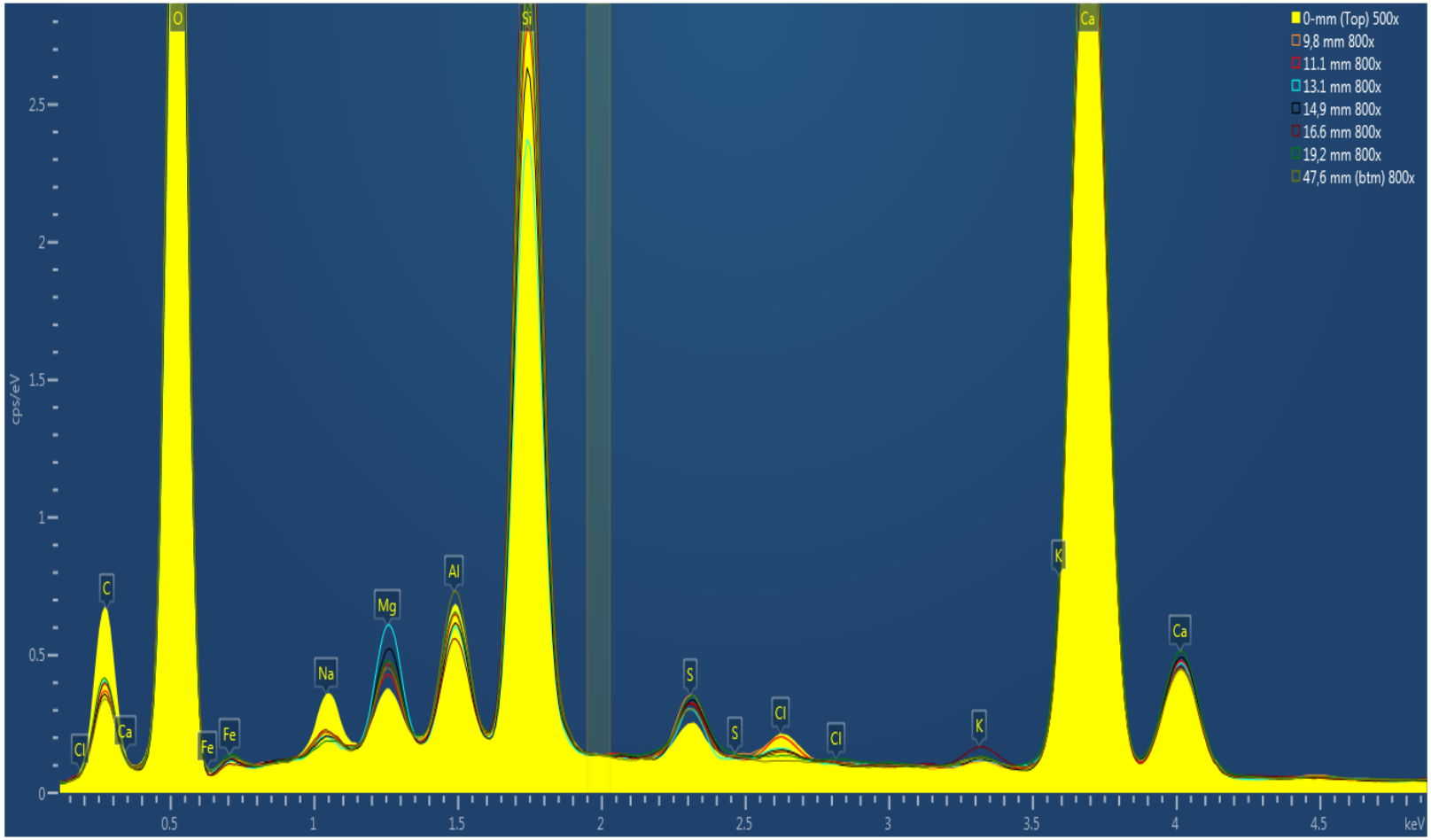

Figure 62. EDS spectrum of NaCl sample

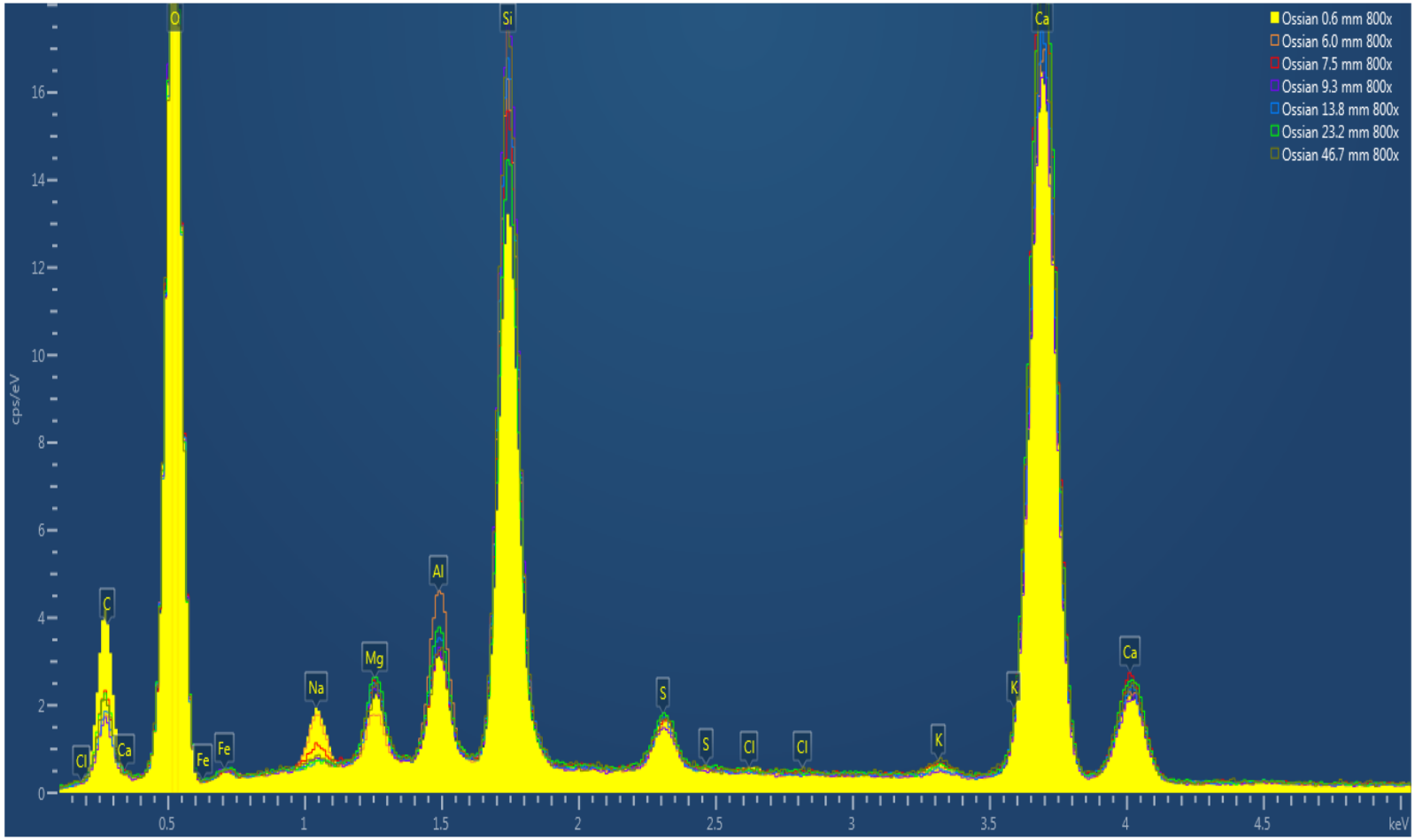

Figure 63. EDS spectrum of Season I sample

APPENDIX C

ORIGINAL DATA

Mass Loss/Strength Loss of Frost-Salt Degradation

Table 16. Strength loss after frost-salt attack

Compressive Strength of mortar cubes after 10 F/T cycles, psi				
Deicer	Sample #	28 day compressive strength, psi	Statistics	
DI Water	S1	9253	std (all results)	2469
	S2	7219	avg (all results)	6792
	S3	3364	std (good results)	80
	S4	7332	avg (good results)	7276
NaCl	S1	4028	std	550
	S2	3942	avg	3996
	S3	4680	std	61
	S4	3335	avg	3985
CaCl2	S1	6495	std	1603
	S2	2917	avg	5275
	S3	5767	std	109
	S4	5921	avg	5844
Season I	S1	9537	std	1571
	S2	9077	avg	7973
	S3	6938	std	422
	S4	6341	avg	6640

Table 17. Strength of mortars in moist curing

	28 day Compressive Strength, psi
1	7569
2	7627
3	9800
4	9915
5	5731
6	7723
7	6764
8	7615
avg	7460

Table 18. Mass loss of mortar cubes in DI water

Deicer/Control	Number of F/T cycles	Sample ID	Weight g	Density g/cm^3	Materials removed g	Weight Loss %	Std of Weight Loss
Deionized Water	0	D1	291.8	2.23			
		D2	295.1	2.25			
		D3	295.1	2.25			
		D4	300.3	2.29			
		AVG	295.6	2.25			
	5	D1	290.4		1.45	0.50	0.06
		D2	293.9		1.15	0.39	
		D3	293.7		1.42	0.48	
		D4	298.7		1.60	0.53	
		AVG	294.2		1.40	0.48	
	10	D1	290.5		1.33	0.46	0.04
		D2	293.6		1.46	0.49	
		D3	293.5		1.62	0.55	
		D4	298.7		1.63	0.54	
		AVG	294.1		1.51	0.51	

Table 19. Mass loss of mortar cubes in Sodium Chloride Solution

Deicer/Control	Number of F/T cycles	Sample ID	Weight g	Density g/cm^3	Materials removed g	Weight Loss %	Std of Weight Loss
Sodium Chloride	0	N1	294.4	2.25			
		N2	298.3	2.28			
		N3	292.3	2.23			
		N4	292.6	2.23			
		AVG	294.4	2.25			
	5	N1	272.6		21.85	7.42	
		N2	274.8		23.48	7.87	
		N3	270.5		21.78	7.45	1.38
		N4	278.4		14.20	4.85	
		AVG	274.1		20.33	6.90	
	10	N1	266.6		27.77	9.43	
		N2	270.4		27.95	9.37	
		N3	264.3		27.97	9.57	1.13
		N4	271.5		21.10	7.21	
		AVG	268.2		26.20	8.90	

Table 20. Mass loss of mortar cubes in Calcium Chloride Solution

Deicer/Control	Number of F/T cycles	Sample ID	Weight g	Density g/cm^3	Materials removed g	Weight Loss %	Std of Weight Loss
Calcium Chloride	0	C1	295.0	2.25			
		C2	296.9	2.26			
		C3	296.3	2.26			
		C4	293.3	2.24			
		AVG	295.4	2.25			
	5	C1	290.5		4.43	1.50	
		C2	283.7		13.21	4.45	
		C3	289.3		7.05	2.38	1.37
		C4	288.7		4.61	1.57	
		AVG	288.1		7.32	2.48	
	10	C1	286.5		8.48	2.87	
		C2	274.1		22.77	7.67	
		C3	283.8		12.59	4.25	2.07
		C4	281.5		11.82	4.03	
		AVG	281.5		13.92	4.71	

Table 21. Mass loss of mortar cubes in Calcium Chloride Solution

Deicer/Control	Number of F/T cycles	Sample ID	Weight g	Density g/cm^3	Materials removed g	Weight Loss %	Std of Weight Loss
Season I	0	O1	293.4	2.24			
		O2	294.1	2.24			
		O3	295.9	2.26			
		O4	296.9	2.26			
		AVG	295.1	2.25			
	5	O1	292.3		1.13	0.39	0.11
		O2	292.7		1.40	0.48	
		O3	294.8		1.10	0.37	
		O4	296.3		0.61	0.21	
		AVG	294.0		1.06	0.36	
	10	O1	291.5		1.89	0.64	0.14
		O2	291.9		2.24	0.76	
		O3	294.0		1.85	0.63	
		O4	295.7		1.23	0.41	
		AVG	293.3		1.80	0.61	

Scaling Rate

Sample ID	Ponding Area, in^2	1st 5 F/T cycles	Mass Loss, g	Unit mass loss, g/m^2	Cumulative Unit Mass Loss, g/m^2	Scaling Rating	Visual Rating
D1	72.38	Jan 1 - 6	0.00	0.00	0.00	0	0
D2	72.38		0.00	0.00	0.00	0	0
N1	72.50		21.00	448.97	448.97	2	2
N2	72.50		23.10	493.86	493.86	2	2
C1	72.38		15.90	340.52	340.52	2	2
C2	72.38		14.70	314.82	314.82	2	2
S1	72.25		0.00	0.00	0.00	0	0
S2	72.25		0.00	0.00	0.00	0	0

2ed 5 F/T cycles	Mass Loss, g	Unit mass loss, g/m^2	Cumulative Unit Mass Loss, g/m^2	Scaling Rating	Visual Rating
Jan 6 - 11	0.10	2.14	2.14	0	0
	0.08	1.71	1.71	0	0
	27.94	597.34	1046.31	3	2
	24.23	518.02	1011.88	3	2
	11.42	244.57	585.09	3	2
	9.27	198.53	513.35	3	2
	0.34	7.29	7.29	0	0
	0.64	13.73	13.73	0	0

3rd 5 F/T cycles	Mass Loss, g	Unit mass loss, g/m^2	Cumulative Unit Mass Loss, g/m^2	Scaling Rating	Visual Exam
Jan 11 - 16	0.10	2.14	4.28	0	1
	0.10	2.14	3.85	0	1
	17.90	382.69	1429.00	4	4
	21.50	459.66	1471.54	4	4
	7.90	169.19	754.28	3	3
	11.40	244.15	757.49	3	3
	0.20	4.29	11.58	0	1
	0.09	1.93	15.66	0	1

4th 5 F/T cycles	Mass Loss, g	Unit mass loss, g/m^2	Cumulative Unit Mass Loss, g/m^2	Scaling Rating	Visual Exam
Jan 17-22	0.10	2.14	6.42	0	1
	0.10	2.14	6.00	0	0
	12.40	265.10	1694.10	4	4
	10.60	226.62	1698.16	4	4
	9.20	197.03	951.31	3	3
	3.90	83.52	841.02	3	3
	0.00	0.00	11.58	0	1
	0.00	0.00	15.66	0	1

5th 5 F/T cycles	Mass Loss, g	Unit mass loss, g/m^2	Cumulative Unit Mass Loss, g/m^2	Scaling Rating	Visual Exam
Jan 27-31	0.00	0.00	6.42	0	1
	0.00	0.00	6.00	0	1
	5.80	124.00	1818.10	4	4
	6.40	136.83	1834.99	4	4
	1.80	38.55	989.86	3	3
	2.20	47.12	888.13	3	4
	0.00	0.00	11.58	0	1
	0.10	2.15	17.81	0	1

6th 5 F/T cycles	Mass Loss, g	Unit mass loss, g/m^2	Cumulative Unit Mass Loss, g/m^2	Scaling Rating	Visual Exam
Feb 3-8	0.80	17.13	23.56	0	1
	0.20	4.28	10.28	0	1
	1.30	27.79	1845.89	4	4
	1.90	40.62	1875.61	4	4
	0.80	17.13	1006.99	3	3
	0.30	6.42	894.56	3	4
	0.10	2.15	13.73	0	1
	0.00	0.00	17.81	0	1

7th 5 F/T cycles	Mass Loss, g	Unit mass loss, g/m^2	Cumulative Unit Mass Loss, g/m^2	Scaling Rating	Visual Exam
Feb 9-14	0.20	4.28	27.84	0	1
	0.00	0.00	10.28	0	1
	1.20	25.66	1871.55	4	4
	2.70	57.72	1933.33	4	4
	0.80	17.13	1024.13	3	3
	4.90	104.94	999.50	3	4
	0.00	0.00	13.73	0	1
	0.00	0.00	17.81	0	1

8th 5 F/T cycles	Mass Loss, g	Unit mass loss, g/m^2	Cumulative Unit Mass Loss, g/m^2	Scaling Rating	Visual Exam
Feb 14-19	0.00	0.00	27.84	0	1
	0.00	0.00	10.28	0	1
	0.70	14.97	1886.51	4	4
	0.20	4.28	1937.61	4	4
	0.20	4.28	1028.41	3	3
	2.40	51.40	1050.90	3	4
	0.00	0.00	13.73	0	1
	0.00	0.00	17.81	0	1

9th 5 F/T cycles	Mass Loss, g	Unit mass loss, g/m^2	Cumulative Unit Mass Loss, g/m^2	Scaling Rating	Visual Exam
Feb 20-25	0.80	17.13	44.97	0	0
	0.00	0.00	10.28	0	0
	0.60	12.83	1899.34	4	4
	0.60	12.83	1950.44	4	4
	0.00	0.00	1028.41	3	3
	0.90	19.27	1070.17	3	4
	0.10	2.15	15.88	0	1
	0.00	0.00	17.81	0	1

10th 5 F/T cycles	Mass Loss, g	Unit mass loss, g/m^2	Cumulative Unit Mass Loss, g/m^2	Scaling Rating	Visual Exam
Mar 2-7	0.00	0.00	44.97	0	1
	0.00	0.00	10.28	0	1
	0.10	2.14	1901.48	4	4
	0.00	0.00	1950.44	4	4
	0.00	0.00	1028.41	3	3
	0.70	14.99	1085.16	3	4
	0.00	0.00	15.88	0	1
	0.00	0.00	17.81	0	1

Air Permeability Data

DI Water Group Air Permeability

	Ch1	Ch2	Ch3	Ch4	OPI	8.035639
Diameter,in	4.02	4.03	4.02	4.02		
	4.01	4.03	4.02	4.03		
	4.00	4.05	4.01	4.01		
	4.00	4.01	4.07	4.03		
Thickness, in	0.93	0.94	0.98	0.92		
	0.93	0.94	0.98	0.91		
	0.93	0.95	0.98	0.91		
	0.93	0.95	0.99	0.91		
Ave thickness, m	0.0236	0.0240	0.0250	0.0232		
Area, m2	0.0081	0.0082	0.0082	0.0082		
Volume (m3)	0.004976	0.004821	0.004862	0.004899		
Slope	6.99793E-06	6.27523E-06	5.00869E-06	4.19044E-06		
Coefficient of permeability, k (m/s)	**1.15959E-08**	**1.01230E-08**	**8.47191E-09**	**6.65775E-09**		

Volume (cm3)			
ch1	ch2	ch3	ch4
4976	4821	4862	4899
Volume (m3)			
ch1	ch2	ch3	ch4
0.004976	0.004821	0.004862	0.004899

acceleration	g (m/s2)	9.81
universal gas constant	R (Nm/K mol)	8.3130
temperature	K	298.0
molecular mass of air	ω (g/mol)	28.97

NaCl Group Air Permeability

	Ch1	Ch2	Ch3	Ch4	OPI	8.1
Diameter,in	4.03	4.01	4.41	4.04		
	4.05	4.03	4.07	4.05		
	4.04	4.02	4.07	4.03		
	4.09	4.02	4.02	4.02		
Thickness, in	0.95	0.99	1.01	1.09		
	0.92	0.98	1.03	1.03		
	0.93	0.98	1.01	1.07		
	0.96	0.98	1.03	1.07		
Ave thickness, m	0.0239	0.0250	0.0259	0.0271		
Area, m2	0.0083	0.0082	0.0087	0.0082		
Volume (m3)	0.004976	0.004821	0.004862	0.004899		
Slope	4.58285E-06	5.12671E-06	########	1.80640E-06		
Coefficient of permeability, k (m/s)	**7.50616E-09**	**8.64124E-09**	**########**	**3.32892E-09**		

Volume (cm3)				acceleration	g (m/s2)
				universal gas constant	R (Nm/K mol)
ch1	ch2	ch3	ch4		
4976	4821	4862	4899	temperature	K
				molecular mass of air	ω (g/mol)
Volume (m3)					
ch1	ch2	ch3	ch4		
0.004976	0.004821	0.004862	0.004899		

$CaCl_2$ Group Air Permeability

	Ch1	Ch2	Ch3	Ch4	OPI	7.8
Diameter,in	4.04	4.07	4.03	4.08		
	4.06	4.06	4.05	4.00		
	4.04	4.03	4.01	4.03		
	4.02	4.01	4.00	4.04		
Thickness, in	1.07	1.06	1.05	1.06		
	1.06	1.04	1.05	1.04		
	1.05	1.07	1.05	1.05		
	1.07	1.04	1.04	1.05		
Ave thickness, m	0.0270	0.0267	0.0266	0.0267		
Area, m2	0.0083	0.0083	0.0082	0.0083		
Volume (m3)	0.004976	0.004821	0.004862	0.004899		
Slope	1E-05	9.212E-06	7.818E-06	6.67779E-06		
Coefficient of permeability, k (m/s)	########	1.6448E-08	1.4151E-08	1.2118E-08		

Volume (cm3)				acceleration	g (m/s2)	9.8
				universal gas constant	R (Nm/K mol)	###
ch1	ch2	ch3	ch4			
4976	4821	4862	4899	temperature	K	###
				molecular mass of air	ω (g/mol)	###
Volume (m3)						
ch1	ch2	ch3	ch4			
0.004976	0.004821	0.004862	0.004899			

Season I Group Air Permeability

	Ch1	Ch2	Ch3	Ch4	OPI	7.912
Diameter,in	4.05	4.06	4.03	4.06		
	4.02	4.07	4.07	4.05		
	4.02	4.06	4.03	4.01		
	4.04	4.07	4.05	4.01		
Thickness, in	1.08	0.98	1.00	1.07		
	1.08	0.99	0.99	1.09		
	1.07	0.98	0.99	1.09		
	1.07	0.99	1.01	1.08		
Ave thickness, m	0.0273	0.0250	0.0253	0.0275		
Area, m2	0.0082	0.0084	0.0083	0.0082		
Volume (m3)	0.004976	0.004821	0.004862	0.004899		
Slope	6.98130E-06	9.73240E-06	6.22116E-06	4.83562E-06		
Coefficient of permeability, k (m/s)	**1.32068E-08**	**1.60839E-08**	**1.06043E-08**	**9.06898E-09**		

Volume (cm3)				acceleration	g (m/s2)	9.81
				universal gas constant	R (Nm/K mol)	8.3130
ch1	ch2	ch3	ch4			
4976	4821	4862	4899	temperature	K	298.0
				molecular mass of air	ω (g/mol)	28.97
Volume (m3)						
ch1	ch2	ch3	ch4			
0.004976	0.004821	0.004862	0.004899			

Water Absorption Mass Change

Water absorption (DI Water Sample 1)

Test Time	Test Time in Seconds	s^(1/2)	Mass (gr)	ΔMass (gr)	I (mm)
0	0	0	957.35	0.00	0
60 s	60	8	957.67	0.32	0.038407
5 min	300	17	957.73	0.38	0.045608
10 min	600	24	957.79	0.44	0.05281
20 min	1200	35	957.83	0.48	0.057611
30 min	1800	42	957.91	0.56	0.067212
60 min	3600	60	957.98	0.63	0.075614
2 h	7200	85	958.05	0.70	0.084015
3 h	10800	104	958.10	0.75	0.090017
4 h	14400	120	958.19	0.84	0.100819
5 h	18000	134	958.24	0.89	0.10682
6 h	21600	147	958.27	0.92	0.11042
1 d	90000	300	958.82	1.47	0.176432
2 d	180000	424	959.26	1.91	0.229242
3 d	270000	520	959.53	2.18	0.261648
4 d	360000	600	959.74	2.39	0.286853
5 d	450000	671	959.87	2.52	0.302456
6 d	540000	735	960.07	2.72	0.32646
7 d	630000	794	960.28	2.93	0.351665
8 d	720000	849	960.39	3.04	0.364867

Water absorption (DI Water Sample 2)

Test Time	Test Time in Seconds	s^(1/2)	Mass (gr)	ΔMass (gr)	I (mm)
0	0	0	1018.15	0.00	0
60 s	60	8	1018.49	0.34	0.041625
5 min	300	17	1018.58	0.43	0.052643
10 min	600	24	1018.69	0.54	0.06611
20 min	1200	35	1018.75	0.60	0.073455
30 min	1800	42	1018.83	0.68	0.083249
60 min	3600	60	1018.92	0.77	0.094268
2 h	7200	85	1019.01	0.86	0.105286
3 h	10800	104	1019.09	0.94	0.11508
4 h	14400	120	1019.21	1.06	0.129771
5 h	18000	134	1019.34	1.19	0.145686
6 h	21600	147	1019.42	1.27	0.15548
1 d	90000	300	1020.01	1.86	0.227711
2 d	180000	424	1020.32	2.17	0.265663
3 d	270000	520	1020.56	2.41	0.295045
4 d	360000	600	1020.81	2.66	0.325652
5 d	450000	671	1021.09	2.94	0.359931
6 d	540000	735	1021.29	3.14	0.384416
7 d	630000	794	1021.59	3.44	0.421143
8 d	720000	849	1021.88	3.73	0.456647

Water absorption (NaCl Sample 1)

Test Time	Test Time in Seconds	s^(1/2)	Mass (gr)	ΔMass (gr)	I (mm)
0	0	0	1044.1	0.00	0
60 s	60	8	1044.5	0.42	0.051
5 min	300	17	1044.5	0.47	0.057
10 min	600	24	1044.6	0.53	0.064
20 min	1200	35	1044.7	0.61	0.074
30 min	1800	42	1044.7	0.65	0.079
60 min	3600	60	1044.8	0.75	0.091
2 h	7200	85	1044.9	0.82	0.1
3 h	10800	104	1044.9	0.86	0.105
4 h	14400	120	1045	0.97	0.118
5 h	18000	134	1045.1	1.01	0.123
6 h	21600	147	1045.2	1.10	0.134
1 d	90000	300	1045.7	1.62	0.197
2 d	180000	424	1046.2	2.11	0.256
3 d	270000	520	1046.4	2.36	0.287
4 d	360000	600	1046.7	2.59	0.315
5 d	450000	671	1046.8	2.75	0.334
6 d	540000	735	1047	2.90	0.352
7 d	630000	794	1047.1	3.07	0.373
8 d	720000	849	1047.2	3.13	0.38

Water absorption (NaCl Sample 2)

Test Time	Test Time in Seconds	s^(1/2)	Mass (gr)	ΔMass (gr)	I (mm)
0	0	0	995.46	0.00	0
60 s	60	8	995.72	0.26	0.0316
5 min	300	17	995.79	0.33	0.0401
10 min	600	24	995.83	0.37	0.045
20 min	1200	35	995.87	0.41	0.0499
30 min	1800	42	995.93	0.47	0.0572
60 min	3600	60	996.04	0.58	0.0706
2 h	7200	85	996.11	0.65	0.0791
3 h	10800	104	996.20	0.74	0.09
4 h	14400	120	996.23	0.77	0.0937
5 h	18000	134	996.32	0.86	0.1046
6 h	21600	147	996.36	0.90	0.1095
1 d	90000	300	996.87	1.41	0.1715
2 d	180000	424	997.21	1.75	0.2129
3 d	270000	520	997.39	1.93	0.2348
4 d	360000	600	997.63	2.17	0.264
5 d	450000	671	997.77	2.31	0.281
6 d	540000	735	997.85	2.39	0.2908
7 d	630000	794	998.07	2.61	0.3175
8 d	720000	849	998.14	2.68	0.3261

Water absorption ($CaCl_2$ Sample 1)

Test Time	Test Time in Seconds	s^(1/2)	Mass (gr)	ΔMass (gr)	I (mm)
0	0	0	886.96	0.00	0
60 s	60	8	887.23	0.27	0.0328
5 min	300	17	887.31	0.35	0.0426
10 min	600	24	887.35	0.39	0.0474
20 min	1200	35	887.39	0.43	0.0523
30 min	1800	42	887.43	0.47	0.0572
60 min	3600	60	887.51	0.55	0.0669
2 h	7200	85	887.60	0.64	0.0779
3 h	10800	104	887.66	0.70	0.0852
4 h	14400	120	887.72	0.76	0.0925
5 h	18000	134	887.79	0.83	0.101
6 h	21600	147	887.83	0.87	0.1058
1 d	90000	300	888.25	1.29	0.1569
2 d	180000	424	888.58	1.62	0.1971
3 d	270000	520	888.73	1.77	0.2153
4 d	360000	600	888.95	1.99	0.2421
5 d	450000	671	889.10	2.14	0.2604
6 d	540000	735	889.27	2.31	0.281
7 d	630000	794	889.35	2.39	0.2908
8 d	720000	849	889.43	2.47	0.3005

Water absorption ($CaCl_2$ Sample 2)

Test Time	Test Time in Seconds	s^(1/2)	Mass (gr)	ΔMass (gr)	I (mm)
0	0	0	998.35	0.00	0
60 s	60	8	998.88	0.53	0.0622
5 min	300	17	998.91	0.56	0.0657
10 min	600	24	998.98	0.63	0.074
20 min	1200	35	999.04	0.69	0.081
30 min	1800	42	999.10	0.75	0.0881
60 min	3600	60	999.19	0.84	0.0986
2 h	7200	85	999.31	0.96	0.1127
3 h	10800	104	999.38	1.03	0.1209
4 h	14400	120	999.46	1.11	0.1303
5 h	18000	134	999.60	1.25	0.1468
6 h	21600	147	999.69	1.34	0.1573
1 d	90000	300	1000.45	2.10	0.2465
2 d	180000	424	1001.03	2.68	0.3146
3 d	270000	520	1001.45	3.10	0.3639
4 d	360000	600	1001.94	3.59	0.4215
5 d	450000	671	1002.11	3.76	0.4414
6 d	540000	735	1002.37	4.02	0.472
7 d	630000	794	1002.49	4.14	0.486
8 d	720000	849	1002.61	4.26	0.5001

Water absorption (Season I Sample 1)

Test Time	Test Time in Seconds	s^(1/2)	Mass (gr)	ΔMass (gr)	I (mm)
0	0	0	886.96	0.00	0
60 s	60	8	887.23	0.27	0.0328
5 min	300	17	887.31	0.35	0.0426
10 min	600	24	887.35	0.39	0.0474
20 min	1200	35	887.39	0.43	0.0523
30 min	1800	42	887.43	0.47	0.0572
60 min	3600	60	887.51	0.55	0.0669
2 h	7200	85	887.60	0.64	0.0779
3 h	10800	104	887.66	0.70	0.0852
4 h	14400	120	887.72	0.76	0.0925
5 h	18000	134	887.79	0.83	0.101
6 h	21600	147	887.83	0.87	0.1058
1 d	90000	300	888.25	1.29	0.1569
2 d	180000	424	888.58	1.62	0.1971
3 d	270000	520	888.73	1.77	0.2153
4 d	360000	600	888.95	1.99	0.2421
5 d	450000	671	889.10	2.14	0.2604
6 d	540000	735	889.27	2.31	0.281
7 d	630000	794	889.35	2.39	0.2908
8 d	720000	849	889.43	2.47	0.3005

Water absorption (Season I Sample 2)

Test Time	Test Time in Seconds	s^(1/2)	Mass (gr)	ΔMass (gr)	I (mm)
0	0	0	1042.19	0.00	0
60 s	60	8	1042.53	0.34	0.0417
5 min	300	17	1042.56	0.37	0.0454
10 min	600	24	1042.57	0.38	0.0466
20 min	1200	35	1042.61	0.42	0.0515
30 min	1800	42	1042.62	0.43	0.0528
60 min	3600	60	1042.67	0.48	0.0589
2 h	7200	85	1042.75	0.56	0.0687
3 h	10800	104	1042.78	0.59	0.0724
4 h	14400	120	1042.83	0.64	0.0785
5 h	18000	134	1042.89	0.70	0.0859
6 h	21600	147	1042.93	0.74	0.0908
1 d	90000	300	1043.36	1.17	0.1436
2 d	180000	424	1043.61	1.42	0.1743
3 d	270000	520	1043.80	1.61	0.1976
4 d	360000	600	1043.96	1.77	0.2172
5 d	450000	671	1044.17	1.98	0.243
6 d	540000	735	1044.31	2.12	0.2602
7 d	630000	794	1044.56	2.37	0.2909
8 d	720000	849	1044.66	2.47	0.3031

Electrical Resistivity

Table 22. Electrical Resistivity Readings by Wenner Probe

Deicer/Control	Sample ID	Resistivity Readings										
		0°	90°	180°	270°	0°	90°	180°	270°	Average	Average	Range
DI water	D1	12.0	11.6	11.2	12.7	12.1	11.3	11.8	11.8	11.8	11.8	high
	D2	12.2	11.2	12.1	11.8	12.6	11.3	12.1	12.1	11.9		
	D3	11.7	12.6	11.0	11.9	11.6	11.9	11.3	11.3	11.7		
3% NaCl	N1	12.2	10.9	11.3	11.1	11.5	10.9	11.6	11.6	11.4	11.4	high
	N2	12.0	11.1	11.4	10.9	11.0	11.2	11.3	11.3	11.3		
	N3	12.1	11.7	10.9	11.9	12.1	11.7	10.5	11.5	11.6		
4% $CaCl_2$	C1	12.6	12.2	13.1	11.8	12.5	11.9	12.6	12.6	12.4	12.0	moderate
	C2	11.6	10.9	11.5	11.2	10.8	11.9	12.0	12.0	11.5		
	C3	12.1	11.5	12.1	11.7	12.0	12.2	12.1	11.9	12.0		
Season I S1	O1	18.1	19.3	15.1	17.9	18.7	19.1	15.6	15.6	17.4	16.9	moderate
	O2	13.9	14.5	16.7	16.2	14.3	14.8	13.7	13.7	14.7		
	O3	19.0	18.4	18.7	19.6	18.8	17.5	18.0	18.0	18.5		

Skid Resistance Measurement

Table 23. Summary of skid resistance results

Deicer/Control	Concentration (weight percent)	Test Surface	BPN Value Average	Temperature ℉
Deionized Water	-	SG	79.6	65.3
		PCC	68.9	74.9
Sodium Chloride	3%	SG	77.4	66.4
		PCC	68.9	74.8
Calcium Chloride	4%	SG	76.8	66.2
		PCC	69.3	74.6
Season I	-	SG	46.8	67.5
		PCC	58.7	74.6

BPN Values and Temperature of each trial

Test Date		10/21/2012		
Test Surface		SG		
Deicer/Control	Concentration (weight percent)		BPN Values	Temperature °F
Deionized Water		1	80.0	65.3
		2	80.0	65.1
		3	79.0	65.3
		4	80.0	65.5
		5	79.0	65.3
		Average	79.6	65.3
Sodium Chloride	3%	1	77.0	66.6
		2	78.0	66.4
		3	78.0	66.4
		4	77.0	66.4
		5	77.0	66.4
		Average	77.4	66.4
Calcium Chloride	4%	1	77.0	66.2
		2	77.0	66.2
		3	77.0	66.0
		4	76.0	66.2
		5	77.0	66.2
		Average	76.8	66.2
Ossain Season 1		1	46.0	67.5
		2	47.0	67.5
		3	47.0	67.0
		4	47.0	67.5
		5	47.0	67.8
		Average	46.8	67.5

Test Date	10/24/2012		Site 1	
Test Surface	PCC			
Deicer/Control	Concentration (weight percent)		BPN Values	Temperature °F
Deionized Water		1	71.0	74.6
		2	70.0	74.5
		3	71.0	74.5
		4	70.0	74.6
		5	70.0	74.6
		Average	70.4	74.6
Sodium Chloride	3%	1	69.0	74.5
		2	68.0	74.5
		3	69.0	74.5
		4	69.0	73.9
		5	69.0	74.4
		Average	68.8	74.4
Calcium Chloride	4%	1	69.0	73.8
		2	69.0	74.3
		3	70.0	74.3
		4	70.0	74.4
		5	70.0	74.4
		Average	69.6	74.2
Season I Season 1		1	60.0	74.4
		2	60.0	74.4
		3	59.0	74.5
		4	60.0	74.4
		5	59.0	74.4
		Average	59.6	74.4

Test Date	10/24/2012		Site 2	
Test Surface	PCC			
Deicer/Control	Concentration (weight percent)		BPN Values	Temperature °F
Deionized Water		1	65.0	75.1
		2	64.0	75.2
		3	65.0	74.9
		4	64.0	74.9
		5	64.0	74.9
		Average	65.0	75.0
Sodium Chloride	3%	1	64.0	74.8
		2	65.0	74.8
		3	64.0	74.7
		4	64.0	74.8
		5	65.0	74.8
		Average	64.4	74.8
Calcium Chloride	4%	1	64.0	74.8
		2	65.0	74.8
		3	65.0	74.7
		4	65.0	74.7
		5	64.0	74.7
		Average	64.6	74.7
Season I Season 1		1	55.0	74.6
		2	54.0	74.5
		3	55.0	74.4
		4	55.0	74.4
		5	55.0	74.4
		Average	54.8	74.5

Test Date	10/24/2012		Site 3	
Test Surface	PCC			
Deicer/Control	Concentration (weight percent)		BPN Values	Temperature °F
Deionized Water		1	71.0	75.3
		2	72.0	75.2
		3	71.0	75.2
		4	71.0	75.2
		5	71.0	75.1
		Average	71.2	75.2
Sodium Chloride	3%	1	73.0	75.2
		2	74.0	75.3
		3	73.0	75.2
		4	74.0	75.2
		5	74.0	75.1
		Average	73.6	75.2
Calcium Chloride	4%	1	73.0	75.1
		2	74.0	75.1
		3	74.0	74.8
		4	73.0	74.9
		5	74.0	74.8
		Average	73.6	74.9
Season I Season 1		1	62.0	74.8
		2	61.0	74.7
		3	62.0	74.8
		4	62.0	74.8
		5	62.0	74.7
		Average	61.8	74.8

Test Date	3/11/2013		Site 1	
Test Surface	PCC			
Deicer/Control	Concentration		BPN Values	Temperature
Ossain Season 1		1	56.0	35.6
		2	55.0	36.9
		3	56.0	37.4
		4	55.0	36.7
		5	56.0	35.5
Sodium Chloride	3%	1	71.0	38.6
		2	72.0	37.5
		3	71.0	37.9
		4	72.0	33.2
		5	71.0	36.5
Ossain Season 1 after 2 hr		1	55.0	43.8
		2	54.0	44.6
		3	54.0	43.2
		4	55.0	41.9
		5	55.0	44.3
		Average	54.6	43.6
Sodium Chloride after 2 hr	3%	1	72.0	44.1
		2	72.0	45.3
		3	72.0	44.4
		4	72.0	44.8
		5	73.0	42.9
Ossain Season 1 after 4 hr		1	51.0	24.3
		2	52.0	24.9
		3	52.0	28.6
		4	51.0	25.6
		5	52.0	27.2
Sodium Chloride after 4 hr	3%	1	75.0	23.5
		2	75.0	24.9
		3	76.0	22.6
		4	75.0	21.5
		5	76.0	23.3

Test Date	3/11/2013		Site 2	
Test Surface	PCC			
Deicer/Control	Concentration		BPN Values	Temperature
Ossain Season 1		1	59.0	33.8
		2	59.0	35.6
		3	60.0	36.2
		4	60.0	36.1
		5	59.0	34.7
Sodium Chloride	3%	1	73.0	37.8
		2	72.0	37.7
		3	72.0	37.4
		4	72.0	36.5
		5	72.0	33.8
Ossain Season 1 after 2 hr		1	59.0	41.9
		2	58.0	41.8
		3	59.0	42.1
		4	58.0	44.5
		5	59.0	42.8
		Average	58.6	42.6
Sodium Chloride after 2 hr	3%	1	73.0	43.6
		2	73.0	42.2
		3	72.0	43.8
		4	72.0	43.5
		5	72.0	41.9
Ossain Season 1 after 4 hr		1	55.0	22.9
		2	55.0	21.6
		3	54.0	22.8
		4	55.0	27.4
		5	55.0	25.6
Sodium Chloride after 4 hr	3%	1	72.0	23.6
		2	72.0	25.7
		3	72.0	25.7
		4	73.0	25.1
		5	72.0	22.9

Test Date	3/11/2013		Site 3	
Test Surface	PCC			
Deicer/Control	Concentration		BPN Values	Temperature
Ossain Season 1		1	56.0	36.9
		2	57.0	37.1
		3	57.0	37.5
		4	56.0	34.0
		5	57.0	35.9
Sodium Chloride	3%	1	68.0	38.6
		2	69.0	37.5
		3	68.0	37.9
		4	68.0	33.2
		5	69.0	36.5
Ossain Season 1 after 2 hr		1	55.0	43.7
		2	56.0	42.6
		3	56.0	45.1
		4	55.0	43.8
		5	56.0	44.6
		Average	55.6	44.0
Sodium Chloride after 2 hr	3%	1	71.0	41.5
		2	70.0	44.7
		3	70.0	43.7
		4	71.0	43.8
		5	70.0	42.4
Ossain Season 1 after 4 hr		1	56.0	23.3
		2	55.0	21.7
		3	56.0	23.5
		4	55.0	22.7
		5	56.0	22.9
Sodium Chloride after 4 hr	3%	1	70.0	23.7
		2	71.0	23.2
		3	70.0	25.4
		4	70.0	21.2
		5	70.0	22.5